NTNU – Trondheim
Norwegian University of
Science and Technology

Use of Telecom Energy for Smart Grid

Muhammad Usman

Master of Science in Electric Power Engineering
Submission date: September 2013
Supervisor: Tore Marvin Undeland, ELKRAFT

Norwegian University of Science and Technology
Department of Electric Power Engineering

Use of Telecom Energy for Smart Grid

Problem Description

The trends of global warming and increased energy demand drive the need for increased use of renewable energy. However, the production of electricity from renewable energy is typically distributed and intermittent. On the energy demand side, the demand for electricity can vary strongly with time. Hence, the combination of:

- Unpredictable and intermittent electricity production from renewable energy sources
- Distributed electricity production in a grid designed for a traditional, more central electricity production with energy transmission bottlenecks
- Varying electricity demands

create challenges both for avoiding an energy demand – supply gap and for the electricity quality at the distribution grid. An alternative to investing in additional conventional electricity production and grid, one approach could be to exploit the energy storage capacities in the distribution grids to time-shift the energy demand and thereby to reduce the distribution grid quality issues. Telecom infrastructure and back-up systems for power generation and distribution/transformation involve existing battery storage that could be exploited to this end.

This Master Thesis will address the following tasks:

- Describe and analyse the opportunities and challenges for the implementation of Smart Grid; how Telecom power infrastructure and other energy storage units could support for the future grid.
- Analyse the relevant power quality challenges faced by the power utilities today, with the help of available measurements and literature studies.
- Describe the different methods to address the relevant power quality issues with the existing telecom energy storages and other technologies.
- Develop and demonstrate a method for exploiting the distributed telecom energy storage for reducing the challenges faced by the power utilities. This involves:
    - Make a simulation model for a distribution grid in the selected region including the typical telecom energy storage, and with representative loads and grid quality issues.
    - Propose a method to control the power flow using the telecom energy storage, in the bidirectional power flow case. A local control method can be implemented to control the flow of power.
    - Demonstrate and analyse the results with simulations.

Supervisor **:** Prof. Tore Marvin Undeland, ELKRAFT, NTNU

Co-supervisor: Dr. Ole Jakob Sørdalen, ELTEK Norway AS.

Abstract

With increasing electricity demand and environmental concerns, utilities are looking for improved network operations and efficient energy consumption. Telecom sites with their flexible energy storage and controllable power flows have significant potential to improve reliability, efficiency, security and quality of electricity supply in the AC distribution system.

Power quality events such as voltage sags, flickers and energization of power devices cause disturbances in the operational grid. Moreover, extensive use of power electronics devices requires additional reactive power from the grid and cause distortion in the source current waveforms. These power quality problems were identified both from the literature studies and measurements obtained from Sintef Energy, a research organization in Norway.

Line rectifiers are being used as grid/utility interfaces for the telecom sites. In this master thesis, an idea is proposed to replace rectifiers with bi-directional AC/DC converters. Operational control schemes for up-to three converters have been developed with the help of vector control technique. These converters with the battery banks on DC side; are not only capable of supplying power for telecommunication services but also of providing the possibility of voltage support, harmonics and reactive power compensation.

Basic distribution network models were developed in the software package MATLAB/SIMULINK® to analyse the impact of connected telecom converters both for the voltage support and ancillary services. Simulations were performed and it was observed that the Total Harmonic Distortion (THD) was reduced to maximum 3.4%, reactive power drawn from the grid became zero and voltage dip in case of wind distributed generation rises from 83.5% to 97.5% when three Telecom sites started supporting the grid. It was also seen that with proper energy management system, Telecom sites can also support utilities by supplying active power during peak hours load demand and for islanding operation.

THD level within the IEEE, IEC, EN power quality standards, compensation of reactive power and provision of voltage support prove that the efficiency of a network can be improved by properly implementing Smart Grid together with the support from distributed telecom sites.

Keywords:

Smart Grid, power quality issues, Telecom Power Infrastructure, power electronics, voltage source converter, vector oriented control, harmonics, active and reactive power, voltage support.

Preface

This master thesis has been written in the department of Electric Power Engineering at the Norwegian University of Science and Technology (NTNU) during the spring 2013. It has been very interesting and remarkable experience of my student life during which I learnt how to work independently and as a team member.

The thesis title was proposed by the department of Research and Development of Eltek Norway AS. This is the continuation of my specialization project during autumn semester project 2012. The autumn project and thesis work provided me an exciting opportunity to visualize the future grid and analyse how Telecommunication companies can contribute to achieve benefits of Smart Grid.

This is an honour for me to be the student of Prof. Tore Marvin Undeland, my supervisor. He has given me this great opportunity to explore the field of power electronics. I would like to express my heartiest gratitude for his timely advices, kind support and encouragement; he has always been a source of inspiration for me.

Without the knowledge, guidance and positive spirit of Dr. Ole Jakob Sørdalen, my co-supervisor from Eltek, I would have not been able to finish my master thesis. His timely discussions and meetings helped me in understanding the areas of research and kept me on track. I would also like to thank PhD student and my friend, Nadeem Jelani for his assistance in building software models and report writing. Nadeem Jelani, I am grateful in every possible way for your endless support.

My special thanks goes to my father, Muhammad Nazir and other family members who have always been there with me whenever I felt alone, thousands of miles away from my home. Their encouragement and support kept me sincere with my work. I would also like to thank Muhammad Shahbaz and other friends for supporting me and keeping my moral high.

Finally, I would like to say that this master thesis is a tiny piece of research in this vast field. I wish reader will find my work interesting and that my dissertation can play a role in the future research.

Muhammad Usman

Trondheim, September 2013

Table of Contents

List of Figures

List of Tables

Acronyms

LV	:	**L**ow **V**oltage
MV	:	**M**edium **V**oltage
DG	:	**D**istributed **G**eneration
SAF	:	**S**hunt **A**ctive **F**ilter
ICT	:	**I**nformation & **C**ommunication **T**echnologies
DER	:	**D**istributed **E**nergy **R**esource
PCC	:	**P**oint of **C**ommon **C**oupling
THD	:	**T**otal **H**armonic **D**istortion
UPS	:	**U**ninterruptable **P**ower **S**upply
VSC	:	**V**oltage **S**ource **C**onverter
TSC	:	**T**hyristor **S**witched **C**apacitor
TCR	:	**T**hyristor **C**ontrolled **R**eactor
CHP	:	**C**ombined **H**eat and **P**ower

Chapter 1: Introduction

In this chapter, the scope of the thesis work and report outlines is presented as a reader's guide, but first it explains the motivation behind this work.

1.1. Motivation

Fossil fuelled conventional power plants produce a large part of manmade CO2 emissions to the atmosphere; such emissions cause global warming and contribute to the negative environmental and health issues [1]. The poor net efficiency of the existing grid infrastructure and climate changes tend to increase the share of distributed renewable energy sources and to improve efficiency of the traditional grid infrastructure. An estimate shows that the cost of improving the efficiency of the power system is less than the investments in new power generation plants and the cost of the abatement of greenhouse gas emissions [2]. A new future grid concept also known as Smart Grid, improves the efficiency of the power system, contributes to the reduction of the global warming, increases the transmission & distribution lines capacities, offers ancillary services support and facilitates the utilities ability to supply power during peak load hours or when there are faults in the grid lines [3], [4].

The use of Power Electronic (PE) devices in adjustable speed drives, utility interfaces with energy storage units or renewable energy sources and in electric or hybrid electric vehicles have significantly increased in the recent few years. Such an expansion of solid state devices is due to the fact that they are low cost, less weight and offer more flexible, reliable and efficient power conversion solutions [5].

AC distribution grids have different Power quality issues such as voltage dips, current harmonics, reactive power consumption, etc. [6]. The loads connected with utility PE interfaces generally behave as non-linear loads for the system; they draw harmonic currents and reactive power from the network which causes disturbances and instability for the distribution grid. In addition to this, if the induction machine wind power turbine is connected to the grid as a Distributed Generation (DG) source, it draws reactive power from the grid which can easily be compensated with the help of capacitor banks. But in case of occurrence of faults in the lines, induction generator will draw even more reactive power from the distribution grid, causing severe problems in the grid. Different ways of handling these issues will affect the performance of the AC system. Allowing the injection of measured currents by using PE interfaces would give possibility of voltage support and improvement in the source current waveforms [7].

Nowadays, numerous Telecom sites are located across the populated areas. Battery banks at these sites supply power to the telecommunication load and are recharged with the help of rectifiers on these locations from AC distribution grids. If line rectifiers are replaced with AC/DC bi-directional converters then PE interfaces will behave as Shunt Active Filters

(SAF). With the help of SAF, Stored energy in these battery banks can be used for two purposes, in addition to their primary back-up power mission. First, it could inject harmonics current and reactive power; secondly, it can be utilized to support the grid with active power during peak load demand.

Although with increasing number of Telecom sites or energy storage units, there will be less stress on individual PE interfaces and on discharging cycles of battery banks but the control of these converters will become more complex due to increasing number of nodes.

1.2. Scope of the Thesis Work

The thesis work is mainly focused on the understanding of smart grid, various power quality issues in the distribution grid and how the Telecom sites connected in parallel with AC grid supply can address these power quality issues. The main objectives of thesis work are mentioned as follows:

- Understanding the basics behind the need of Smart Grid and relationship between Smart Grid and Telecom power infrastructure.
- Understanding of storage devices and their usage for Smart Grid application.
- Identification of various driving factors and barriers in the implementation of Smart Grid.
- Investigation of different power quality events from Literature studies and measurements analysis.
- Understanding of different techniques for the Harmonics and reactive power compensation in the AC distribution grid.
- Development of the control strategies for up-to three bi-directional AC/DC converters
- Understanding the effects of using PE interfaces for the injection of Harmonics current and reactive power both for power factor correction and grid voltage support.
- Analysing the consequences of using battery bank for import and export of active power, in addition to supplying power to DC load.

1.3. Report Outlines

Each chapter of the thesis addresses a specific topic. Main points of each chapter are highlighted as follows:

Chapter 1: Introduction: This chapter describes the motivation behind the thesis work, scope of the thesis and explains how the report is structured.

Chapter 2: Smart Grid: An Overview: Explains reasons behind the Smart Grid and relationship between Telecom Power Infrastructure and Smart Grid. This chapter also elaborates on the various driving factors and barriers in the implementation of Smart Grid.

Chapter 3: Power Quality in the AC Distribution Network: Literature review: Investigates the different power quality events in the LV/MV AC distribution grid with the help of available measurements and literature studies. It explains the impact of different loads and reasons behind the current harmonics & reactive power consumption in the AC distribution grid. Different methods are also analysed to address these challenges.

Chapter 4: Telecom sites in the AC Distribution Network: Describes the basic distribution model implemented in the MATLAB/SIMULINK® software package and provides the details about converters control schemes.

Chapter 5: Power Quality Improvement: Results and Discussion: Presents the results obtained from simulation of the test model. The results basically elaborate the improvement in the performance of the system regarding ancillary service provided by the Telecom sites.

Chapter 6: Grid Voltage Support: Presents the basic model for distributed wind power generation implemented in the MATLAB/SIMULINK® software package and explains the results obtained for the grid voltage support.

Chapter 7: Conclusion and Future Work: Concludes the thesis work by summing up the thesis and proposing some valuable suggestions for the improvement of work in future.

Chapter 2: Smart Grid: An Overview

Electric power grid is an interconnected network for delivering power from generating stations to the consumers. Today, most of the power plants use fossil fuels to generate electricity; Green House Gas (GHG) emissions from these power plants are causing global warming and have serious threats to the environment. Environmental changes and poor efficiency of conventional electric power system requires an electric grid which has better efficiency and a significant share of energy from renewable energy sources.

In this chapter, a new grid concept known as Smart Grid is introduced which ensures the reliable, efficient, secure and better quality of supply together with the integration of renewable energy sources and two way digital communication technologies. Visions of different nations towards the implementation of Smart Grid are presented. In addition to this, several driving factors and barriers for the deployment of Smart Grid are also briefly explained before summarizing the chapter.

2.1. Towards the Smart Grid

Generally, electricity has been generated far off places from the populated areas and is transferred to the consumers via transmission and distribution networks. Most of the European countries and USA's power infrastructure and the principles of operation for interconnected power systems were established before 1960s, before the emergence of extensive computer and communication networks [8]. This power infrastructure is now beyond its life and needs replacement and up-gradation which requires big investments and professional expertise. In many countries to meet the load demand, distributed generation has been delayed for up-to 10 years due to difficulties in obtaining rights of way and environmental permits. Therefore, in many cases, T&D lines are operating at their peak capacities [9]. When the overhead lines operate at their peak capacities, it is necessary to avoid thermal constraints. Thermal constraints are the ultimate limits of their power transfer capability. This leads to the reduction in the life time of the equipment and increasing incidents of the faults. Due to the passage of high current, the conductor lengthens, the sag of catenary increases and clearance to the ground is decreased which is not environmentally feasible and can cause personal damage [9], [10]. Moreover, the security of supply is not fully guaranteed in the traditional grid e.g. if a fault occurs, other than the disconnection of the faulty part, there is no solution and the supply to the customer is disturbed.

With the development of ICT, it has become possible to de-carbonise, control and modernize the existing power system at a realistic cost. For example capacity of lines can be increased by diverting the power flow through the less loaded lines; intelligent post fault reconfiguration can ensure the continuity of power supply and Demand side energy management can lead to voltage and frequency stability; Thus, heading towards the Intelligent Grid or Smart Grid.

Key drivers with some limitations for the implementation of Smart Grid will be explained later in the chapter.

Smart Grid is seen as an environment friendly and cost effective move towards green energy in all over the world. Many countries are encouraging this technology not only because of its vulnerability but also as an economic/commercial opportunity to develop new products and services. Here are some of the future visions from different parts of the world.

2.1.1. China

Although the concept of Smart Grid was introduced in 2007 in China; work was already being carried out to digitalize the power systems and it planned to reduce carbon emission per unit of GDP will reduce to 40%-45% by the end of 2020 as compared to 2008. Enormous attention has been paid by the government, commercial enterprises, manufacturers and research institutions, etc. to the Smart grid. The State Grid Corporation of China (SGCC) has released a medium long term plan for the development of Smart Grid as [11]:

“A Strong and robust electric power system which is backboned with Ultra High Voltage (UHV) networks based on co-ordinated networks at different voltage levels, supported by ICT, characterised as in formalized, automated and interoperable power system.”

2.1.2. USA

The US Department of Energy (DoE) has laid down the policy for the Perfect Power System project. State DoE in co-operation with the other companies plan to develop comprehensive solution to the loss in time and power outages. Perfect power system will incorporate micro grid technologies in the loop system to reduce the costly outages. It states that [12]:

“The perfect power system will include self-sustaining electricity infrastructure, an intelligent distribution system, onsite electricity production, Demand response capability, green buildings and technology ready infrastructure.”

2.1.3. The European Union

The Smart grid Technology platform of the Europe issues vision and progress every year for the Smart Grid in Europe. It states that [3]:

“It is vital that Europe’s electricity networks are able to integrate all low carbon generation technologies as well as to encourage the demand side to play an active part in the supply chain. This must be done by upgrading and evolving the networks efficiently and economically”

The goal is to reduce 20% less CO2 emission, 20% increment in the efficiency of the network and 20% increment in the use of renewable energy sources by the end of year 2020. It also aims to strengthen the grid including its extension to Offshore by developing a decentralized control scheme.

Norway

Norway produces electricity almost entirely from hydroelectric power plants and has signed Kyoto Protocol under which it agreed to reduce carbon emissions to no more than 1% above 1990 levels by 2012 [13].

The Smart Grid centre in Norway has the vision to modernize the national Grid with the help of ICT. A sketch of future smart grid has been proposed, according to this [14],

"Norway will deploy Smart Grid that will be effective, robust and environment friendly with the maximum share of renewable energy sources. Norway aims to contribute internationally for the development of Intelligent Grid for household, commercial and industrial consumers by sharing and providing services, products and expertise with the other countries."

In this master thesis, potential for the implementation of Smart Grid with the help of Telecom power infrastructure is identified by addressing various power quality issues in the conventional grid.

2.2. What is the Smart Grid

The concept of Smart Grid can be realized with the help of different Information & Communication Technologies (ICT), Power Electronics and Distributed Energy Resources (DERs). It is hard to find a particular definition for the Smart grid; every author, company, energy organization or stakeholder defines it in their own way. Some of the definitions are presented here:

US DoE defines the Smart Grid as [12]:

"A smart grid is a less centralized and more consumer interactive network that uses two way digital communication technologies to improve reliability, security and efficiency of the electric system, from the large generations through distributed generations and storage resources."

European Technology platform for the implementation of Smart Grid, states that [3]:

"A Smart Grid is an electricity network that can intelligently integrate the actions of all users connected to it; generators, consumers and those that do both; in order to efficiently deliver sustainable, economic and secure electricity supply."

National Institute of Technology (NIST) has its own understanding about the Smart Grid. NIST describes the Smart Grid as [15] :

"Smart grid uses two way digital data communication technologies with automated controls which allow the two way flow of information and electricity from generating stations to customers".

Author of [9] pays attribute to Smart Grid as; it manages the consumer demand and response data with the help of smart meters, smart appliances Distributed Generation (DG), and electricity storage by providing the dynamic pricing information of electricity. It encourages the consumers to adjust their load demands according to the pricing information available. Figure below summarizes the functioning of Smart grid [16].

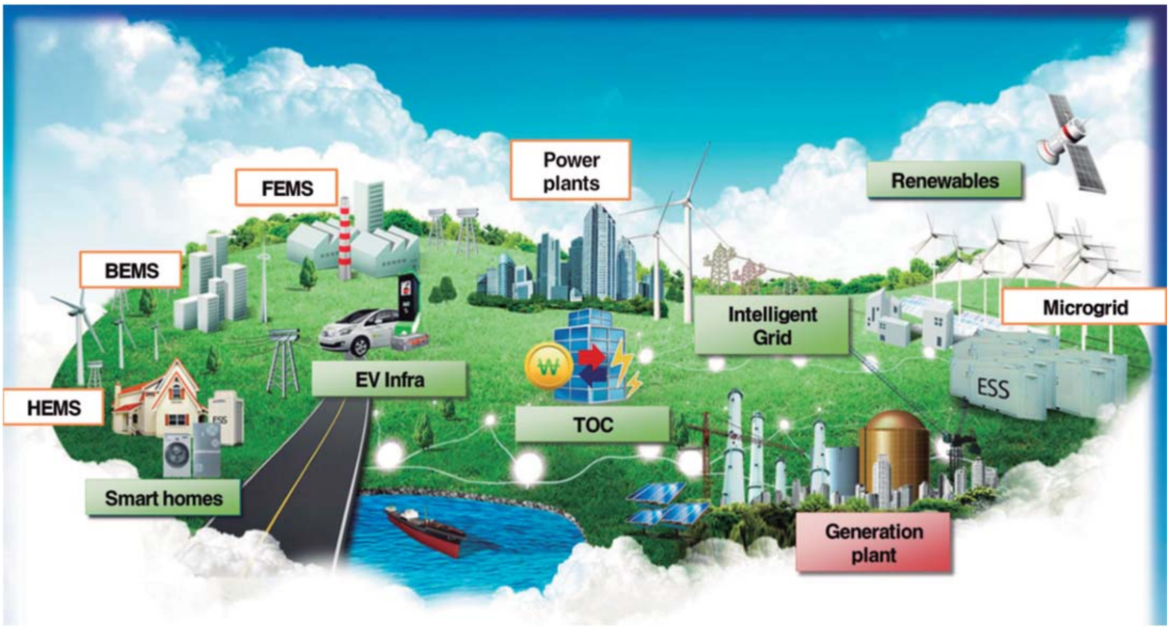

Figure 2. 1: Applications and Implementation of Smart Grid **[16]**.

In general, Smart Grid can be described stated as: A network of networks that uses ICT to control the flow of two way information and electric power on the network between utility companies and consumers for secure, efficient, reliable and economically feasible usage of electricity.

2.2.1. Smart Grid vs Conventional Grid

Smart Grid is an emerging technology and many countries are investing for its implementation. The UK, Germany, France and Italy are the leading investors. Only EU has invested about €1.8 billion up-to 2012 in 281 projects; Denmark is the most actively involved country in Research and Development (R&D) projects, spending the most per capita per kWh energy demand. It is therefore important to extract the fundamental differences between a conventional Grid and a Smart Grid; Author of [17] has identified some key differences, tabulated as:

	Conventional Grid	**Smart Grid**
System topology	Hierarchical	Multiple PF routes
System operations	Electromechanical	Digital
Communications	One-way	Two-way
Power generation	Centralized	Centralized & Distributed
Co-ordination mechanism	With few Sensors	With sensors Throughout
Monitoring	Blind	Self-Monitoring
Disturbance response	Manual Restoration	Self-Healing
Reliability	Failures & blackouts	Adaptive & Islanding
Maintenance operations	Manual check/Test	Remote Check/Test
Power flow control	Limited Control	Automated
Customer interaction	Few Customer Choices	Many customer choices

Table 2. 1: Differences between conventional grid and smart grid **[17]**

Table 2.1: has highlighted the key differences between Smart Grid and Conventional Grid. It explains that the power flow is bi-directional, communication is two way mechanisms and monitoring is self-monitoring in Smart Grid as compared to the blind monitored unidirectional conventional grid.

2.2.1.1. Technologies required for the Smart Grid

Power generation becoming more decentralized, system becoming more and more complex with millions of end points will require number of advanced technologies to control the overall system. Existing Energy Management System (EMS) and Supervisory Control and Data Acquisition (SCADA) will have to be integrated with Distribution Management System (DMS) and new application such as Advanced Metering Infrastructure (AMI) [9]. In addition to these, several other new security protocols need to be defined.

2.3. Distributed and Renewable Energy Resources

As described in the previous sections, in the traditional grid generation is centralized and power flows only in one direction with limited control. On the other hand, Smart grid enables the decentralized generation and two-way automated flow of power, which supports the idea of micro or large scale distributed power generation such as power from micro turbines, fuel cells, energy storage units, photovoltaic, wind and other renewable energy resources.

Reduction of CO2 and GHG emissions highly encourages the growth of renewable energy sources as DERs; only Europe tends to increase the share of renewable energy up-to 20% of its total consumption by 2020. DG allows the production of electricity by the utilities or the individuals, close to the point of power consumption, thus reducing the T&D losses, serving the utilities for peak shaving, lowering the over-all cost, improving reliability, reducing emissions and expanding the energy options [18]. Enterprises that specialize in ICT and electricity market are expected to benefit from the new market and business opportunities created by the integration of DERs.

2.3.1. Distributed Energy Storage

Un-predictable nature of renewable energy sources puts multiple stresses on the conventional grid. Fluctuating load demand and supply can be met with highly flexible conventional generation, automated power flow with ICT or with stored energy. Stored Energy is becoming a necessity with high penetration of renewable energy sources; In fact this is promising technology which can convert renewable power generation into dispatch-able generation for the utility companies.

Grid operators with access to hydropower can store energy by pumping water back to the reservoirs and use it when the demand is high. The countries with no or very little access to hydropower are looking for the other storage technologies e.g. Combined Heat and Power (CHP) plants, home heat pumps or EV batteries. Other storage technologies include Lead acid, Sodium Sulphur (NaS), Zinc Bromide, Lithium Ion and Nickel Cadmium batteries at distribution level. Lithium Ion is gaining its place in distributed energy storage system particularly in Electric Vehicles and Nickel metal hydrides are also becoming promising future options [9], [19]. **Appendix [A.1]** explains the benefits of different distributed storage technologies along with their limitations on Discharging cycles.

EV batteries can also be a better option for energy storage when the grids have excess of renewable power production.

2.3.2. Electric Vehicles (EVs)

The deployment of EVs and Smart Grid go hand-in-hand, making the grid more reliable and efficient. Electric transportation not only helps to reduce CO2 but also stores energy and facilitates the grid for ancillary services and peak shaving by providing energy back to the grid known as Vehicle to grid (V2G).

The number of EVs is increasing day by day; International Energy Agency (IEA) predicts the sale of EVs to reach up-to 3 million per year by 2020 and 8 million per year by 2035. Globally, Norway is the country with the largest EV ownership per capita in the world, with Oslo recognized as the electric car capital. EV car sales in 2012 represented a 3.1% market share of passenger car sales in the country, up from 1.6% in 2011 [20]. V2G vehicles are also expected to rise with the passage of time.

From 2015 to 2020, only V2G vehicle units are projected to grow from 103,900 to 1.06 million respectively. The compound annual growth rate is projected to increase by 59.0% annually, which gives rise to a big business opportunity globally e.g. by the end of 2020, V2G vehicle market value, V2G infrastructure market value, V2G technology market value and V2G total revenues are targeted to $26.6 billion, $6.7 billion, $10.5 billion and $2.9 billion respectively [21]. USA, China, Japan, Germany, UK and Denmark will be the largest business centres in future for V2G markets.

2.3.2.1. Electric Vehicles, Telecom sites, Utility Stations & Smart Grid

This is a modern era of Telecommunication in which exchange of information is done very fast with the help of internet and other electronic means. Mobile services provided by the different telecom companies, have data centres and communication sites at numerous locations of earth. Communication/Telecom sites are connected to the LV/MV distribution grids, deliver their services powered by the battery banks on these locations and these battery banks are charged from the grid supply. Battery banks placed at telecom sites behave same as that of V2G batteries and energy storage units at utility stations.

Co-ordinated and joint operation of these energy storage units can play a very important role in achieving the benefits of Smart Grid with the help of other technologies.

Even though, charging and discharging cycles of battery banks effect the battery life time but in rare cases they can be used. E.g. Norway has good standards of power quality and in case of short duration disturbances; the discharging of battery banks can be negotiated.

2.4. Active Distribution Grid

With the deployment of DG, Digital Communication Technologies, Power Electronics Technologies and other required principles of operation, the conventional grid will behave like a modern grid or Smart grid. Figure shows the schematics of such a distribution network known as active distribution network [9].

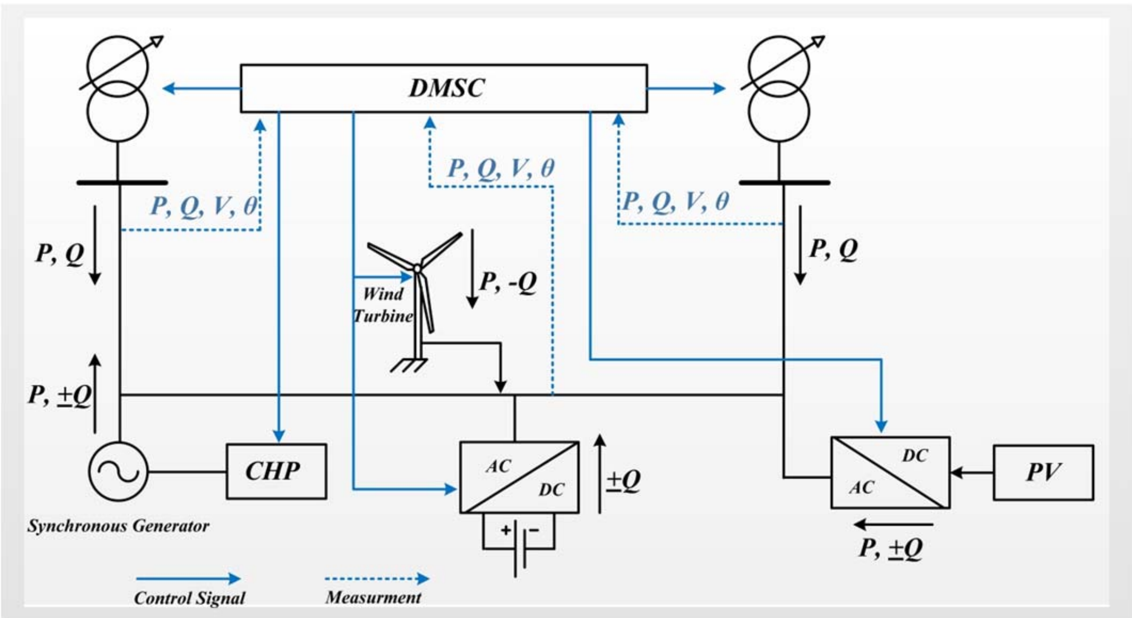

Figure 2. 2: Active Distribution Grid **[9]**

Figure shows a simple distribution network with DG. There are many features of this network enlisted below.

- Power flow is not unidirectional; rather it is bi-directional.
- The direction of power flows and the voltage magnitude on the network depend upon demand and supply of the network.
- DG give rise to fault currents and hence complex protection and co-ordination settings are required to protect the network.
- The reactive power flow in the network can be controlled independently.
- Many DGs connected with PE interface can inject harmonics in the network.
- Central control mechanism Distribution Management System Controller (DMSC) controls the over-all operation of the network.

In this master thesis, batteries at telecom sites will behave as DGs. A network model with proper control strategies for PE interfaces will be developed in which above mentioned features of Smart grid will be achieved. Development of control mechanism for DMSC is out of scope of this thesis work.

2.5. Barriers and driving factors for the Smart Grid

Adoption of the Smart Grid will enhance the features of the electric power system from generation, transmission, distribution levels to the consumption level. Policy makers and private sector is spending or encouraging to spend, billions of Dollars in this field. However, the day to day advancements in the technologies, regulatory changes and varying customer interests make it difficult for them to decide where to put money for the long term. Driving factors along with some barriers for the implementation of Smart grid in Europe are briefly discussed here.

2.5.1. Driving Factors

The growing population is driving an even greater increase in the demand of electricity. In addition to this, environment experts and governments are focusing on reducing the emission of CO2. The reduction of CO2 and increasing the share of renewable energy are the most important driving factors for the implementation of Smart Grid [22].

2.5.1.1. Environmental Considerations and the System Efficiency

With the growing population and electricity demand, an estimate of 1 GW power plants is needed every week for the next 20 years but according to an estimate; today, almost 80% of the primary energy is lost from generation to consumption by the consumer [23]. On the other hand, a significant amount of global electricity comes from thermal power plants and they are causing 17% of GHG emissions worldwide and it will continue to increase with the increasing energy demand; such an emissions cause global warming and contribute to negative environmental and health effects. These factors work as a driving force for the consumers, policy makers and the other state actors to embrace the renewable energy sources and focus on the power system efficiency.

The efficient handling of electrical energy have a much lower GHG emission reduction cost than investment in any power generating unit. Smart Grid technology and applications have potential to increase the efficiency of electricity distribution as well as the efficiency of electricity use in the household appliances [23]. This is a great incentive for policy makers, utility companies and other stakeholders to set precedence for the development of Smart Grid.

2.5.1.2. Security and Quality of Supply

Most of the countries in the world depend upon imported fossil fuels. Only Europe imports 53% of its total energy requirements in the form of gas and oil [1]. Addition of renewable energy sources, energy storage devices and efficient power system that will be achieved by the grid optimization; will make less dependent on imports. At the same time, up gradation of old fashioned grid and introduction of smart grid technologies will guarantee the more reliable electricity infrastructure and increase security & reliability of the supply.

Even though quality of supply in Europe is better than for example U.S, where the average annual duration of interruption in 2007 was 240 minutes with an average annual frequency of 1.5. However, Japan has the best reliability measures with average annual duration of interruption in 2007 was only 2 minutes with frequency of 0.05 [24]. DG together with energy storage system and Smart Grid technologies will help in power factor correction, peak shaving, and reduce losses & outages which cause significant losses to GDP.

2.5.1.3. Economic Benefits

According to an assessment, by 2050 the electricity price will go up by almost 50% if the Smart Grid is deployed. If not, the average electric bill will go up by almost 400%. Such trends inspire consumers to focus more on efficiency of the system and implement the Smart Grid technologies such as energy storage and Demand response management systems.

Moreover, with the deployment of Smart Grid, local renewable energy sources and consumer interaction, utilities can save a lot of energy and money by avoiding peak load. For example, Europe's five to eight per cent of the installed capacity is used for only one per cent of the time and is reserved for the peak demand but with the Smart Grid, 44% of the peak demand could be achieved with reduction of up-to €67 billion investment needed for the peak power plants. In this way maximum installed power generation capacity also could be used with the maximum limits of transmission and distribution lines [2].

In addition to these benefits, development of Smart Grid will also increase GDP and create jobs and business opportunities in the power sector.

2.5.1.4. New Technologies

Information and Communication Technologies (ICT) have developed a lot in the recent few years and the costs related to Grid connected ICT solutions are reduced considerably which makes the smart grid implementable. Moreover, according to [2] , electric vehicles, integration of increased power generation from renewable energy sources and CHP plants, depend upon each other as shown in and require the Smart Grid to become operational. Furthermore, battery storage technology and electricity generation from the renewable energy sources are also gaining efficiency to the point where power generation from PV and wind parks is almost cost-competitive with fossil fuels.

Beside all these driving factors, there are several advantages for the customers to adopt Smart Grid. For example with smart Energy Management System (EMS), it is possible for the customers to easily switch between different power suppliers and choose the suitable one. Additionally, consumers are more informed about the price of electricity with time which makes them more flexible to adjust their electricity bills.

2.5.2. Barriers for the Implementation of Smart Grid

Besides a number of drivers both for the network operators and customers, still there are some strong barriers in the implementation of concept of Smart Grid. High capital investments in the beginning, inconsistent policies, uncertainty about who will reap the benefits, resistant to adopt new technologies, different standards for different utility companies and less awareness about the advantages of Smart Grid to the customers are major concerns in implementing the Smart Grid. Some barriers are briefly discussed here.

2.5.2.1. Energy Policies and Regulations

Benefits of Smart Grid could be better achieved if it is adopted in a wide range but energy policies and rules & regulations in energy sector vary considerably. For example in some states, policies and incentives encourage power consumption rather than saving. On the other hand, in some states energy suppliers are responsible for the installation of smart meters; in others, grid operators are responsible. Some markets like Poland offer regulated tariffs, making customized pricing schemes difficult for the customers. On the other hand, markets like Germany, Sweden offer dynamic and customized tariffs schemes in which the pricing of electricity is different during day timings than night times.

Also, the policies and regulations were made for the traditional grids; taking Smart Grid into account, some changes should be made in the present policies and regulations in favour of clean renewable energy and customer interactions.

2.5.2.2. Market Uncertainty and technology Barriers

One of the bigger obstacles for the deployment of Smart Grid is expected financial decline for the utility companies. Electricity of €18.2 billion is projected to be produced by the residential customers in future only in Europe if the new technologies are applied. In this way, a new business model could replace the old fashioned conventional business model with more interaction of consumers and power producers.

The implementation of Smart Grid will require huge investments and stakeholders are doubtful about who will invest and who will reap the benefits. On the other hand, competition in electricity market doesn’t allow the utility companies to make electricity more expensive and invest some money in Smart Grid projects. That is why; Governments should come forward and support the stakeholders to come out of this situation in addition to provide incentives for the renewable energy sources.

On the other hand, operating costs of new technologies are still high in the early phases of deployment, resulting in long payback time and making the investors hesitant in this field [25].

Another important aspect of Smart Grid is the energy storage devices. A lot of developments have been made in this technology but charging a fairly efficient battery system is at best 70 to 80% efficient. Returning that energy back to grid includes DC power back to the AC grid with efficiencies of about 90% yields 63 to 72% energy return to system. This needs to be increased by increasing and making the cycles of battery banks more efficient.

2.5.2.3. Lack of Customer Involvement

Without customer awareness and involvement, it is not possible to introduce new technologies and concepts in the existing grid infrastructure. European consumers are getting more awareness about the need to reduce the use of fossil fuels and GHG emissions. They are also becoming familiar about the use of renewable energy sources and to improve the efficiency of the power system.

However, still there is a lot of work to do in order to engage more people and to create the positive awareness about Smart Grid among them. Besides providing them access to the modern communication tools as well. If the people are able to use electricity more efficiently by managing their daily routines, it will be a key success factor for the utilities that wish to embrace the opportunities of Smart Grid [2].

Summary

In this chapter, various complications in the conventional electric grid are highlighted and it is discussed that there is a need of new power grid infrastructure, equipped with renewable generation sources and modern two way communication technologies.

It is seen that how different countries e.g. USA, China and Norway are looking towards their future electric grids to reduce GHG emissions and to improve reliability, efficiency, security and quality of the supply by introducing renewable energy sources and new ICT respectively. It is also observed that the cost of improving efficiency of the whole power system is less than the investments on new power generation plants and the cost on the abatement of GHG emissions.

Smart Grid is a promising future technology that uses ICT and decentralized power generation to control the two way flow information and power between power plant and the consumer that enables the secure, efficient, reliable and economically feasible usage of electricity.

Implementation of Smart Grid is driven by various strong factors e.g. environmental & economic benefits can be obtained with cost effective new technologies for the secure and reliable supply of electricity.

Having all these benefits, still there are some serious challenges need to be addressed for the deployment of Smart Grid such as lack of customer interest and uncertainties about the energy markets.

Chapter 3: Power Quality in the AC Distribution Network: Literature review

The term *power quality* refers to a wide variety of electromagnetic phenomena that characterize the voltage and current at a given location on the power system [26]. AC distribution system supplies power in the medium voltage and low voltage networks. In this chapter several *power quality* events along with their possible reasons and solutions, are presented in terms of voltage characteristics in the distribution network. Measurements in the power system are used to classify different kinds of events. The events can be divided into three main categories [6].

- Fault related events:
  - Voltage Dips
  - Interruptions
- Switching related events:
  - Induction motor starting
  - Transformer saturation
- Non-linear loads related issues:
  - Current Harmonics
  - Reactive Power consumptions

3.1. Power System Event

A *power system event* is recorded or observed current or voltage excursion outside the pre-determined monitoring equipment thresholds. A *power disturbance* is a recorded or observed current or voltage excursion which results in an undesirable reaction in the electrical system [6], [27].

Terms event and disturbance are basically used to describe significant deviation from the ideal waveforms, these are measured by triggering on an abnormality in the voltage or current as shown in Figure 3.1 (a).

Transient voltage may be detected when the peak magnitude exceeds a specified threshold. *'rms'* voltage variations e.g. sag and interruption may be detected when it exceeds a specified level. While the term variations is used to describe small deviations from nominal values. These include normal *'rms'* voltage variations and harmonic distortion [28]. An example of steady state variation is given in Figure 3.1 (b).

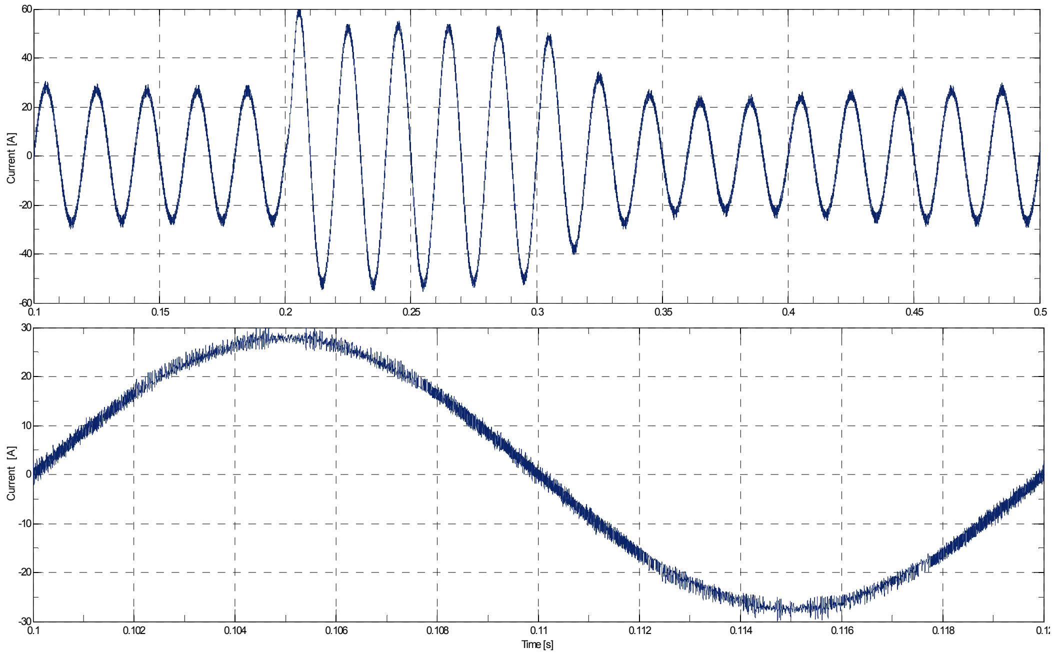

Figure 3. 1: Power System event and variations; (**a**) Power system event, (b) Harmonic distortion **[6]**.

Table 3.1 summarizes different categories of electromagnetic phenomena that may appear in the power system [26]. This classification is done on the basis of Spectral Contents, voltage magnitude and typical duration of these disturbances. Some of the reasons for a few disturbances are as:

- Impulsive transients are caused by lightning while switching actions like back to back capacitor switching cause the impulsive transients.
- Short duration voltage variations like voltage sags, swells, noise, etc. are almost always caused by fault conditions, the energization of large loads that require high starting current or intermittent loose connections in the power wiring.
- A large numbers of industrial, commercial and household loads using semiconductor devices e.g. VFDs, some of the household loads like computers, UPS, fluorescent lamps, etc. draw reactive power from the source, introduce harmonics into the network and cause waveform distortion.

For some of the electromagnetic phenomena listed in Table 3.1, the protection system will operate. For example during the fault on cable or line, the protection system will isolate that part of the network. The objective of the protection system is to disconnect the affected parts of Electric Power System in order to minimize any equipment damage, process outage costs and risks to the personnel [29]. However for some of the events protection system is not expected, for example the power electronic loads cause an increase in THD and power factor variation. Switching of large induction machines might cause an increase in load current and a voltage dip but normally no action is taken by the protection system [6].

Categories	**Typical Spectral Content**	**Typical Duration**	**Typical Voltage Magnitude**
1.0 Transients			
1.1 Impulsive			
1.1.1 Nanosecond	5 nsec rise	< 50 nsec	
1.1.2 Microsecond	1 µsec rise	50 nsec – 1 msec	
1.1.3 Millisecond	0.1 msec rise	> 1 msec	
1.2 Oscillatory			
1.2.1 Low Frequency	< 5 kHz	0.3 – 50 msec	0 – 4 pu
1.2.2 Medium Frequency	5 – 500 kHz	20 µsec	0 – 8 pu
1.2.3 High Frequency	0.5 – 5 MHz	5 µsec	0 – 4 pu
2.0 Short Duration Variations			
2.1 Instantaneous			
2.1.1 Sag		0.5 – 30 cycles	0.1 – 0.9 pu
2.1.2 Swell		0.5 – 30 cycles	1.1 – 1.8 pu
2.2 Momentary			
2.2.1 Interruption		0.5 cycles – 3 sec	< 0.1 pu
2.2.2 Sag		30 cycles – 3 sec	0.1 – 0.9 pu
2.2.3 Swell		30 cycles – 3 sec	1.1 – 1.4 pu
2.3 Temporary			
2.3.1 Interruption		3 sec – 1 min	< 0.1 pu
2.3.2 Sag		3 sec – 1 min	0.1 – 0.9 pu
2.3.3 Swell		3 sec – 1 min	1.1 – 1.2 pu
3.0 Long Duration Variations			
3.1 Interruption, Sustained		> 1 min	0.0 pu
3.2 Under Voltages		> 1 min	0.8 – 0.9 pu
3.3 Over Voltages		> 1 min	1.1 – 1.2 pu
4.0 Voltage Unbalance		Steady state	0.5 – 2 %
5.0 Waveform Distortion			
5.1 DC Offset		Steady state	0 – 0.1 %
5.2 Harmonics	0 – 100th H	Steady state	0 – 20 %
5.3 Inter-harmonics	0 – 6 kHz	Steady state	0 – 2 %
5.4 Notching		Steady state	
5.5 Noise	Broad band	Steady state	0 – 1 %
6.0 Voltage Fluctuations	< 25 Hz	Intermittent	0.1 – 7 %
7.0 Power Freq. Variations		< 10 sec	

Table 3. 1: Summary of different electromagnetic phenomena with their spectral contents, time duration and magnitude **[6]**.

3.2. Benefits of Power Quality Monitoring

There are several benefits for monitoring *power quality* both for customers and the utilities; in fact they share similar benefits. The most important reason for *power quality* monitoring is the economic damage produced by electromagnetic phenomena in critical loads. On the other hand it also helps in the identification of problem conditions, prioritize system improvements and access overall performance of utility and customer power systems [30]. There are several other aspects of solving such problems which include the technological and non-technological solutions.

Monitoring requires an investment in equipment, time and education. In many cases management, production and plant engineers must be sufficiently convinced of the benefits of monitoring. Author of [31] has justified the investment in monitoring by its increased availability due to the following:

- Improvement in the availability of the power.
- Preventive and predictive maintenance.
- Determining the need for mitigation equipment.
- Ensuring Equipment performance
- Sensitivity assessment of process equipment to disturbances.

In short, monitoring is an essential component of the customer care process for his business. It can help to identify *power quality* problems, minimize losses in the power system and increase the reliability. In this master thesis technological solutions will be provided for some of the power *quality problems* in the distribution network.

Data Collection

Data presented in this chapter is on voltage and frequency, taken from some of the measurements and literature studies. These measurements come from
SINTEF Energy Research, SINTEF is a Norwegian research Organization.

3.3. Overvoltage/Voltage Swell

In general three phase source is used to supply single phase loads in commercial, industrial and big residential buildings, which is divided equally in all three phases. Single phase load is connected between one phase and neutral. When a single phase to ground fault occurs, other two phases are subjected to phase to phase voltage with respect to earth. It means an overvoltage or voltage swell will appear on other two phases and it will be sustained until the fault is cleared. Voltage swell is defined as [26]:

"Sudden increase in the supply between 110% and 180% of the nominal value for the duration of 10 milliseconds to 1 minute"

Voltage swell is caused by switching off a large inductive load, single line to ground fault and energizing the large capacitor banks, etc. Figure 3.2, shows the measurement for a voltage swell due to single line to ground fault in the system.

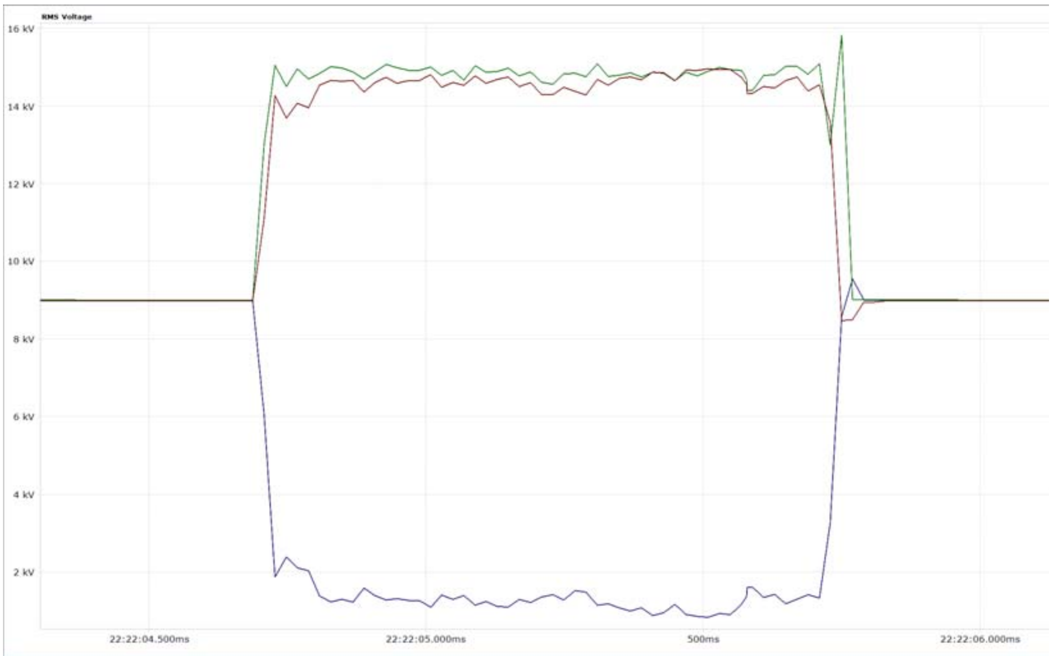

Figure 3. 2: Measurement for Voltage swell due a to single line to ground fault

It is shown in the Figure that a single line to ground fault occurs at time 4.5 sec. and continues till 5.5 sec and the swell on the other two phases remains for almost 1 sec. During fault, voltage on fault line drops to 1.5 [kV] while on the other two phases, it goes to about 15 [kV].

3.4. Voltage Dip

Voltage Dips are one of the major *power quality* concerns that customers have to face since sensitive equipment like PCs, digital control systems and electronic devices have been widely used in industrial and residential facilities [32]. According to European standard EN 50160,

"Temporary reduction of the voltage at a point in the electricity supply system below a specified start threshold is known as voltage dip."

The largest (with respect to deviations in per cent) and most seriously voltage dips are mainly due to short circuits in the network. In addition to this, automatic reclosures against permanent faults and connections of large loads in weak distribution systems are also major sources of voltage dips [33]. For the purpose of this standard start threshold is equal to 90% of the reference voltage and duration is from 20ms up to and including 1min depending upon the operating time of protection devices during fault.

3.4.1. Voltage dip magnitude

Voltage dip can be characterized by its magnitude and the duration; sag/dip magnitude can be defined as the minimum '*rms'* voltage during the event and the duration is the time that the *'rms'* remains below the threshold [34]. Effects of the voltage dip can be experienced by the sensitivity of the equipment while magnitude can be calculated at the point of common interest in the radial system and it depends upon the type and resistance of the fault as given by the equation 3.1. Figure 3.3(**a**), shows the schematics for a fault on a radial distribution system.

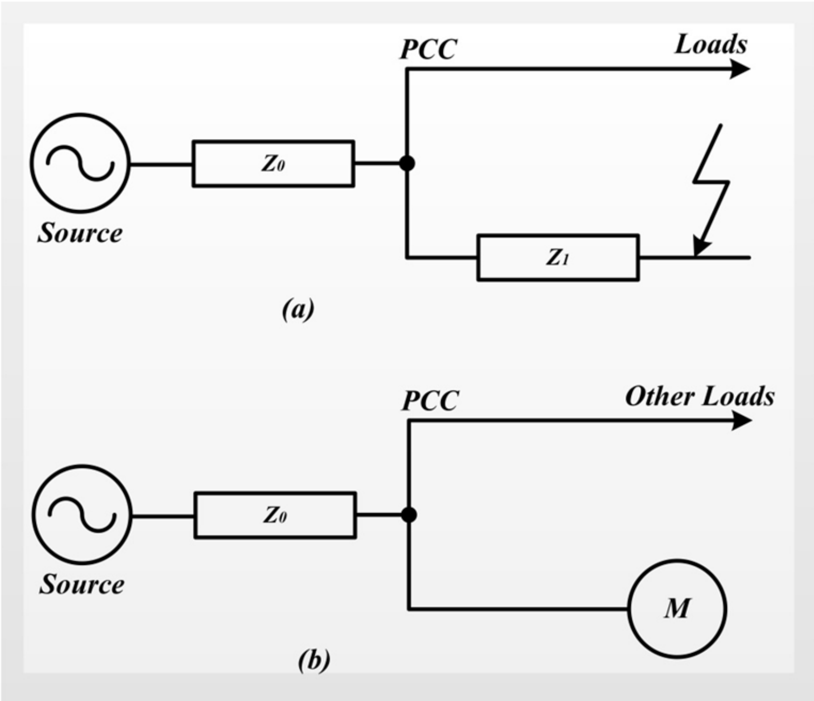

Figure 3. 3: Fault on radial system: (**a**), fault on lines. (**b**), Induction motor starting

Z_0 is the source impedance and Z_1 is the impedance between fault and PCC. The dip magnitude at the load position is the same as that of PCC and is given as:

$$V_{dip} = \frac{Z_1}{Z_0 + Z_1} E \tag{3.1}$$

where

'E' is the source voltage.

3.5. Reasons behind Voltage Dips

Short circuits in the power system have been an essential field of interest due to their importance for the stability of the power system. They are one the main sources of voltage dips. A detailed analysis on different reasons behind voltage dips is given below:

3.5.1. Symmetrical/Asymmetrical Faults

Symmetrical and Asymmetrical faults in the power system are the major reasons behind voltage dips. In symmetrical three phase faults only positive sequence impedance is needed and in Asymmetrical faults, positive, negative and zero sequence impedances are required [35]. Figure below shows the representation of three phase fault and single line to ground fault:

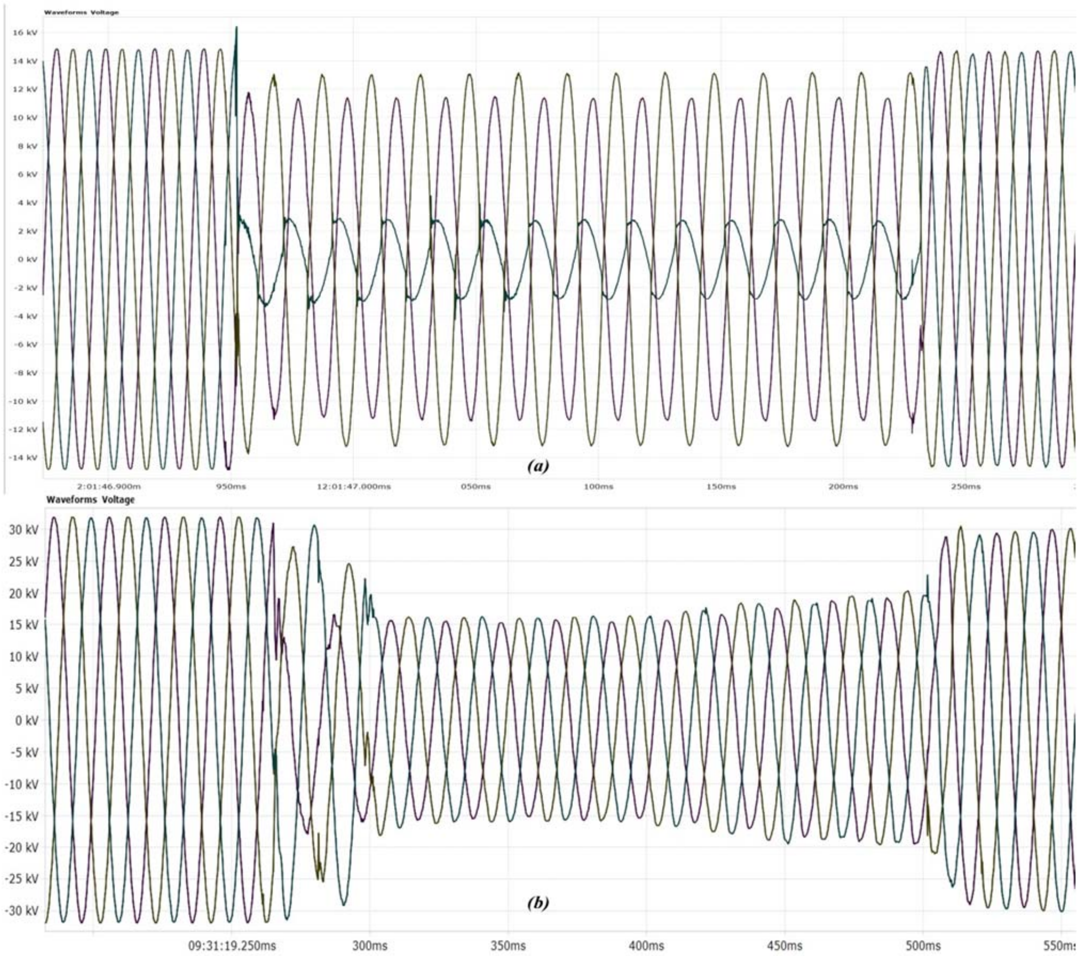

Figure 3. 4: Measurements for Voltage dips due to faults: (**a**), Voltage dip for symmetrical fault. (**b**), Voltage dip for asymmetrical fault

Figure 3.4(**a**), is the representation of voltage dip caused by an asymmetrical fault at PCC. It shows that three phase fault clearing time is 300ms. This is shown that when fault occurs, three phases are not symmetric any more and each phase has different voltage magnitude.

Figure 3.4(**a**), shows that three phase fault occurs at time t=19.250 sec. and the clearing time is 270 msec. It is clear that the voltage returns to normal after fault clearing operation. It is also shown that all three phases forms symmetrical shapes, fault clearing is fast and it forms a rectangular shape when compared to fundamental voltage magnitude.

3.5.2. Phase angle jump

In Asymmetrical faults phase angle jump depends upon *'X/R'* ratio, if *'X/R'* ratio of source and feeder are equal than phase angle jump is zero and vice versa. Author of [6] has made a statistical analysis on phase angle jumps of rectangular voltage dips. The recordings were made for a medium voltage network (33kV and 11kV) over a one month period. Analysis contains the phases that present a voltage dip of magnitude larger than 0.10 pu. Figure 3.5, shows the graphical results for the analysis. It can be seen that more negative values than positive values.

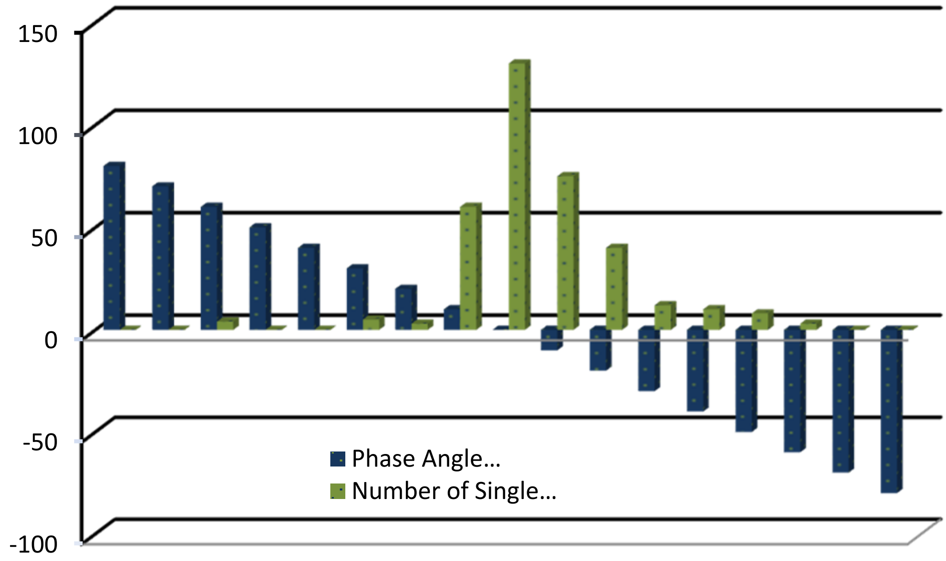

Figure 3. 5: Phase angle jump analysis **[6]**.

Figure shows that there are more negative values than positive values.

3.5.3. Earth Faults

Faults like earth faults might disappear before any protection operation starts due to the self-extinction of the fault due to zero crossing of the fault current. This more likely happens in reactance grounded systems [36]. The event causes a short duration voltage dip accompanied by an overvoltage on healthy phases, low fault current, slow voltage recovery and an oscillatory zero-sequence voltage [37].

There is another kind of voltage dips known as multistage dips. Multistage stage dips are due to the faults but they present different magnitude levels before they come to the pre-fault value. Analysis of measurements showed that about 20% of the measured voltage dips are multistage dips. These steps in the multistage dips are either due to the changes in system configuration or due to the nature of the faults. A measurement for mutstage voltage dip is given in the **Appendix [B.1].**

3.5.4. Induction motor starting

Starting of induction motors is also one of the reasons for voltage dip in the network. Induction motor draws five to six times more current than the normal value, when it starts. This current remains high until motor doesn't come to normal speed and it continues from several seconds to one minute [38]. Large amount of starting current causes a voltage dip in the system and this voltage dip depends upon the system parameters. However, soft starters can be used to start the motor but it is an expensive method. For the system given in the Figure 3.3(**b**), magnitude of voltage dip at Point of Common Coupling (PCC) can be written as:

$$V_{dip} = \frac{Z_M}{Z_0 + Z_M} E \tag{3.2}$$

Where 'E' is the source voltage, 'Z_0' is source impedance and 'Z_m' is the motor impedance.

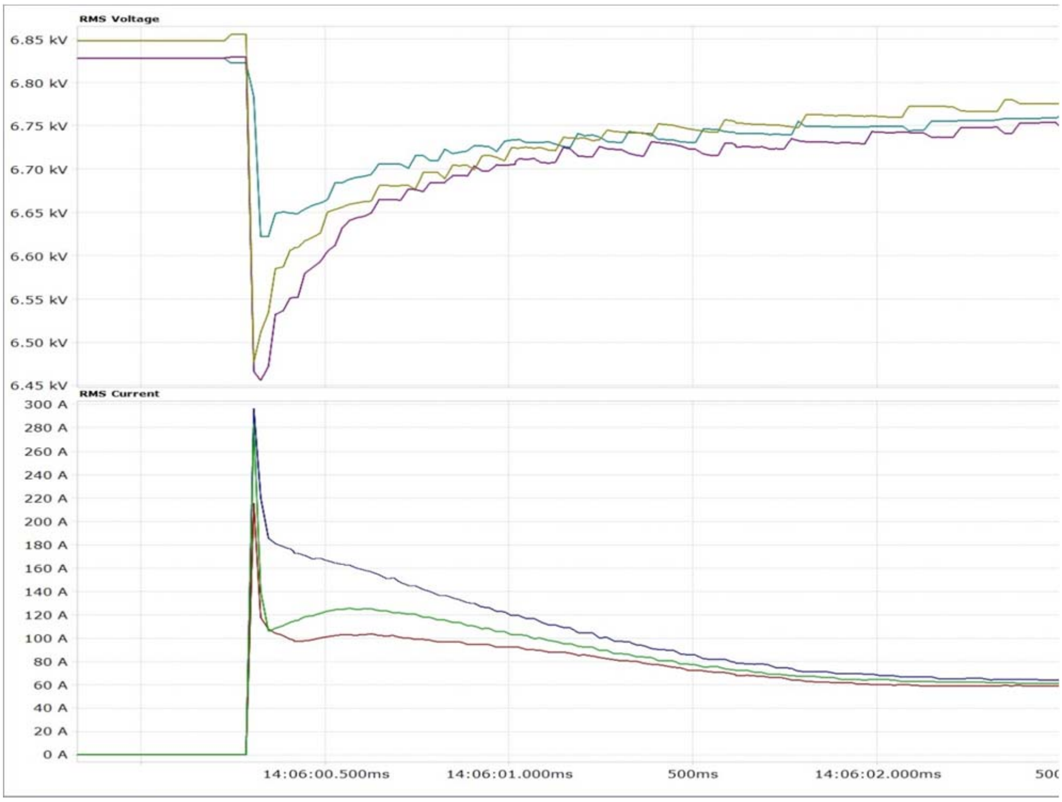

Figure 3. 6: Measurements for motor start: (**a**), Voltage dip. (**b**), Starting current

Figure 3.6 shows the measurements for motor start. Figure 3.6(a), shows that when motor starts at time t=0.500ms the voltage drops down to 6.45[kV] from 6.85[kV]. And it draws a significant amount of starting current e.g. it is shown in the Figure that the starting current of motor rises to 300 [A] but after 1.2 sec. it starts drawing normal current i.e. 80 [A].

3.6. Non-fault Interruptions

There are many other interruptions that are not caused by the faults, for example opening of lines for the maintenance purposes also cause interruption in the supply voltage. Switching of different components in the power system cause interruption in the supply voltage but they exist for few moments. Some of the switching actions include:

- Energizing of the feeder
- Load switching
- Reactive power compensation switching

The details of these measurements are well explained in [6] but most frequent and interesting measurements have been discussed and analysed.

3.7. Current Harmonics

Source current waveform distortion is due to the presence of harmonics. Harmonics have always been present in the power system. Recently due to the widespread of PE switching devices presenting non-linear loads, have extensively increased, resulting in an increase in their magnitude. Non-linear nature of the rectifier's load cause harmonic pollution in power distribution systems. Harmonic is defined as [39], [40]:

"A harmonic of a wave is a component frequency of the signal that is an integer multiple of the fundamental frequency i.e. if fundamental frequency is f, the harmonics have frequencies 2f, 3f, 4f, etc."

Harmonic number is the harmonic frequency; the first harmonic is the fundamental frequency (50 Hz in this case), the second harmonic is the component that is two times the fundamental frequency and so on. Figure 3.7 shown below, differentiates between second, third and fourth harmonic components compared to the fundamental frequency component.

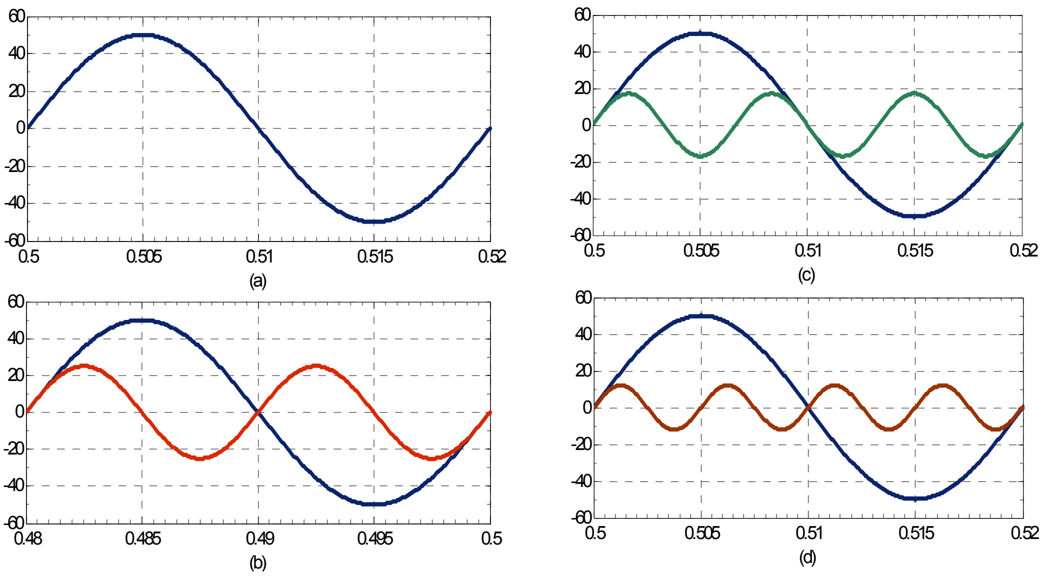

Figure 3. 7: Harmonic Components compared to fundamental component: (**a**), Fundamental frequency component. (**b**), Fundamental and second harmonic components. (**c**), Fundamental and third harmonic components. (**d**), Fundamental and fourth harmonic components **[40]**.

3.7.1. Decomposition of Distorted waveforms

The ratio of harmonic frequency to the fundamental frequency is harmonic order, waveforms containing different order harmonics are not purely sinusoidal in nature, and rather they are distorted waveforms. Mathematically, these distorted waveforms can also be decomposed into various components with the help of Fourier analysis.

Fourier analysis establishes a relationship between a function in time and frequency domains. Mathematical relationships are given as [41]:

$$f(t) = F_o + \sum_{h=1}^{\infty} f_h(t) = \frac{1}{2}a_o + \sum_{h=1}^{\infty}\{a_h \cos(h\omega t) + b_n \sin(h\omega t)\} \quad (3.3)$$

where

f (t)= non-sinusoidal periodic function

$F_o = \frac{1}{2} a_o$ = *average value of the function f (t)*

$a_o = \frac{1}{2\pi} \int_0^{2\pi} f(t) d(\omega t)$

ω= 2π/T, 'T' is the periodic function of the function f (t) and T=1/f

f= frequency

a_h and b_n are series co-efficient that can be determined a:

$$a_h = \frac{1}{\pi} \int_0^{2\pi} f(t) \cos(h\omega t) d(\omega t); \qquad h= 1,2,3,4,,,, \tag{3.4}$$

$$b_h = \frac{1}{\pi} \int_0^{2\pi} f(t) \sin(h\omega t) d(\omega t); \qquad h= 1,2,3,4,,,, \tag{3.5}$$

Therefore, the Fourier series can be expressed as:

$$f(t) = F_o + F_{m1} \sin(\omega t + \phi_1) + F_{m2} \sin(\omega t + \phi_2) + ... + F_{mh} \sin(\omega t + \phi_h) \tag{3.6}$$

where

F_0= DC component

F_{m1}= DC maximum value of fundamental component

F_{m2}= DC maximum value of 2^{nd} order harmonic component

F_{m3}= DC maximum value of 3^{rd} order harmonic component

F_{mh}= DC maximum value of 'h' order harmonic component

ω= angular frequency

Φ_1= phase shift of fundamental component

Φ_2= phase shift of 2^{nd} order harmonic component

Φ_h= phase shift of 'h' order harmonic component

3.8. Parameters of Harmonics

Some harmonics are part of the power system and some are generated by the switching of power electronic devices. Order of harmonics generated by the switching power devices is given by:

(2n ± 1), where ‘n’ is the phase order.

These harmonics are known as characteristic harmonics, and those which are already part of the electrical system, are known as non-characteristic harmonics [42]. Any harmonic component can be represented by as a percentage of the fundamental or a percentage of the *‘rms’* value of the total current, with the formula:

$$I_h = 100\frac{I_n}{I_1} \tag{3.7}$$

where

I_h *= amplitude of current harmonic ‘h’*

I_n *= amplitude of current harmonic ‘n’*

I_1 *= amplitude of fundamental current harmonic component*

For the harmonic voltages same approach is used. The ratio of the *‘rms’* value of the sum of all harmonic components up to a specified order to the *‘rms’* value of the fundamental component is known as Total Harmonic Distortion (THD) and can be represented as:

$$THD = 100\sqrt{\sum_{n=2}^{\infty} I^2{}_h} \tag{3.8}$$

This can also be written as:

$$THD = 100\sqrt{\sum_{n=2}^{\infty}\left(\frac{I_n}{I_h}\right)^2} \tag{3.9}$$

These parameters are used for LV, MV and HV applications.

3.9. Measurement

In power system, harmonic analysis is used to determine the impact of harmonic producing load on a power system. The main Harmonic analysis method used by the measurement devices is the Fourier Transform (FT) and its modifications and improvements. This method can be applied to an arbitrary function, both periodic and non-periodic functions. Its special case is a periodic function whose spectrum is discrete and its lines are components: the fundamental and the harmonic [40].

Discrete Fourier Transform or Fast Fourier Transform (DFT or FFT) analysis is a digital application of classical Fourier analysis. The use of digital method is significant because the PWM *‘On’* and *‘Off’* times are quantized to evenly spaced and well defined time intervals. In contrast, *‘On’* and *‘Off’* times produced by the equivalent analogue method vary continuously and are not quantized. In practice, for FFT analysis, the signal is analysed in a limited time interval *‘Tw’* by using limited number of samples *‘M’* of the actual signal. FFT analysis with its detailed working principles, advantages and limitations has been well explained by the author of [40]. Figure 3.8, below shows harmonic analysis using FFT approach of a current waveform. Where *'Tw'* is taken is (1.5-1/50) second and *'M'* is selected as 2000 samples.

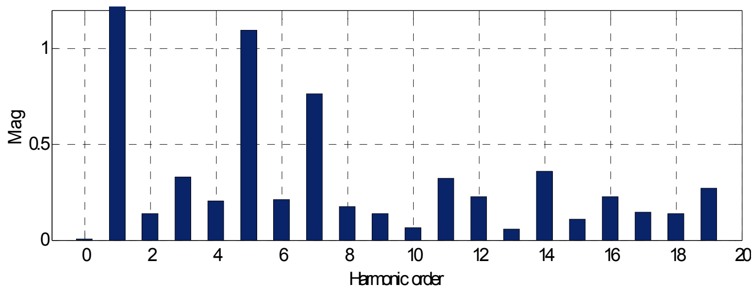

Figure 3. 8: FFT Analysis of a current waveform

3.10. Sources of Current Harmonics

In the power system, sources of current and voltage harmonics can be divided into three categories.

- Magnetic core equipment, like transformers, generators, etc.
- Fluorescent lamps, arc furnaces, welding equipment, etc.
- Electronic and power electronic equipment.

3.10.1. Magnetic Core equipment

Transformers are the first source of harmonics in the history of power system. The non-linearity between magnetizing force and flux density is shown in the magnetization curve in the Figure 3.9.

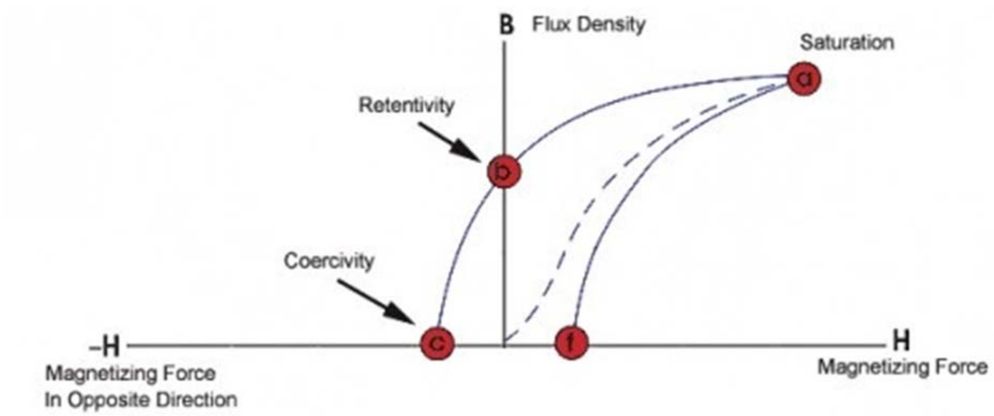

Figure 3. 9: Non-linearity between magnetizing force and flux density **[40]**

Figure shows that the relationship is strongly non-linear and its location within the saturation region causes distortion of the magnetizing current. Transformers are designed so that the magnetizing current doesn't increase more than 1-2% of the nominal current. As a result, even if the large numbers of transformers are operating, they are not the major cause of harmonics. In transmission systems, *Y/Y* connected transformers are used; with this winding connection they may cause significant distortion in the supply current. On the other hand, *delta/Y* connection guarantees a low impedance delta connected circuit for the third harmonic. Therefore, this harmonic doesn't distort the secondary voltage waveforms. In distribution networks, *delta/Y* transformers are commonly used. In the same way, motors can also generate harmonic currents in order to produce a magnetic field. Their contribution however is very small due to much more linear characteristic of the air gap as compared to the transformers.

3.10.2. Arc Furnaces and Fluorescent lamps

Distortion in the voltage and current waveforms due to arc furnaces is of significant importance because of their common use and large in comparison to the short circuit capacity at the point of connection. It is found that the arc at electrode is basically a voltage clamp with a trapezoidal shape. The highest level of the current distortion occurs during melting phase; however it is much lower in the other phases. Fluorescent lamps have poor power factor and high THD; they are not a major problem for the *power quality* as long as they don't constitute an enormous amount of the distributed load [43]. However, the traditional filament lamps are being replaced by Compact fluorescent lamps (CFLs) with good power factor and low THD.

3.10.3. Power Electronic Equipment

With the advent of the power electronics, large numbers of industrial, commercial and household loads are becoming non-linear loads, e.g. some of the household loads; computers, UPS, etc. are not linear loads. Induction motor load, the main load of industry is now equipped with a rectifier and inverter for the purpose of achieving adjustable speed control. These non-linear loads have resulted from the proliferation of power electronic converters using semiconductor devices such as diodes, Thyristors Insulated Gate Bi-polar Devices (IGBTs), Gate Turn-off Thyristors (GTOs) and so on. These solid state switching devices have quick response in controlling their voltages and currents but drawbacks of using these are: they may draw significant amount of harmonics and reactive power from the grid [44]. Two types of switching devices are described as:

3.10.3.1. Switched Mode Power Supplies SMPS

With the rapid development of PE and semiconductor technology, switching power supplies are used in almost all applications with output power level above one watt including communication equipment, data centres, and computers and so on [38]. The main difference in these devices from the older units is in the lack of transformer and rectifier; these are replaced by direct controlled rectification of the supply to charge the capacitor from which load is fed.

Several advantages like size, cost and reduced weight can be achieved with these SMPS. But there is a disadvantage for using such devices e.g. they draw pulses of current instead of continuous current which causes third order and higher order harmonics in the source current. Figure 3.10 above shows the voltage and current waveform drawn by one of the single phase rectifier.

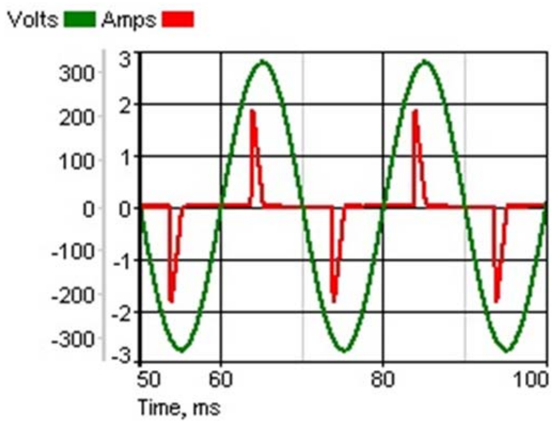

Figure 3. 10: Voltage and current waveform drawn by single phase rectifier **[45]**

3.10.3.2. Three phase rectifier

Equipment containing static converter like large UPS units are based on three phase bridge converters. These bridge converters produce harmonics of the order of *(6n $\pm$ 1),* which means one more and one less than each multiple of six. The magnitude of harmonic should be equal to the reciprocal of harmonic order which means there would be 20% of the 5th harmonic and 9% of the 11th harmonic [40]. Figure below 3.12 shows the current waveform drawn by the three phase bridge rectifier along with the phase voltage. FFT analysis has provided the harmonic analysis of the current drawn by the rectifier.

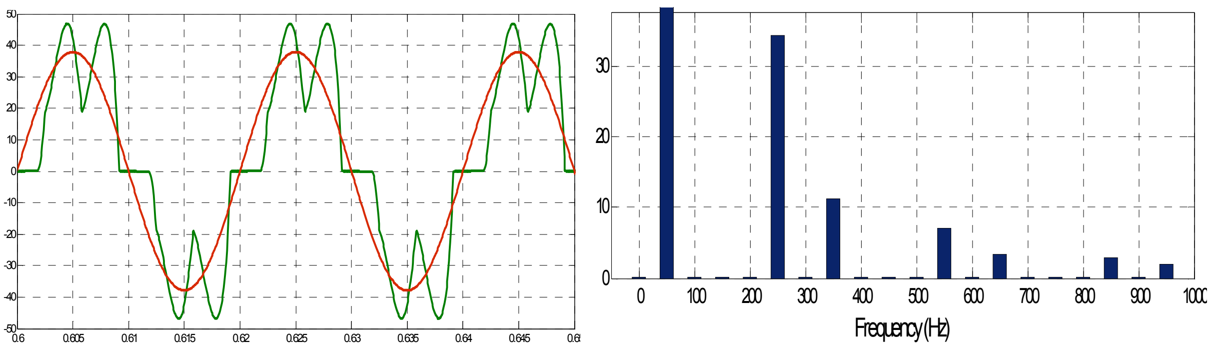

Figure 3. 11: Phase ‘a’ representation of three phase rectifier current and FFT analysis

3.11. Problems associated with Harmonics

Harmonics create many problems in the power system. Various standards and guidelines have been established that specify limits on the magnitudes of harmonic current and harmonic voltage distortion at various harmonic frequencies. These limits are given in the **Appendix [B.2]** [38]. Authors of [40], [44] and [38] have very well explained the Details about the problems associated with Harmonics, some of them are listed and briefly explained here.

- Harmonic components current/voltage, induce high frequency magnetic flux in motors and in the cores of transformers, which results in high losses and overheating of these machines.
- Capacitors can generally be used for power factor correction. If the combination of line reactance and capacitor has a resonance at the same frequency as harmonic

current generated by non-linear load, an over current may flow through the capacitor which causes the overheating of the capacitor.

- Harmonic current can cause the voltage waveform distortion that can interfere with the operation of the other electronic devices.
- If the frequency spectra generated by non-linear loads is below the line frequency, this may cause flicker in the supply voltage which is a very uncomfortable effect for the eyes of people.

3.11. Reactive Power Consumption

Reactive power impact is main reason for the voltage fluctuation that can easily lead to electrical devices actions, malfunctions and damage, and thus further leads to large economic losses. It is a common phenomenon which is observed when the loads such as motors, mills and PE loads are connected to the grid. The impact is shorter, bigger and appears frequently in the LV/MV networks [46]. Several sources of reactive power are mentioned in the literature, some of them are briefly discussed here.

3.11.1. Generators

Conventional electric power generators supply active power. Additionally a generator also supports voltage by producing reactive power when over-excited and absorbing reactive power when under-excited. Reactive power is continuously controlled. The ability of generator to provide reactive support depends upon its ability to produce active power. Author of [47] explains the methods and limits for a generator to produce active and reactive power with the help of respective graphical analysis.

3.11.2. Power transfer components

Interfaces and Power transfer components are also one of the main sources for producing the reactive power which include transformer, transmission/distribution lines, converters, etc. These are briefly discussed as:

3.11.2.1. Transformers

Transmission & Distribution transformers are designed to operate in their linear region. However, with the flow of low frequency currents such as Geo-magnetically Induced Current (GIC), the operating point is shifted slightly into the saturated region. This shift reduces the effective core impedance and causes a corresponding increase in the reactive power absorbed by the transformer. Absorbed reactive power increases when core becomes saturated with the low frequency current components. It is also observed that reactive power due to low frequency currents for a given transformer is linear and constant which varies between 0.05-0.2 p.u. [48].

3.11.2.2. T&D Lines and cables

T&D lines and cables generate and absorb reactive power at the same time, are given by:

$$Q_{gen} = V^2 B \tag{3.10}$$

where

B= shunt susceptance

$$Q_{con} = I^2 X \tag{3.11}$$

where

X=line/cable reactance

In this master thesis, line capacitances are neglected due to short distance between the load and the source. Line reactance is taken as a parameter for absorbing the reactive power.

3.11.2.3. PE Converters

The line voltage, the line frequency commutated converters operate at lagging power factor and hence draw reactive power from the Grid. It is given by the equation 3.12 [38].

$$Q = 1.35 V_{LL} I_d \sin\alpha \tag{3.12}$$

where

α= firing angle

For the desired real power transfer, the reactive power should be minimized as much as possible. Similarly 'I_d' should be kept as small as possible to minimize 'I^2R' losses.

PE Converters connected in distribution system draw reactive current which causes the poor power factor and reactive power to increase and hence the real power transfer to decrease. The apparent power drawn from the grid is given by [44]:

$$S_{3\phi} = 3VI\cos(\phi_v - \phi_i) + j3VI\sin(\phi_v - \phi_i) \tag{3.13}$$

where

$P = 3VI\cos(\phi_v - \phi_i)$

$Q = j3VI\sin(\phi_v - \phi_i)$

Equation 3.13 shows that for constant grid supply, the real power will decrease with an increase in the reactive power drawn by the load and the lines reactance.

3.11.3. Reactive Loads

Voltage characteristics are closely related to the load characteristics. The reactive power consumption or generation by the connected loads has great impact on the voltage profile. The response of loads to voltage changes, have large effect on stability. For the transient voltages, dynamics characteristics of induction machines are very important, briefly discussed as:

3.11.3.1. Induction motors

Electrical motors consume around 55% of the total consumed energy in which 96% of energy consumption goes to induction motors. Around 67% of the total induction motors are below 55 kW which shows that 85% of the energy loss is dissipated in these motors [49]. The active power drawn by the motors is independent of the voltage levels while reactive power is more sensitive to the voltage levels. As voltage level drops reactive power decreases first and then increases as the voltage drops further.

3.11.3.2. Induction Generators

Wind power generation is increased on large scale in the recent few years due to increasing emphasis on renewable energy. Recent study on wind power generation shows that the induction wind generator systems have been widely used because of their advantages over the synchronous generators such as smaller size, lower cost and lower requirement of maintenance [49]. However induction generators require significant amount of reactive power which is usually supplied by the capacitor banks connected at the terminals of the turbine but in case of faults on T&D lines and cables, the reactive power is drawn from the network which can lead to low voltage and further losses in the network. There are some other loads which also absorb the reactive power such as discharging lights, arc furnaces; Constant Power loads (CPLs), etc.

3.12. Reactive Power and Harmonics Compensation

The reactive power change together with harmonics has the most adverse effect on the voltage regulation [38]. Reactive power is managed to improve overall performance of the AC grid with the help of several compensation techniques. Reactive power and harmonics compensation should

- Improve the system power factor to balance the real power drawn from the supply, compensate voltage regulation and eliminate the current harmonic components produced by large and fluctuating non-linear loads.
- Stabilize and improve the capacity of system by increasing the maximum active power flow. It should also maintain the regulated voltage at all voltage levels.
- Reduce voltage fluctuation and keep the voltage within standard limits by providing the voltage support via reactive power compensation techniques.
- Optimize the system losses.

3.13. Reactive Power and Harmonics Compensation Techniques

The reactive power can be compensated with VAr generators connected either in series or parallel configuration. Series and shunt VAr compensation alters the neutral characteristics of the system e.g. series compensation modifies the T&D system parameters while shunt compensation changes the impedance of the load. The overall objective of reactive power and harmonics compensation is to improve the performance of AC system. Some of the compensation methods can be categorized as:

3.13.1. Fixed or mechanically switched capacitors

Leading current characteristics of capacitors make the realization of reactive compensation. The amount of leading current or size of capacitor bank depends upon the lagging current drawn by the load. In case of widely fluctuating loads, the amount of reactive power also varies and fixed capacitor may lead to either over compensation or under compensation. In this situation, compensation is achieved by switched capacitors and switching is achieved by relays and circuit breakers [50]. But switching actions have disadvantages, for example they generate high inrush currents and require frequent maintenance.

3.13.2. Synchronous Condensers

Traditionally, synchronous condensers have also been used as VAr compensators. This is a machine connected to the system. After it gets synchronised, the field current is adjusted to absorb or generate reactive power. This has been successfully used on transmission and distribution levels to improve the stability of the system. However, today synchronous condensers are rarely used because they require space and maintenance. Moreover their losses are much higher than that of static compensators [51].

3.13.3. Static VAr Compensators

The objective of reactive compensation can be achieved with the development of static compensators known as Static VAr compensators (SVCs). SVCs consist of reactive and capacitive elements and have the advantage of fast response time on synchronous condensers. The reactors and capacitors are switched to control the variable reactive power. They are grouped into two main types, as discussed below.

3.13.3.1. Thyristor Switched Capacitors

Thyristor Switched Capacitor (TSC) consists of two major parts, capacitor '*C'* and Thyristor switches '*Sw1'* and '*Sw2'*. There is also a small inductor '*L'* used to limit the raise of current through Thyristor and to provide resonance with the network. TSC has advantages e.g. it provides step wise control and an average delay of one half cycle with no generation of harmonics [50].

Figure 3.12 (**a**) shows circuit arrangement of different components for a single phase TSC.

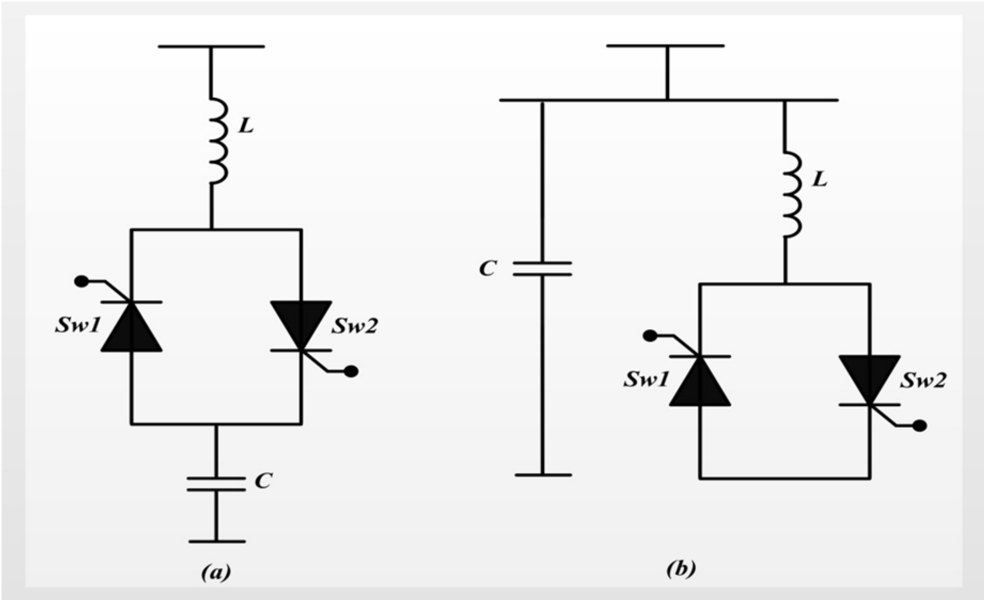

Figure 3. 12: Thyristor Switched Capacitor and Thyristor Controlled Reactor: (**a**), TSC Configuration. (**b**), TCR Configuration **[50]**.

Despite having several advantages, there are also some limitations for using the TSC as a compensator. For example, the VAr compensation is not continuous; each capacitor bank requires a separate switch which makes the construction not feasible. Moreover, the steady state voltage across non-conducting thyristor is twice the peak supply voltage and thyristor must be rated or protected by external means [50]. A solution for the described limitation is to replace one of thyrsitor switches with a diode. In this case inrush currents are eliminated when thyristor is switched at the right time. Figure 3.13 below shows the typical arrangement for that particular TSC.

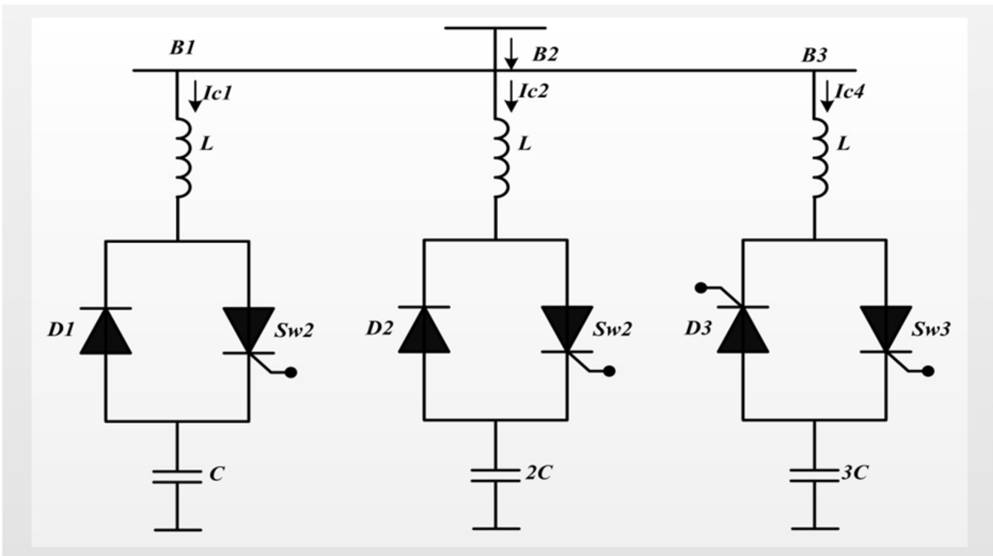

Figure 3. 13: Binary Thyristor Diode Switched Capacitor **[52]**.

3.13.3.2. Thyristor Controlled Reactor

Figure 3.12 (**b**), shows the schematics for Thyristor Controlled Reactor (TCR) for single phase which also includes capacitor for low order harmonics. Each of three phases include inductor '*L'* and Thyristor switches '*Sw1'* and '*Sw2'*. Reactors may be both switched controlled or phase angle controlled [38]. Phase angle control gives continues range of reactive power but it gives rise to the generation of odd harmonic current components.

In order to eliminate low frequency current components delta configuration (for zero sequence harmonics) and passive filters may be used as described in [52].

3.13.3.3. Combined TSC and TCR

Reactive power compensation is a step wise and continues process for of switched capacitors and controlled reactors methods respectively. However, if both of these methods are combined together as shown in the Figure 3.14, better compensation can be achieved. In combined form if reactive power is required to absorb, entire capacitor bank can be disconnected and vice versa. With the development of co-ordinated control, it is possible to realize a step-less control.

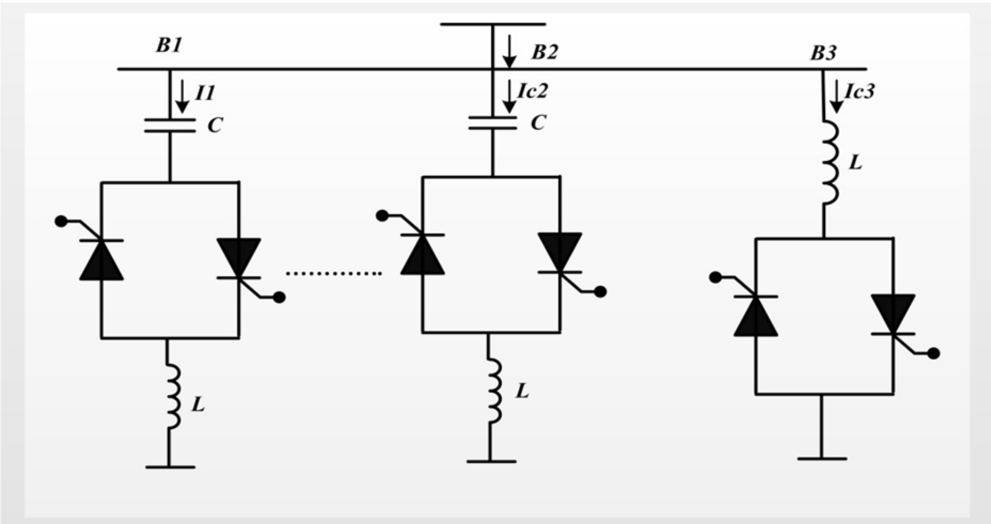

Figure 3. 14: Combined TSC and TCR Configuration **[52]**.

Collective operation of TSC and TCR retains some advantages e.g. they create very less harmonics with practically no transients and has flexibility in control operations. Besides these advantages there is a serious concern of cost behind the implementation of such compensators in the practical networks.

Other than these thyristor technologies, there is another series configuration known as Thyristor-Controlled Series Compensation (TCSC). TCSC technology specifically addresses damping issues in the large electrical transmission systems. Control operation of TCSC along with its advantages and disadvantages, has been explained in [52].

3.13.4. Self-Commutated VAr Compensators

With the help of modern gate commutated semiconductor devices, it has become possible to design and implement self-commutated converters also known as force-commutated compensators. Several approaches can be adopted e.g. Current Source Converter (CSC) and Voltage Source Converters (VSC) are among those as shown in the Figures 3.15. In general, CSC is not preferred for low power applications due to complexity of its control and sensitivity of the inverter circuit to current variations in the DC link inductor. Force commutated converters can be implemented to achieve [53].

- Harmonics Compensation
- Reactive power compensation
- Phase Balancing
- Load Balancing
- Combination of two or more of above mentioned usages

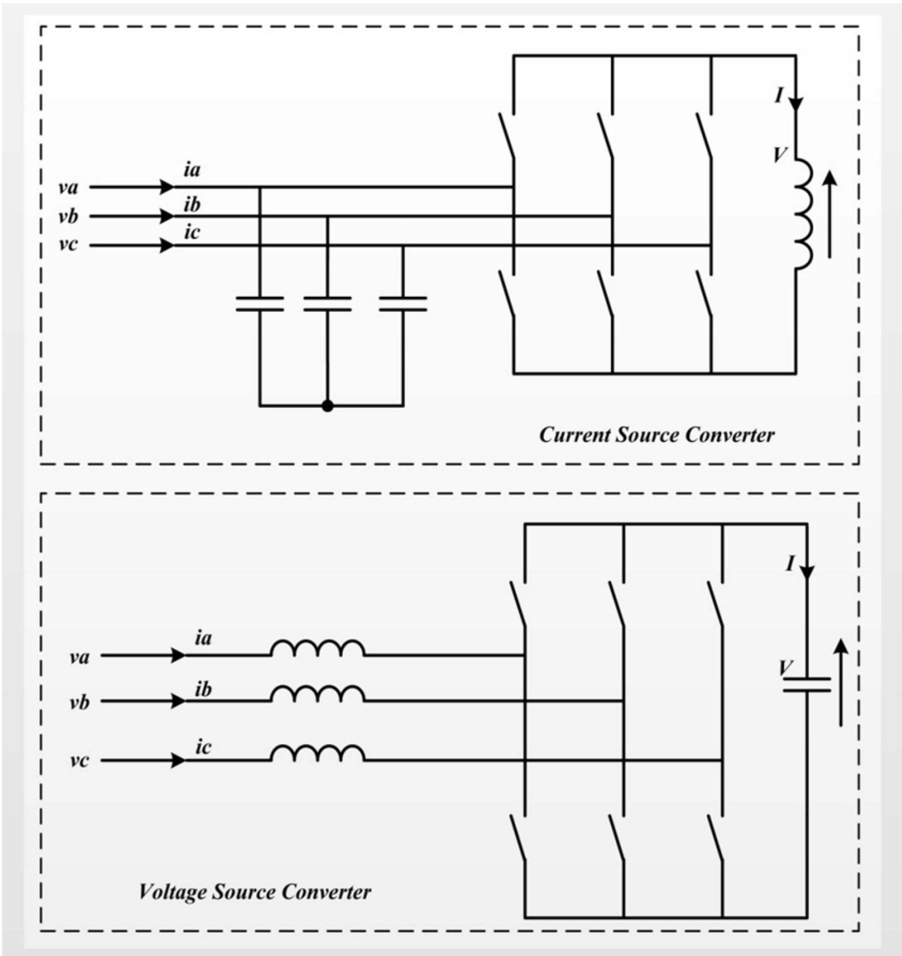

Figure 3. 15: Current Source Converter CSC and Voltage Source Converter VSC **[53]**.

Force-commutated converter also known as Shunt Active Filter (SAF) has smaller size and the installation cost is much lower because in this case, large number passive elements are minimized and the power ratings of switching devices are reduced. The amplitude of compensator output voltage can be controlled by changing the switching pattern modulation Index or Pulse Width Modulation (PWM) [38]. Some of the self-commutated converters with brief explanation are given below:

3.13.4.1. STATCOM

A Static Compensator (STATCOM) consists of a voltage source implemented with an inverter and coupling reactor in parallel configuration to the power system. This is like a synchronous machine connected at the PCC but without any inertia and overload capability. STATCOM generates output voltage at an angle and frequency as calculated from the PCC. Figure 3.16 shows one of the schematics being used in the power system.

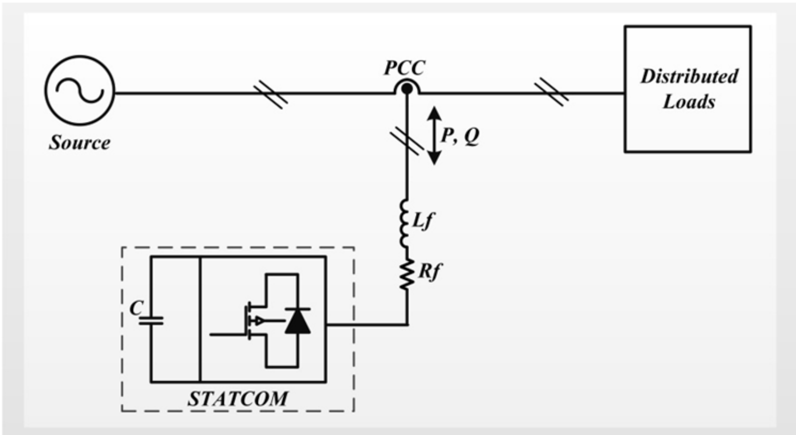

Figure 3. 16: Grid Connected STATCOM **[52]**.

3.13.4.2. SSSC

STATCOM is connected in parallel to the supply network. However, VSC can also be implemented with the supply lines in series. Such an arrangement is known as Static Synchronous Series Compensator (SSSC). SSSC injects voltage in series to the line, 90^0 phase shift with the load current, operating as series controlled capacitor. Only difference as compared to the series capacitor is that the voltage injected by an SSSC is not related to the line current and can be independently controlled [54]. Circuit diagram 3.17 for a SSSC is shown below.

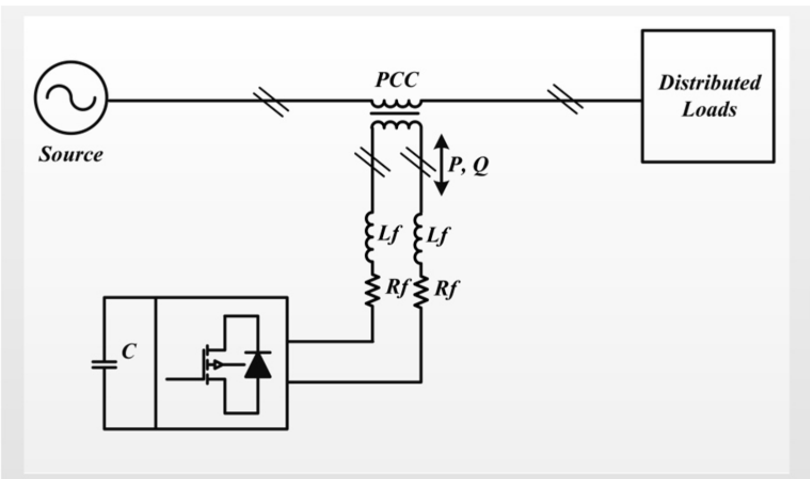

Figure 3. 17: SSSC **[54]**.

3.13.4.3. DVR

One of serious *power quality* issues as mentioned before is the voltage Sag/swell. To overcome these problems, power electronic device known as Dynamic Voltage Restorer (DVR) has come to existence. This is one of the most efficient and effective modern custom power device used in the power distribution networks which monitors the voltage on side and injects the appropriate amount of voltage across the lines [55]. It has also gained an increasing role in protecting industries against remote faults.

In addition to the force-commutated converters, there are some other devices as well that are being used for the reactive and harmonics compensation generally on transmission levels. These devices include Unified Power Flow Controllers (UPFCs), Interline Power Flow Controllers (IPFCs), etc. The details of these compensators are explained in [52].

3.14. Comparison between Thyristorized and Self-Commutated Converters

Self-Commutated compensators have number of advantages over Thyristorized compensators which make them preferable for the compensation in the voltage network. Table 3.2 summarizes the comparative analysis of compensators [52].

	Synchronous Condenser	Static Compensator		Self-commutated Compensator
		TCR (with shunt capacitors if necessary)	TSC (with TCR if necessary)	
Accuracy of Compensation	Good	Very good	Good, very good with TCR	Excellent
Control Flexibility	Good	Very good	Good, very good with TCR	Excellent
Reactive Power Capability	Leading/lagging	Leading/lagging indirect	Leading/lagging indirect	Leading/lagging
Control	Continuous	Continuous	Dis-continuous (Cont. with TCR)	Continuous
Response Time	Slow	Fast 0.5-2 cycles	Fast 0.5-2 cycles	Very fast but depends on control scheme
Harmonics	Very good	Very high (large filters are required)	Good, filters are necessary with TCR	Very good, depends on switching scheme
Losses	Moderate	Good, but increase in lagging mode	Good, but increase in leading mode	Very good, but increase with switching freq.
Phase Balancing Ability	Limited	Good	Limited	Very good
Cost	High	Moderate	Moderate	Low to Moderate

Table 3. 2: Comparison of different compensation schemes **[52]**.

It is clear from the Table 3.2, that force-commutated converters are the best choice for our MV/LV distribution network. A VSC with battery bank on DC side is chosen for addressing the *power quality* issues such as compensation of harmonics and reactive power, import and export of active power and for the voltage sags situation with wind power generation. Control scheme of VSC is developed and discussed later in the chapters.

Summary

In this chapter, different *power quality* events are summarized and analysed by literature studies and measurements from the Sintef Energy Research. It is observed that voltage dips, induction motor starting, current harmonics and reactive power consumption are the most important disturbances in the distribution system. It is also shown that most of the times voltage dips are due to faults on the lines; symmetrical and asymmetrical faults are two kinds of faults.

Current harmonics in the source current are one of the major reasons for power supply disturbance. Magnetic core equipment, arc furnaces and power electronic components are the major sources for the introduction of harmonics in the supply. Consequences of having harmonics in the supply current are also explained later in the chapter. Moreover, it is explained that the reactive power consumption is a major reason for *power quality* disturbance; transformers, T&D lines and reactive loads are main reasons for the absorption of reactive power.

In the end, several techniques are proposed, compared and explained for the compensation of reactive power and harmonics. Among these methods, switched capacitors and static VAr compensators have been previously used but the advancements in power electronics has given rise to the development of self-commutated compensators; STATCOM, SSSC and DVR are among those power electronic devices.

Chapter 4: Telecom Sites in the AC Distribution Network: Case Study

Telecom sites are connected to the LV/MV AC distribution networks through the active rectifiers, as utility interfaces. Rectifiers convert AC power to DC power and allow the charging of battery banks, from where power is supplied to the DC Telecom load. Control Algorithm of active rectifiers allow the power flow only in one direction but if bi-directional power flow becomes possible then surplus amount of power could also be sent back to the grid in future. In this chapter, basic network model is proposed with several distributed loads and number of telecom sites connected with LV AC distribution network. Control principle of bi-directional PE interface has been developed to enable the control of two way flow of power, from or to these telecom sites.

4.1. Telecom sites and Distributed Loads Connected with AC Distribution System

Telecom stations/sites are located across the cities on different locations. Only In Sør-Trøndelag Norway, telecom companies have more than 300 telecom sites on different locations and these Telecom sites are connected with LV/MV AC distribution network. Figure 4.1 shows the block diagram for n-Telecom sites connected with LV AC grid.

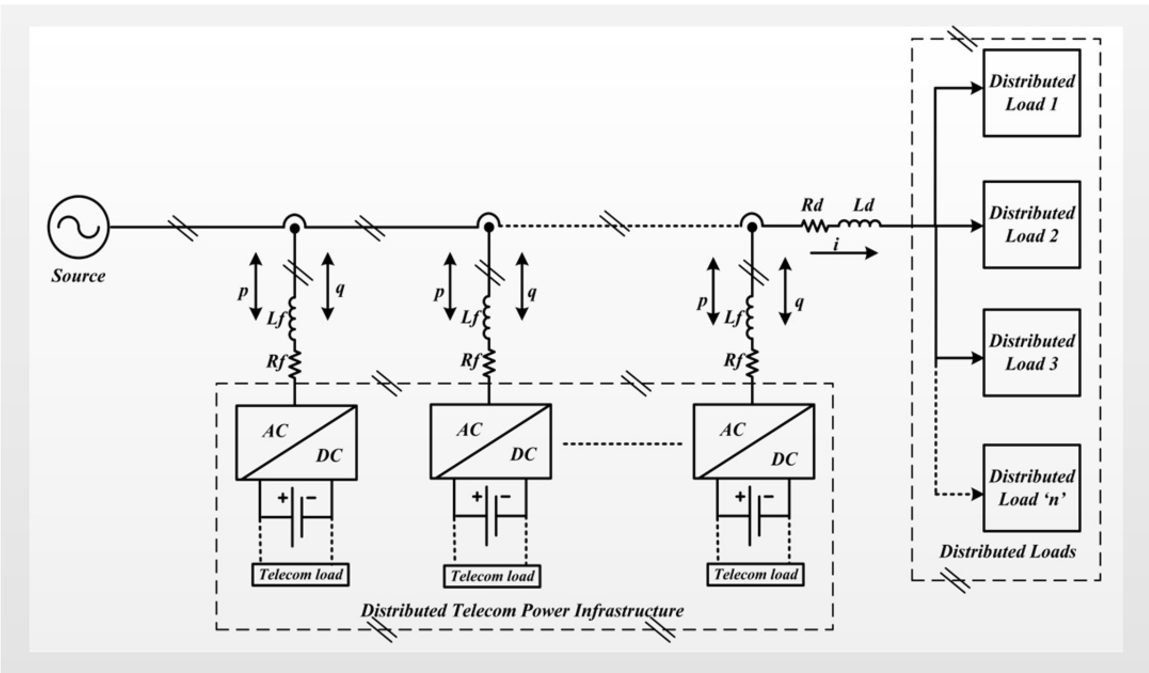

Figure 4. 1: Telecom sites and distributed loads connected with distribution network

A Simulation model will be developed in which different distributed loads such as non-linear and passive loads are connected to three phase AC distribution network. Non-linear loads are supplied by Thyristor and diode bridge rectifiers and passive loads are either delta connected or wye connected. Telecom sites are also supplied by the distribution grid.

Different cases will be developed in which one or more than one telecom sites are connected to the grid. These sites will be used to enhance the reliability, power quality and to provide the ancillary services. Three phase line to line grid voltage is 398 [$V_{L-L,rms}$]. Measurements will be taken from both the ideal and non-ideal voltage sources. In non-ideal voltage source harmonics and voltage unbalance is introduced artificially. Composition of block diagram will be explained later in the chapter.

4.1.1. Telecom Sites

Telecommunication companies install their apparatus for telecom services on different locations across the cities, known as Telecom sites. These sites comprised of DC loads which are fed by battery banks at these localities. Battery banks are charged from the AC source of the network with the help of PE interface. Each telecom site has on average of 3 [kW] DC loads. Composition of one telecom site is shown below.

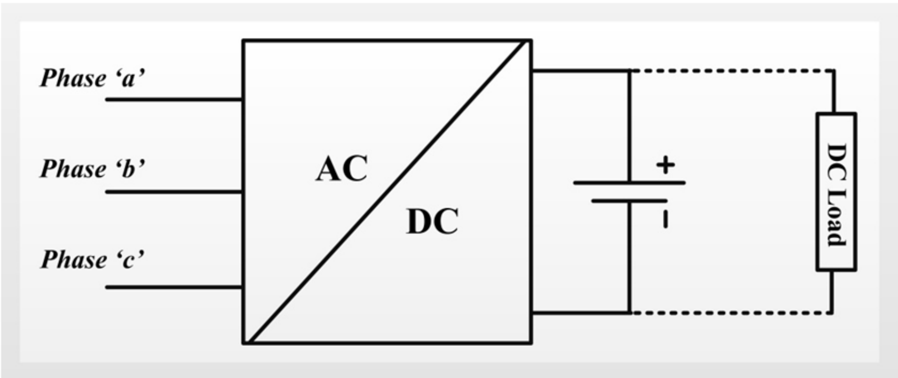

Figure 4. 2: One telecom site

This is shown in the diagram that telecom load is not directly fed from the battery banks; rather there is another DC/DC converter to adjust the required accurate voltage level. But detailed analysis of DC/DC converter is out of scope for this master thesis and on DC side battery voltage is adjusted as 700 [V].

4.1.1.1. Battery banks at each telecom site

Telecom stations or telecom sites are comprised of DC loads. DC loads operate with the help of battery banks installed at these sites. Battery banks are usually high efficient because of the sensitivity of the telecom load. The capacity of these battery banks varies between 3.5 kWh to 6 kWh. Different battery banks with their specifications have been explained in the chapter three. In the proposed model, Lithium Ion battery is used with the efficiency 85% to 95%. Total back up energy capacity is 6 [kWh] and the voltage varies between 700 [V] and 800 [V] depending upon the charging capacity.

Batteries are continuously charged from the grid supply and discharged by supplying power to the DC load. If calculated amount of power is managed properly and fed back to the grid, it can be used for the power quality improvement and other ancillary services. Figure 4.3 shows the charging and discharging characteristics of Li ion battery at given loads.

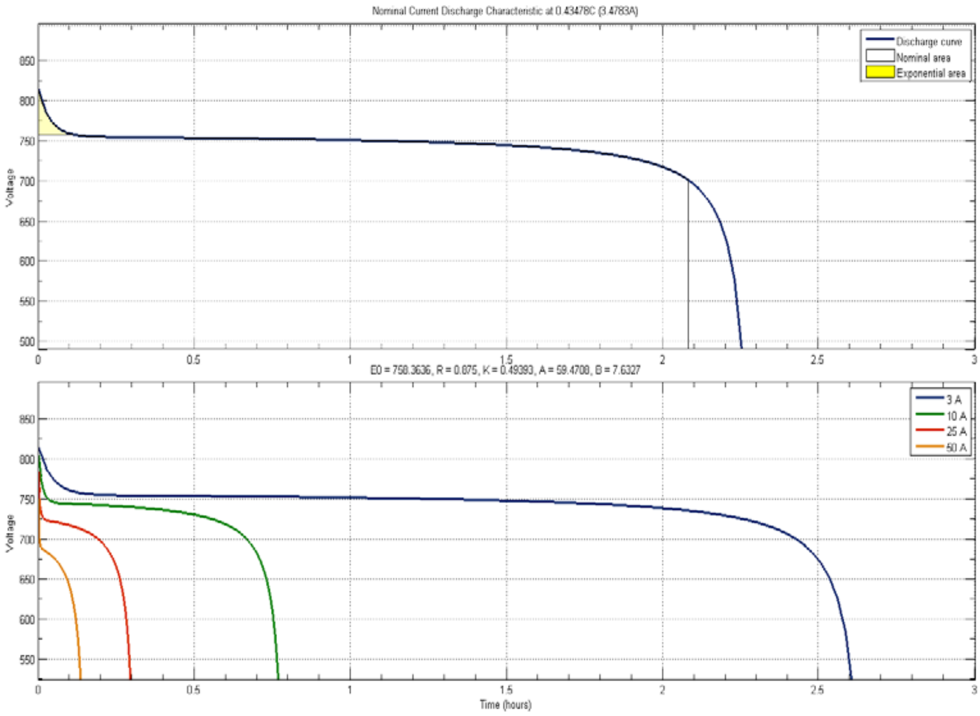

Figure 4. 3: Charging and discharging characteristics of Li-Ion battery for different current ratings

Figure shows that with the varying load demand, discharging current characteristics of a battery bank also varies. For example with required 3 [A] and 50 [A] load demand a Li-ion battery will be discharged completely in 2.6 and 0.12 hours respectively.

4.1.2. AC Distribution Grid

Telecom sites and other distributed loads are connected to three phase voltage supply. In the simulation model, measurements are taken both from the ideal and non-ideal voltage sources. Ideal voltage source supplies three phase AC voltage with zero internal impedance while non-ideal voltage source has its source impedance. Parameters for the LV AC supply are given in the Table 4.1.

Voltage, v_s	398 [$V_{L\text{-}L,rms}$]
Frequency, f	50 [Hz]
Source resistance, R_s	0.01 [mΩ]
Source inductance, L_s	0.01 [mH]

Table 4. 1: Parameters of Distribution Grid

4.1.2.1. Distribution Lines

Distributed loads are connected with LV distribution network. Capacitance of the lines and resistance between different loads can be neglected since they are much smaller than the line reactance [37]. In the same way impedance between telecom sites and distribution lines is neglected due to very small distance while impedance between source and the distributed loads is represented on per kilometre basis. In case of one telecom site, distributed loads are connected at the distance of 1 kilometre from the source. Between site 1 and site 2, there is distance of 100m while the distance between site 2 and site 3 is 200m. Inductance between n^{th} site and distributed loads is represented by L_d.

Network resistance, R_d = 1 [mH]/km

Network inductance, L_d = 1 [mΩ]/km

4.2. Unbalanced and distorted voltage conditions

Now the distribution voltage is taken as unbalanced and distorted voltage. According to [56] voltage unbalance is defined as,

"In a three phase system voltage unbalance takes place when magnitudes of phase or line voltages are different and the phase angles differ from balanced conditions, or both."

In an unbalance system, voltage consists of positive and negative sequence components. It can be written as:

$$\begin{bmatrix} v_{ua} \\ v_{ub} \\ v_{uc} \end{bmatrix} = \begin{bmatrix} v_{ua+} \\ v_{ub+} \\ v_{uc+} \end{bmatrix} + \begin{bmatrix} v_{ua-} \\ v_{ub-} \\ v_{uc-} \end{bmatrix} \tag{4.1}$$

Where 'v_{ua}', 'v_{ub}', 'v_{uc}' are three phase unbalanced voltages, 'v_{ua+}', 'v_{ub+}', 'v_{uc+}' are positive sequence voltage components and 'v_{ua-}', 'v_{ub}'-, and 'v_{uc-}' are negative sequence voltage components respectively. In the given model, voltage unbalance is introduced by reducing the magnitude of phase 'b' by 30 [$V_{L-L,rms}$]. While phase 'a' and phase 'c' has the magnitude of 398 [$V_{L-L,rms}$]. So, the system can be written as:

$$\begin{bmatrix} v_a \\ v_b \\ v_c \end{bmatrix} = 398 \begin{bmatrix} \sin(\omega t) \\ \sin(\omega t - 120°) \\ \sin(\omega t + 120°) \end{bmatrix} - 30 \begin{bmatrix} 0 \\ \sin(\omega t - 120°) \\ 0 \end{bmatrix} \tag{4.2}$$

Equation shows that phase 'a', 'b' and phase 'c' are displaced at 120 degrees but phase 'a' and phase 'b' has voltage of 398 [$V_{L-L,rms}$] while phase 'b' has voltage 368[$V_{L-L,rms}$].

The use of power electronic switches in the distribution network has been significantly increased since last few decades. The non-linear nature of the connected load is the major source of distortion in the supply voltage which sometimes causes serious power quality issues at distribution level. Under such circumstances, supply voltage can be written as the sum of fundamental components and harmonics components of voltage, given as:

$$\begin{bmatrix} v_{da} \\ v_{db} \\ v_{dc} \end{bmatrix} = \begin{bmatrix} v_{af} \\ v_{bf} \\ v_{cf} \end{bmatrix} + \begin{bmatrix} v_{ah} \\ v_{bh} \\ v_{ch} \end{bmatrix} \tag{4.3}$$

Where *'v_{da}'*, *'v_{db}'* and *'v_{dc}'* are distorted three phase voltages, *'v_{af}'*, *'v_{bf}'* and *'v_{cf}'* are three phases of fundamental voltages and *'v_{ah}'*, *'v_{bh}'* and *'v_{ch}'* are three phase harmonic voltages respectively.

SAF can be a solution for such a problem. In the given model, distortion in three phases is introduced by adding 3rd, 5th and 7th order harmonics of magnitudes 30 [$V_{L-L,rms}$], 25 [$V_{L-L,rms}$] and 18 [$V_{L-L,rms}$] respectively. The system after adding I^{3rd}, I^{5th} and I^{7th}, can be written as:

$$\begin{bmatrix} v_a \\ v_b \\ v_c \end{bmatrix} = 398\begin{bmatrix} \sin(\omega t) \\ \sin(\omega t-120°) \\ \sin(\omega t+120°) \end{bmatrix} + 30\begin{bmatrix} \sin(3\omega t) \\ \sin(\omega t-120°) \\ \sin(\omega t+120°) \end{bmatrix} + 25\begin{bmatrix} \sin(5\omega t) \\ \sin(\omega t-120°) \\ \sin(\omega t+120°) \end{bmatrix} + 18\begin{bmatrix} \sin(7\omega t) \\ \sin(\omega t-120°) \\ \sin(\omega t+120°) \end{bmatrix} \tag{4.4}$$

When both the unbalance and distortion are introduced in the supply, it becomes presents a worst scenario. Under these conditions, the system equation behaves as:

$$\begin{bmatrix} v_{uda} \\ v_{udb} \\ v_{udc} \end{bmatrix} = \begin{bmatrix} v_{af} \\ v_{bf} \\ v_{cf} \end{bmatrix} + \begin{bmatrix} v_{a-} \\ v_{b-} \\ v_{c-} \end{bmatrix} + \begin{bmatrix} v_{ah} \\ v_{bh} \\ v_{ch} \end{bmatrix} \tag{4.5}$$

In above equation v_{af}, v_{bf} and v_{cf} are fundamental components of phase a, b and c respectively, which also act as positive sequence components. The whole system under unbalanced and distorted conditions can be written as:

$$\begin{bmatrix} v_a \\ v_b \\ v_c \end{bmatrix} = 398\begin{bmatrix} \sin(\omega t) \\ \sin(\omega t-120°) \\ \sin(\omega t+120°) \end{bmatrix} + 30\begin{bmatrix} \sin(3\omega t) \\ \sin(\omega t-120°) \\ \sin(\omega t+120°) \end{bmatrix} + 25\begin{bmatrix} \sin(5\omega t) \\ \sin(\omega t-120°) \\ \sin(\omega t+120°) \end{bmatrix} + 18\begin{bmatrix} \sin(7\omega t) \\ \sin(\omega t-120°) \\ \sin(\omega t+120°) \end{bmatrix} - 30\begin{bmatrix} 0 \\ \sin(\omega t-120°) \\ 0 \end{bmatrix} \tag{4.6}$$

In the simulation model, circuit diagrams for creating unbalanced and distorted voltages in the given system are given in the Figure 4.4, Figure 4.5 and Figure 4.6:

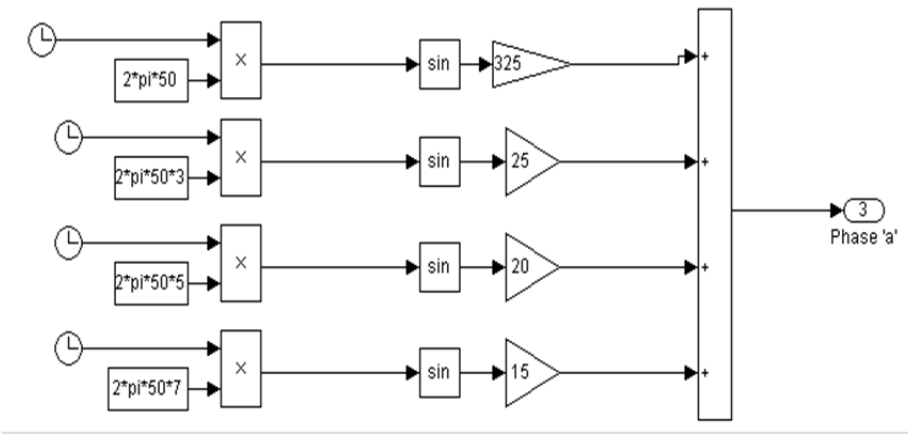

Figure 4. 4: Distortion in phase 'a'

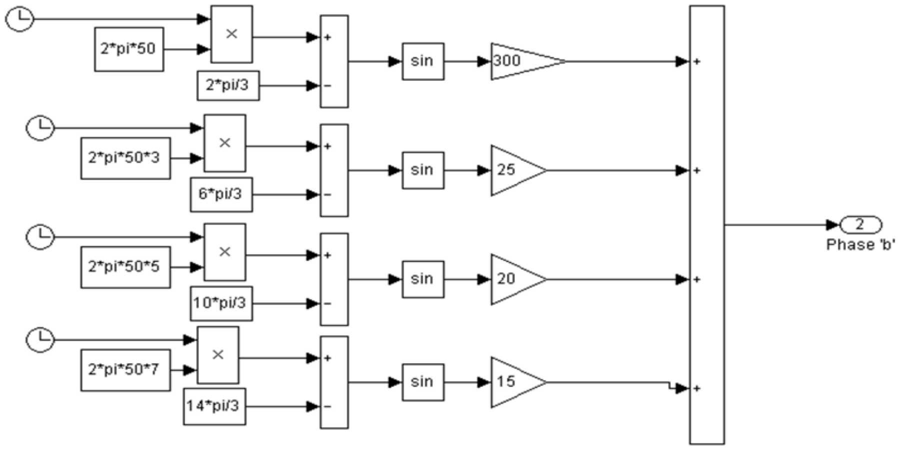

Figure 4. 5: Unbalance and distortion in phase ‘b’

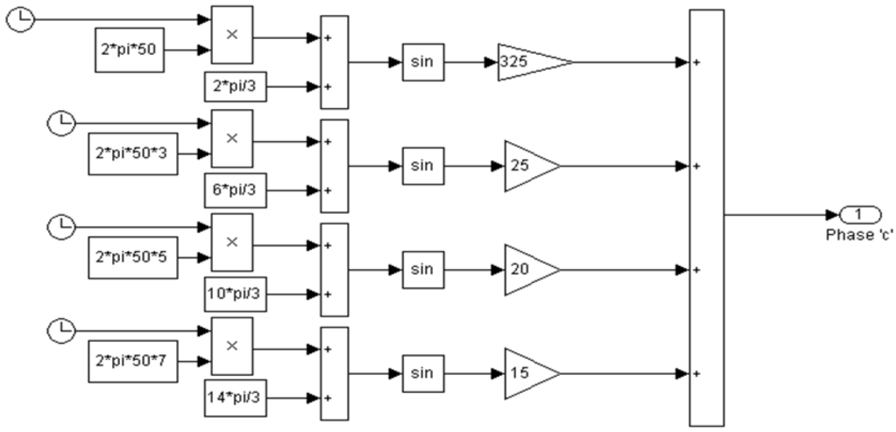

Figure 4. 6: Distortion in phase ‘c’

4.3. Distributed Loads

Figure 4.1 shows that different kinds of loads are connected to the distribution network. In our network model for reactive power and harmonics compensation, loads such as passive loads, diode bridge rectifier’s loads and Thyristor bridge rectifier loads are connected.

To achieve peak load demand, these kinds of additional distributed loads need to be connected and will be explained later in the chapters. Details parameters for these loads are given as:

4.3.1. Passive Loads

Passive load consists of passive elements like resistor, capacitor and inductor. Inductor absorbs reactive power while capacitor acts as a source of reactive power. In this simulation model resistor and inductor are connected as distributed passive loads. In some cases they are connected in wye configuration and in others they are connected in delta arrangement. Values for passive loads are given in Table 4.2. Figure 4.9, shows the circuit configuration wye connected passive loads.

Voltage, v_s	398 [$V_{L\text{-}L,rms}$]
Frequency, f	50 [Hz]
Active power, P	1 [kW]
Reactive power, Q	250 [VAr]

Table 4. 2: Parameters of passive load

4.3.2. Diode Bridge Non-Linear Loads

In the simulation model, distributed non-linear loads are connected with grid via three phase diode bridge rectifiers. Resistive and Inductive loads are connected on DC side of the rectifiers. Same kind of load is connected with all the diode bridge rectifiers.

To achieve peak load demand, some additional non-linear load is connected with the distribution grid on different time intervals. Parameters related to the non-linear loads connected with Diode Bridge rectifiers are tabulated in the Table 4.3.

Voltage, v_s	398 [$V_{L\text{-}L,rms}$]
Frequency, f	50 [Hz]
Resistive load, R_l	50 [Ω]
Inductive load, L_l	50 [mH]
DC side capacitance, C	0.5 [mF]
Snubber resistance, R_s	1 [k Ω]
Snubber capacitance, C_s	0.1 [µF]
Internal resistance, R_{on}	1 [mΩ]
Rated load, *'P'*	5.5 [kW]

Table 4. 3: Diode bridge non-linear loads

4.3.3. Thyristor Bridge Non-Linear Loads

Non-linear loads are connected either with Diode Bridge or Thyristor Bridge rectifiers. These three phase bridge rectifiers are supplied by LV AC grid.

Current and switching harmonics related to bridge rectifiers are explained in the chapter 3. In Figure 4.1 there is one Thyristor bridge rectifier with resistive and inductive loads connected on DC side of the rectifiers. Different parameters for DC loads, firing angle, etc. are summarized in the Table 4.4.

Voltage, v_s	398 [$V_{L\text{-}L,rms}$]
Frequency, f	50 [Hz]
Resistive load, R_l	50 [Ω]
Inductive load, L_l	50 [mH]
DC side capacitance, C	1 [mF]
Firing angle, α	25^o
Snubber resistance, R_s	1 [k Ω]
Snubber capacitance, C_s	0.1 [µF]
Internal resistance, R_{on}	1 [mΩ]
Rated load, *'P'*	5.5 [kW]

Table 4. 4: Thyristor bridge non-linear loads

4.4. Snubber resistance and Snubber Capacitance

Non-linear loads, one of the major reasons for harmonics in the source current are connected with rectifiers. Figure 4.7 and Figure 4.8 show the three phase bridge rectifier.

Simulation model is discrete model, so in order to avoid numerical oscillations snubber values for 'R_s' and 'C_s' are specified for the diode and Thyristor bridge rectifiers [38]. Following formulae are used to calculate appropriate values of 'R_s' and 'C_s'.

$$Rs > 2\frac{Ts}{Cs} \tag{4.7}$$

$$Cs < \frac{Pn}{1000(2\pi f)V^2n} \tag{4.8}$$

where

Pn =nominal power of three phase rectifier [kW]

Vn =nominal line to line voltage [V_{rms}]

f =fundamental frequency [Hz]

Ts =sample time [s]

The rectifier bridges are discretised and the sample time is taken as 1[µs], the internal inductance L_{on} must be taken as zero. R_s and C_s values are derived from two criteria's

- The snubber leakage current at fundamental frequency is less than 0.1% of nominal current when power electronic devices are not conducting.
- The *RC* time constant of snubbers is higher than two times of the sample time.

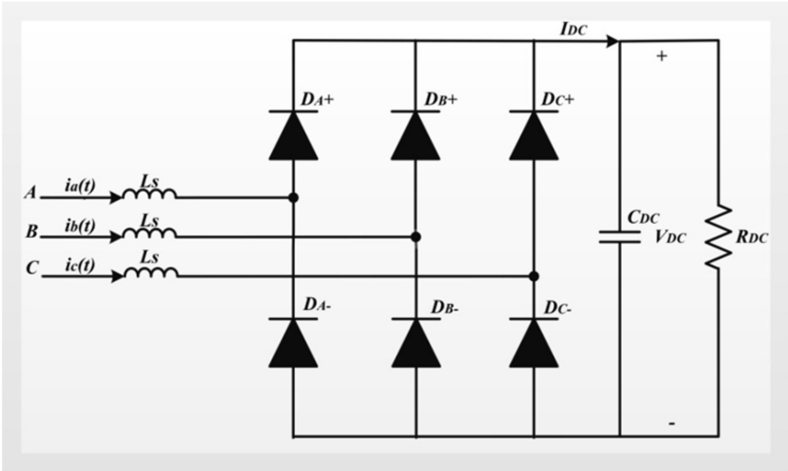

Figure 4. 7: Circuit Configuration of three phase diode bridge rectifier

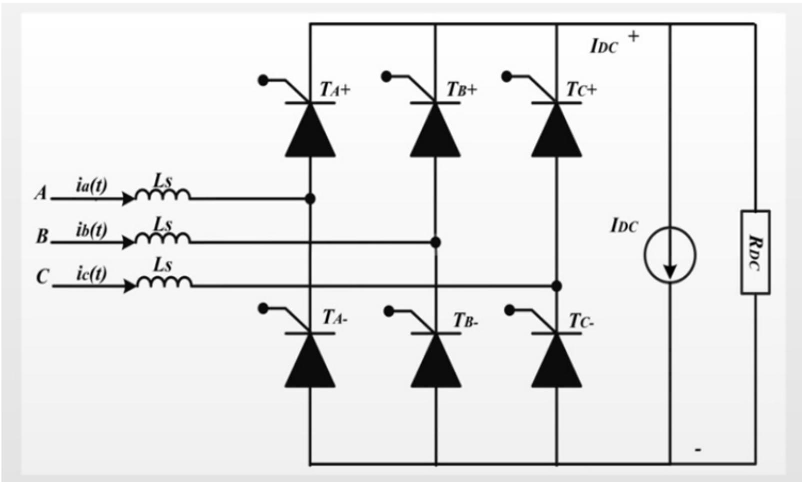

Figure 4. 8: Circuit Configuration of Thyristor bridge rectifier

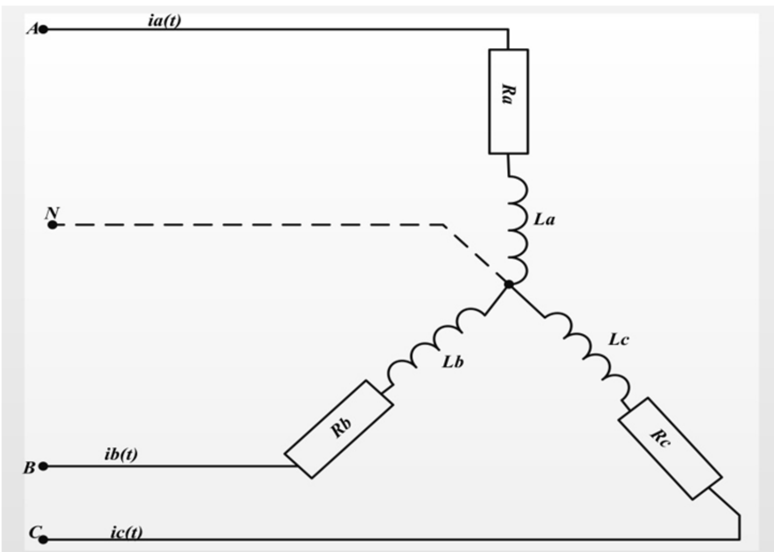

Figure 4. 9: Circuit Configuration of wye connected passive load

4.5. Voltage Source Converter VSC

Voltage source inverters are used to produce sinusoidal ac output whose magnitude and frequency can both be controlled. Chapter 3 explains different kinds of voltage source inverters that how they can be used as SAFs. An inverter performs as a Voltage Source Converter if the switches operate in combination with antiparallel diodes. Converter can be used both as a rectifier and as an inverter. Figure 4.10 shows the schematics of VSC, which will be used as an interface of telecom sites to the LV grid supply.

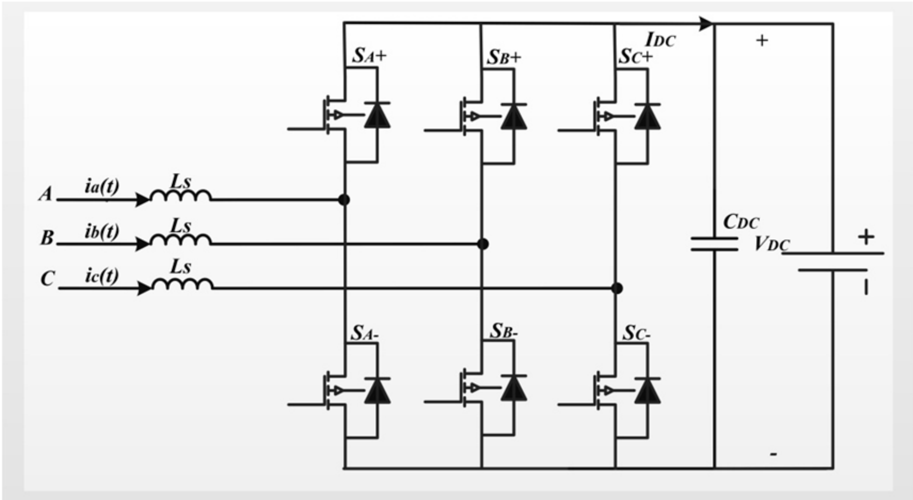

Figure 4. 10: Voltage Source Converter

It consists of six MOSFETs along with antiparallel diodes. Each site has to supply an average telecom load of 3 [kW] and the battery banks are also not of large capacity. MOSFETs have lower on state losses due to the absence of Conductivity modulation and high switching speed. Also, their positive temperature co-efficient make them quit convincing for high current handling capability [38]. All these features make them ideal for such a low power applications but for utility applications, co-ordinated operation of hundreds of Telecom sites is required to meet the power requirements. Switching frequency of 10 [kHz] is selected for VSCs on different sites and a capacitor of 100 [μF] is selected for the DC side of the converter in order to remove oscillations.

During charging of the battery bank VSC acts as a three phase bridge rectifier and supplies power from grid to the battery banks. Battery banks not only supply power to the telecom loads but they will also be used to supply reactive power, active power and harmonics to the grid. During supplying power to the grid switching PE interface will act as an inverter.

4.5.1. Converter Filter

Most of the renewable energy sources like wind, solar, etc. need to be interfaced with the existing grid supply using a power converter. However, power converters introduce undesirable harmonics that will affect nearby loads at a PCC. Hence, such converters have a filter to attenuate the high frequency PWM harmonics to desirable limits. For medium to high power converter applications '*LCL'* filters are proffered to use due to significant smaller size and cost but for the low power application simple '*L'* filter is used to meet the harmonics standards defined in [57]. Since the power ratings at telecom sites is low, so simple '*L'* filter is used in this master thesis, ranging 1-3.5 [*mH*] depending upon the capacity of telecom site.

4.6. Modelling of Voltage Source Converter$_{(s)}$ VSCs

In this chapter, one of the main purposes is to develop a method to control AC/DC bi-directional converter which allows the converter to behave as a rectifier and as an inverter. We will develop a method for one converter and then apply the same method on one, two and three converters by making small changes in their control specifications. Installing these bi-directional converters at telecom sites would make it possible to import/export power from and to the grid according to their current ratings and size of the battery banks.

Telecom sites could be very helpful for the grid support when these sites export power to the grid, e.g. they can mitigate the current harmonics from the source current, provides reactive power to the grid and can export active power as well during peak load demand.

The control of VSC is done by using vector control technique. Block diagram representing the 'n' sites connected at PCC in the Figure 4.11:

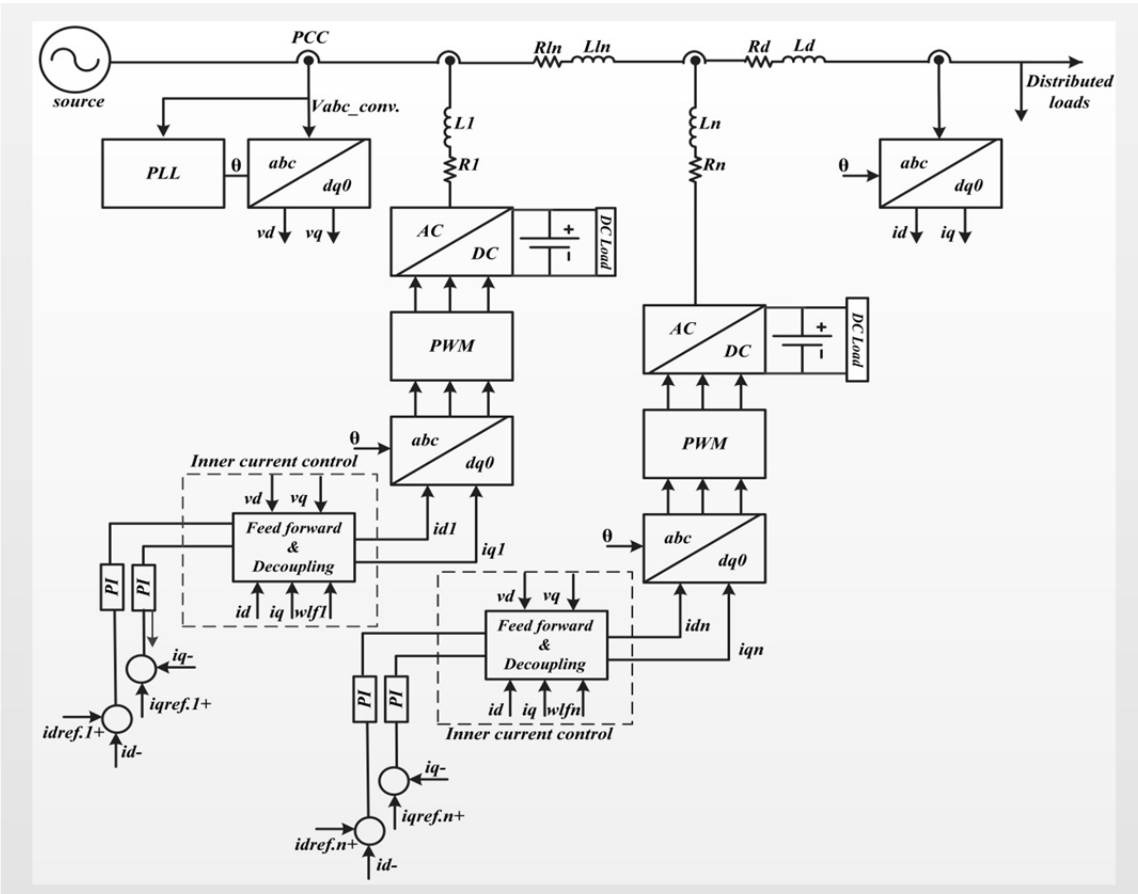

Figure 4. 11: Control Diagram of 'n' converters

Figure shows the individual control schemes from converter *'1'* to converter *'n'*. Detailed analysis of each section of the diagram is given below.

4.6.1. Vector Control Technique

Vector control technique is used to control VSC. The main advantage of vector control technique is its simplicity. This technique helps to obtain fast dynamic response and independent control of active and reactive powers [58]. This transformation is made in two steps.

- Transformations of three phase stationary co-ordinate system to two phase *'αβ'* stationary coordinate system.
- Transformation from *'αβ'* stationary coordinate system to rotating *'dq'* co-ordinate system.

Clark and Park transformations are used in which three phase stationary co-ordinates system is transformed to rotating 'd-*q'* co-ordinate system through *'α-β'* stationary frame of references and vice versa. Figure 4.12 shows the representation of Clark and Park transformation in vector forms.

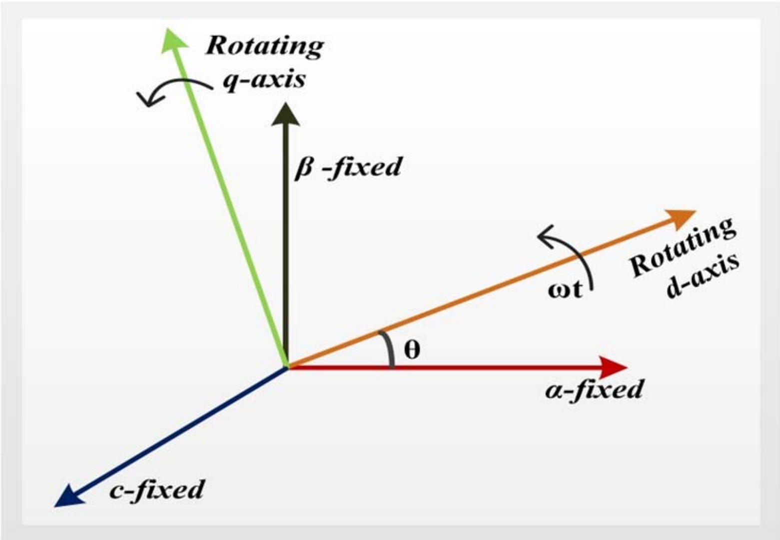

Figure 4. 12: The transformation of axis for vector control **[59]**.

Considering the VSC connected to the grid, defining grid voltages as v_{abc}, currents as i_{abc}, converter input voltages *'v_{abc_conv}'* and resistance *'R'* and inductance *'L'* between grid and converter as shown in the Figure 4.11, the voltage equations on the grid side of the converter can be written as.

$$v_{abc} - v_{abc\_conv} = Ri_{abc} + L\frac{d}{dt}i_{abc} \tag{4.9}$$

Using *'abc'* to *'dq'* transformations, converter currents and voltages are expressed as:

$$v_d - v_{d\_conv} = Ri_d + L\frac{di_d}{dt} - wLi_q \tag{4.10}$$

$$v_q - v_{q\_conv} = Ri_q + L\frac{di_q}{dt} + wLi_d \tag{4.11}$$

Where 'v_d' , 'v_q' are '*d*' and '*q*' components of supply network while 'v_{d_conv}' , 'v_{q_conv}' represent converter '*d*' and '*q*' axis voltage components. '*R*' and '*L*' are the resistance and Inductance between converter and grid. The grid frequency and speed of rotating '*d-q*' frame is given by 'ω'.

The grid voltage vector is defined to be along the '*d-axis*' direction and then a virtual grid flux vector can be assumed to be acting along the '*q-axis*'. With this alignment '$v_q=0$' and instantaneous real and reactive power injected or absorbed by the system is given by:

$$p = \frac{3}{2} vdid \tag{4.12}$$

$$q = -\frac{3}{2} vdiq \tag{4.13}$$

Above Equations show that both active and reactive power can be controlled independently by controlling '*d*' and '*q*' axis currents, through VSC.

The angle between '*α-axis*' of '*α-β*' frame and '*d-axis*' of '*d-q*' frame is used for transformation between '*α-β*' and '*d-q*' frame. The angular position of voltage vector is given by,

$$\theta = \tan^{-1}\left(\frac{v\beta}{v\alpha}\right) \tag{4.14}$$

Where 'v_β' and 'v_α' are components of voltage in stationary two axis reference frame. The value of the 'θ' can be computed using Phase Locked Loop (PLL) [60]. PLL is used to control the flow of active and reactive power by synchronizing the output according to the given references.

Both real and reactive powers have harmonic components and average components given by the equations 4.15 and 4.16 [44]. Both of these are controlled using this technique.

$$p = p_{ave} + p_{osc} \tag{4.15}$$

$$q = q_{ave} + q_{osc} \tag{4.16}$$

Where 'p_{ave}' and 'q_{ave}' are the dc components of active power and reactice power, and 'p_{osc}' and 'q_{osc}' are the harmonic components of active power and reative power. In vector control method 'I_d' and 'I_q' are responsible for controlling the flow of active power and reactive power respectively. By vector control principle

$$I_d = I_{dave} + I_{dosc} \tag{4.17}$$

$$I_q = I_{qave} + I_{qosc} \tag{4.18}$$

So, by controlling the *'Idave'* and *'Iqave'*, real parts of active and reactive power can be controlled and by controlling the 'Idosc' and 'Iqosc', harmonics in the system can be controlled. The overall scheme of vector control for VSC is shown in the Figure 4.13.

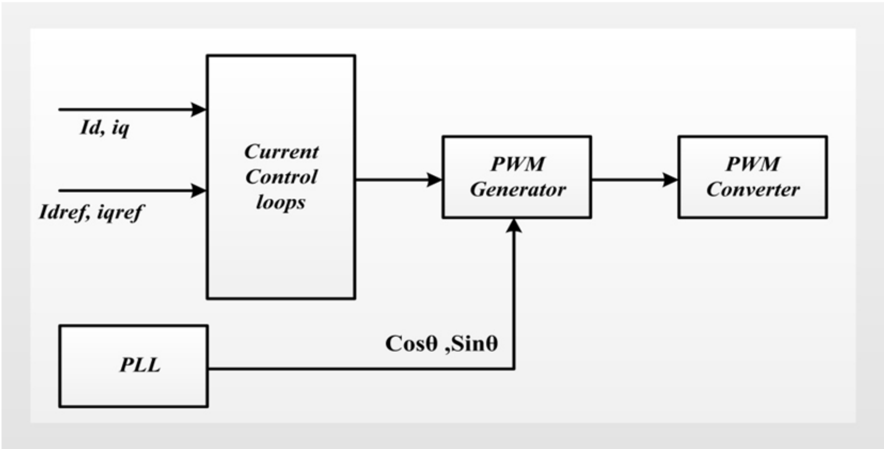

Figure 4. 13: Block Diagram of vector control principle

Principal of Clark and Park transformation has been well explained by the authors of [59]. However, mathematical description of these techniques is also explained in the **Appendix [C.1]** [59]**.**

As vector control offers decoupled control of active and reactive powers. It is fast dynamic in the form of cascade structure possible with two control loops that is, outer current control loop and inner current control loop. Fast inner current control loop controls the AC current. The AC current references are supplied by outer controllers. The outer controller includes the dc voltage controller, active power controller, reactive power controller depending upon the application. The references are supplied by the active power controllers or reactive power controllers. In this master thesis, dc voltage is fixed and maintained by the battery banks at a specified at level. While the active and reactive power is controlled.

4.6.2. Inner Current Controller

The inner current control loop can be implemented in the *'dq'* frame. The control loop consists of PI controllers, decoupling factors and feed forward terms. The current control block diagram is represented by the following general block diagram.

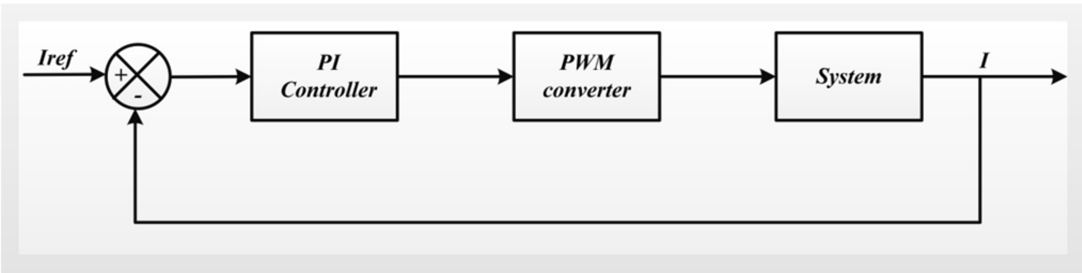

Figure 4. 14: Inner current controller

Inside the current control block, there are two PI regulators, respectively for d and q axis current control. They transform the error between the comparison of d and q components of current into voltage value. In order to have a detail overview of the control system, each block of the system is discussed in details as.

4.6.3. PI Regulators

The representative equation of PI regulator is:

$$R(s) = Kp + \frac{Ki}{s} = Kp\left(\frac{1+Ti.s}{Ti.s}\right) \tag{4.19}$$

Where proportional gain Kp and integral time constant *Ti= Kp/Ki* are the design parameters to be specified. Thus for PI control block,

$$\left\{Iref(s) - Is\right\}\left(Kp + \frac{Ki}{s}\right) = V'conv(s) \tag{4.20}$$

4.6.4. PWM Converter

From the control point of view, the converter is considered as an ideal power transformer with a time delay. The output voltage of the converter is assumed to follow a voltage reference signal with an average time delay equal half of a switching cycle, due to VSC switches. Hence the general expression is

$$Y(s) = \frac{1}{1+Ta.s} \tag{4.21}$$

Where Ta=T_{switch}/2, thus for converter block,

$$V'conv(s).\frac{1}{1+sTa} = Vconv(s) \tag{4.22}$$

4.7. The system

Equation 4.10 represents the complete dynamics of the system. It is shown that in the synchronous frame VSC is a multiple input-output strongly coupled non-linear system. The equations of each axis have speed/frequency induced terms that give cross coupling between the two axes. Cross coupling terms can be considered as disturbance from control point of view. Thus, dual close-loop current controller with decoupled current compensation and feed forward compensation gives a good control performance.

Using separate current controllers *‘i_d’* and *’ i_q’*, gives the voltage references for two independent axis which fed to the converter gives two voltage references for the system. Using equations 4.20 and 4.22 the references are as:

$$V_{dconv} = \left(i_{dref} - i_d\right).\left(Kp + \frac{Ki}{s}\right).\left(\frac{1}{1+Ta.s}\right) \tag{4.23}$$

$$V_{qconv} = \left(i_{qref} - i_q\right).\left(K_p + \frac{K_i}{s}\right).\left(\frac{1}{1+T_a.s}\right) \tag{4.24}$$

When cross coupling and feed forward terms are introduced, then the above equations become

$$V'_{dconv} = -\left(i_{dref} - i_d\right).\left(K_p + \frac{K_i}{s}\right) + \omega L i_q + v_d \tag{4.25}$$

$$V'_{qconv} = -\left(i_{qref} - i_q\right).\left(K_p + \frac{K_i}{s}\right) - \omega L i_q + v_q \tag{4.26}$$

After putting in equation 4.22 and equating to system eq. 4.10, the feed forward terms are cancelled. The remaining terms are given as:

$$v_{d\_conv} = R i_d + L\frac{di_d}{d_t} \tag{4.27}$$

$$v_{q\_conv} = R i_q + L\frac{di_q}{d_t} \tag{4.28}$$

From the above equations, it is clear that both of these have the same parameters. Hence, one equation can be used. By taking the Laplace transformation, the transfer function becomes,

$$G(s) = \frac{1}{R}.\frac{1}{1+s.\tau} \tag{4.29}$$

where $\tau = L/R$, known as constant of line.

4.7.1. Control Block Diagram

Control block diagram of the system is give below.

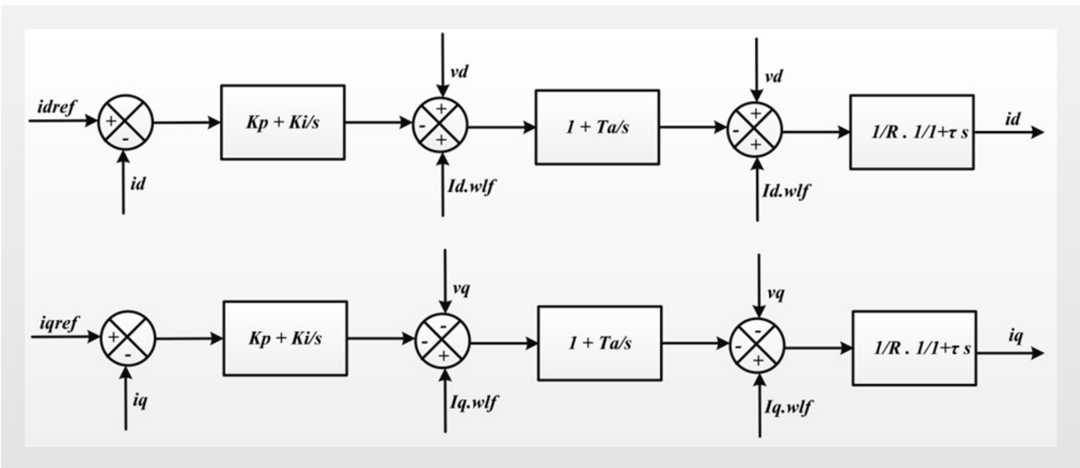

Figure 4. 15: Detailed control block diagram of inner current controller

Where '*vd'*, *'vq'*, *'idwl'* and '*iqwl'* represent the feed forward and decoupling specifications.

4.7.2. Vector Control of Two and three Converters

In this master thesis, 2nd and 3rd telecom sites are located 100m and 200m apart. There are no distributed loads connected between these sites, so the source current remains the same for all three sites. In order to develop control of VSCs reference currents and source voltage is the same for all of these converters since there are minimal losses in the line. Each telecom site provides compensating currents according to the battery capacities they have. They can share total current or can supply according to the capacities. Figure 4.16(a) and Figure 4.16(b) show the inner current controller block diagrams for telecom site 2 and telecom site 3. A and Figure B show the block diagrams for controlling two and three SAFs.

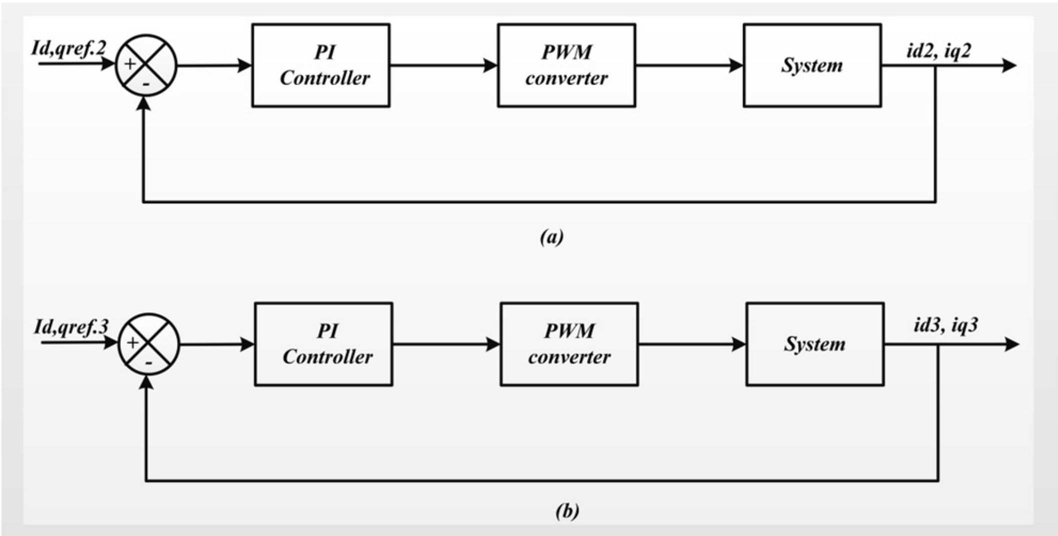

Figure 4. 16: SAF's Inner Current controllers: (**a**), For Telecom site 2, (**b**), For Telecom site 3

The detailed configuration of each parameter in the block diagram has been explained.

4.7.3. Tuning of PI Regulators

The controller must be tuned to obtain improve response of the system. The basic purposes of proportional gain and integral gain are described in [61]; the proportional gain affects the rate of rise after a change has been initiated in the loop. The integral gain produces an output that depends on the integral of the error and it continuously changes the in the direction to reduce error, until the error is restored to zero.

To achieve the above outcomes, Tuning of PI regulators is done manually. By following this method, Ki is kept zero and increase the value of Kp until the output of the loops oscillates, then kp should be set to approximately half of that value for a 'quarter amplitude decay' type response. Then increase Ki until any offset is corrected in sufficient time.

However, too much *Ki* will cause instability.

4.7.4. Pulse Width Modulation PWM

Pulse Width Modulation (PWM) technique is used to convert DC voltage into three phase AC voltages and vice versa. Each phase voltage is displaced by 120 Degrees and is responsible for converter switching. Three phase reference signals are compared with triangular waveforms and sinusoidal voltages are formed in inverter mode of operation. While in rectifier mode, switches operate with anti-parallel diodes such as to have rectifier operation. Details of PWM are found in [38].

Converter should not operate in over modulation. In over modulation peak of control voltage is allowed to exceed the peak of triangular waveform. Because of this, switches will be on or off at the period in which reference voltage is above or beneath the triangular voltage signals which causes the instability in the system. So the modulation index ma should be less or equal to 1. Frequency modulation ratio ‘ m_f ’ is defined as:

$$m_f = \frac{f_s}{f_1} \tag{4.30}$$

Where f_s = the switching frequency of converter.

And f_1 is the switching frequency of triangular waveform.

Figure 4.17: show s the per phase output voltage with PWM for mf=0.8.

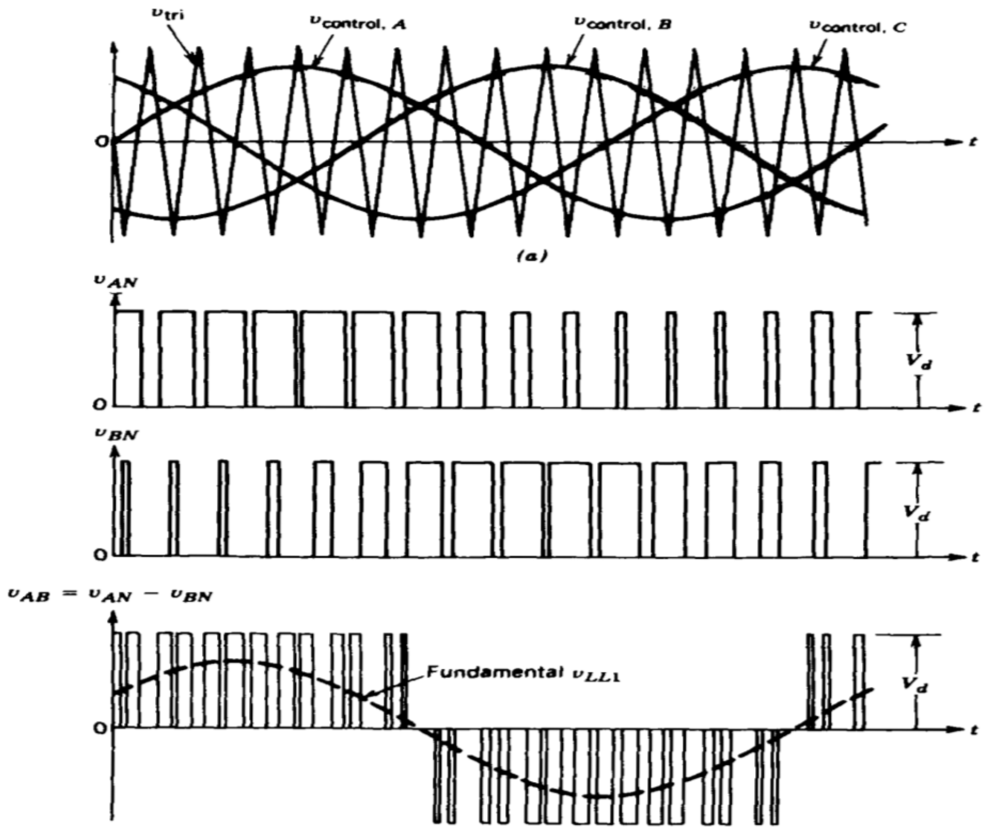

Figure 4. 17: Per phase representation of PWM technique **[38]**.

Summary

In this chapter, network model has been proposed with distributed loads and telecom sites connected to the AC distribution system. It is shown that the active rectifiers have been used as utility interfaces until today but with the development of power electronics, it has become possible to replace rectifiers with bi-directional AC/DC converters which will enable the two way flow of power. Various specifications for different elements such as AC source, Telecom sites, network lines, passive loads and bridge rectifier loads have also been given and explained.

AC source is assumed to be low voltage three phase ideal/non-ideal voltage source. To analyse the converter performances for peak hours load demand, additional three phase and single phase distributed loads are recommended to connect when required. On DC side of the converters, Lithium Ion battery bank is connected because of the high efficiency.

Methods are proposed to introduce artificial distortion and phase un-balance in the supply voltage. A complete algorithm is explained in details to control the utility interface in which vector control principal is applied because it helps to obtain fast dynamic response and to achieve independent control of active and reactive powers. Moreover, it is explained that this method can also be used when more than one Telecom sites are connected to the grid. PWM switching pattern is selected to achieve desired results with MOSFETs as switching devices due to advantages such as fast switching frequency and low on state switching losses.

Chapter 5: Power Quality Improvement: Results and Discussion

Non-linear and passive loads connected to the network draw harmonics and reactive power which cause voltage distortion and grid instability. Control strategies of power electronic interfaces mentioned in Chapter 4 for telecom sites can be used to enhance grid power quality measures. In this chapter, a network model shown in the Figure 4.1 was implemented in the software MATLAB/SIMULINK® to study the impact of power flow with PE interfaces. Different Simulations were carried out for LV AC distribution system with ideal and non-ideal voltage supply. Passive loads and non-linear loads are connected to the grid supply directly and with bridge rectifiers respectively. Telecom sites are also connected with the grid supply, different cases are developed in accordance with number of telecom sites connected to the grid and how do they contribute to address different grid power quality issues.

5.1. Case 1: One VSC for the mitigation of harmonics

Figure 5.1 shows the block diagram for one telecom site connected to the grid. Battery bank supplies power to the DC telecom load via a DC/DC converter between battery bank and telecom load.

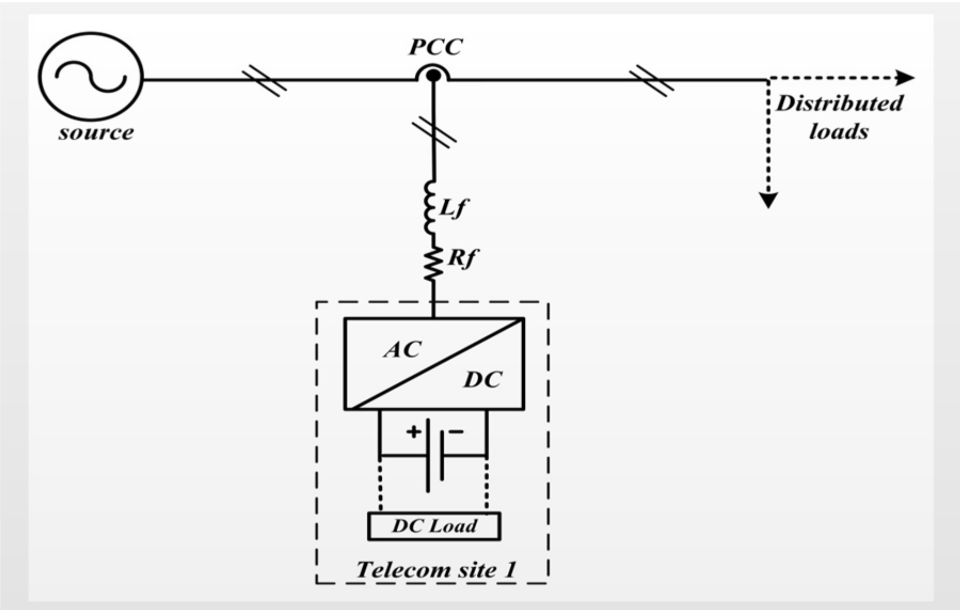

Figure 5. 1: One Telecom site connected to distribution network

Power electronic interface is responsible for addressing the grid quality issues in addition to maintaining the capacity of battery banks for telecommunication services. PI regulators are tuned for controlling the reference current and converter current. The optimal values of *Kp* and *Ki* are given as:

Kp= 9 and *Ki* = 350

Simulation models with proper control scheme for one converter are given in the **Appendix [D.1]**.

5.1.1 Converter performance for harmonics compensation

Different simulations were performed for the rated values of the grid voltage. Non-linear and passive loads parameters as given in the section 4.3, are connected as distributed loads. Supply voltage is 398 [$V_{L\text{-}L,rms}$], the simulation time is 1.5 sec. and converter starts supplying currents at time t=0.4 sec. Simulations results for source current and converter current, before and after the VSC is connected are shown in the Figure 5.2.

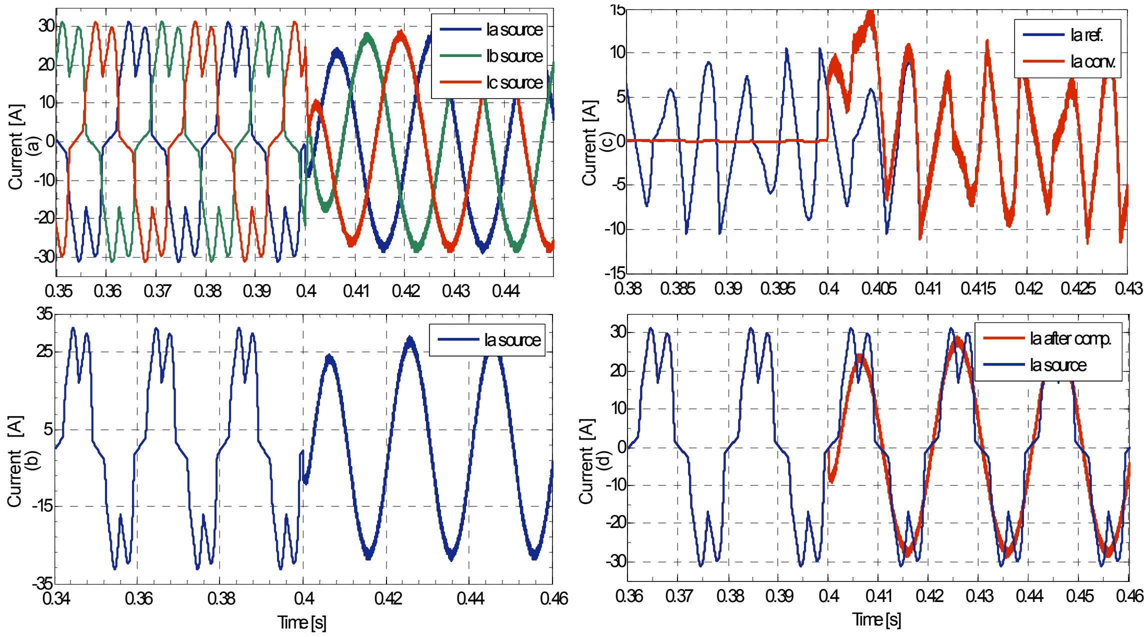

Figure 5. 2: Grid supply and converter currents: (**a**), Three phase source current. (**b**), Source current for the phase ‘a’. (**c**), Reference current and converter current for phase ‘a’. (**d**), Source current at PCC for phase ‘a’.

As the grid voltage supply is three phase AC supply and three phases of supply line are identical to each other. So, it is better and simple to study only single phase instead of all three phases [38]. Converter starts supplying the calculated currents when it is connected to the grid at PCC. Source current is same as that of load current.

In Figure 5.2 (**a**), three phases of the source currents are shown before and after the converter is connected at PCC. It is shown that the source current is distorted and drawing the harmonics before the converter is connected and when converter starts supplying the exact opposite amount of harmonics current at time t=0.4 sec., the source current becomes three phase pure sinusoidal in which each phase displaced by 120^0. Figure 5.2 (**b**), shows the single phase representation of the source current for phase ‘a’. Since all the properties of three phases in a distribution network are identical to each other. So, in this case we will study one phase for simplicity.

Figure 5.2 (**c**) shows the harmonic contents in the phase 'a' of current supplied by the source and current supplied by the converter for phase 'a'. In Figure, *'Ia ref.'* is the harmonic current component of source phase 'a' which acts as the reference current for the converter and *'Ia conv.'* is the current supplied by the converter for phase 'a'. SAF starts supplying current at time t=0.4 sec. It is clear from the Figure that the converter strictly follows the reference and supplies exactly same amount of current as required by the reference current. The peak amplitude of the reference current is $\pm$ 10 [A]. When converter starts supplying the harmonics contents in the source current at PCC, the source current becomes pure sinusoidal. Phase 'a' representation of the source current before and after the converter is connected are shown in the Figure 5.2 (**d**).

Fast Fourier Transform (FFT) Analysis

FFT analysis was performed for the harmonic contents in the source current. Simulations were performed for the supply voltage 398 [V_{rms}] at the frequency of 50 [Hz], simulation time is 1.5 seconds and converter starts working at time t=0.4 sec. Table 5.1 shows the magnitudes of different harmonic contents before and after the VSC is connected to the grid supply.

Parameter	**Harmonic contents before VSC is connected**	**Harmonic contents after VSC is connected**
Fund. 27.44 [A_{peak}]	100%	100%
I_{5th} [% of I_1]	25.99%	0.14%
I_{7th} [% of I_1]	8.64%	0.43%
I_{11th} [% of I_1]	5.67%	0.12%
I_{13th} [% of I_1]	5.40%	0.07%
I_{17th} [% of I_1]	5.30%	0.09%
I_{19th} [% of I_1]	1.58%	0.03%
T.H.D	28.27%	1.35%

Table 5. 1: FFT Analysis for the source current

Table 5.1 shows the harmonic contents in the source current before and after the converter is connected to the distribution network. It is shown that the Total Harmonics Distortion (THD) has been considerably reduced from 28.27% to 1.35% when VSC starts supplying the opposite harmonics at PCC. Table also shows that the major harmonic current components are 5^{th}, 7^{th}, 11^{th} and 13^{th} order harmonics and they are reduced from 25.99%, 8.64%, 5.67% and 5.4% to 0.14%, 0.43%, 0.12% and 0.07% respectively. These are percentages of harmonic contents for different order harmonics are quite within the permissible limits defined in the IEEE, IEC standards [26], [40].

5.1.2 Reactive Power and harmonics Compensation

In the section 5.1.1, harmonics drawn by the non-linear loads were mitigated by injecting same amount of currents with the help of VSC connected to the grid at PCC. VSC is connected in parallel to the grid lines and is supplied by battery storage. Vector Control strategy of the converter also allows the compensation of reactive power, drawn by the line commutated three phase rectifiers, passive loads and the reactance of the lines.

Simulations were performed for the rated grid voltage. Simulation time is 1.5 seconds and VSC is connected at time t=0.4 sec. 13 [kW] of distributed load is connected with the supply which includes non-linear loads and passive loads. Simulation results for source voltage, source current and converter current, before and after the VSC is connected at PCC are shown in the Figure 5.3.

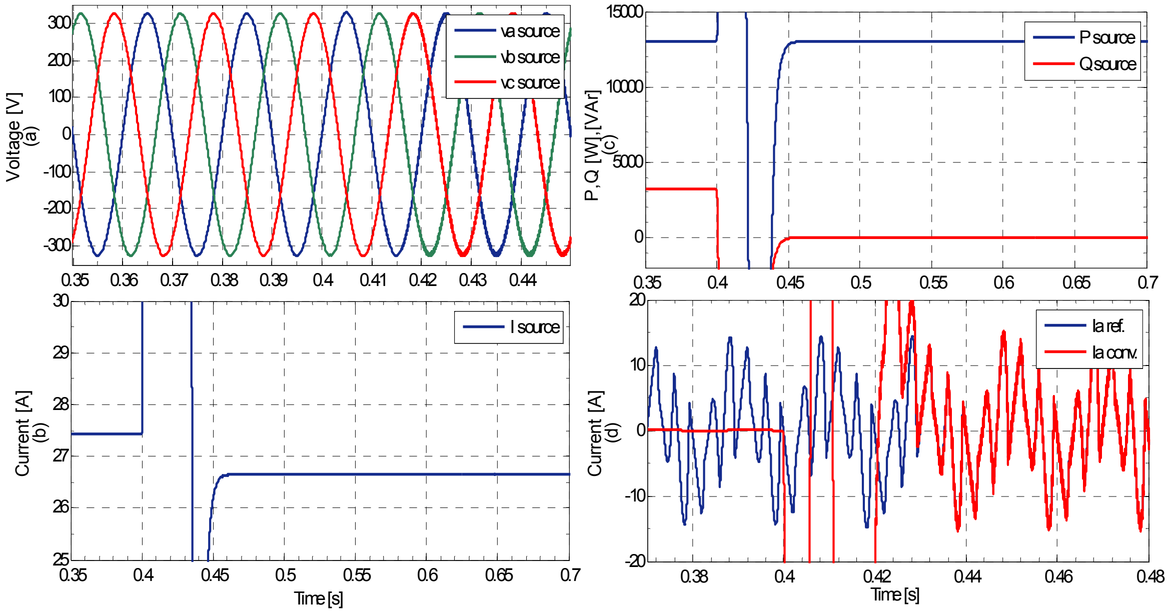

Figure 5. 3: Grid supply and converter performance: (**a**), Three phase supply voltage. (**b**), Current drawn by load connected with the grid. (**c**), Active and reactive powers drawn by the distributed loads. (**d**) Phase 'a' of reference current and the converter current.

Supply voltage is same before and after the VSC is connected to grid. The magnitude of the gird voltage is 398 [$V_{L-L,rms}$]and three phases are displaced by 120^0. Grid voltages are shown in the Figure 5.3 (**a**). It is also shown in the Figure 5.3 (**b**) that the magnitude of supplied current is 27.5 [A] before the converter is connected at PCC. After the converter's grid connection, supply current is reduced from 27.5 [A] to 26.7 [A]. This shows that now the reactive and oscillating current components are being supplied by the VSC and the source current magnitude is reduced by 0.8 [A].

Figure 5.3 (**c**) represents that the magnitude of active power and reactive power absorbed by the load connected to the grid. It is clear from the figure that the active power remains the same before and after the VSC is connected at time t=0.4 sec. and the total active power absorbed by the load is given as 13 [kW]. However, the reactive power is reduced from 3.1 [kVAr] to zero after the connection of SAF at PCC. 100% compensation of reactive power shows that the control of VSC is working according to our requirements. Figure 5.3 (**d**) shows the current required for the compensation of harmonics and reactive power, and the current supplied by the VSC. *'Ia ref.'* shows the phase 'a' of the required current and *'Ia conv.'* shows phase 'a' of the current supplied by the converter. It is clear from the figure that the peak amplitude of the current is $\pm$ 15[A] and converter strictly follows the reference current.

FFT Analysis

FFT analysis was performed for one VSC connected to the LV distribution network, compensating harmonics and reactive power. It showed that the THD was reduced from 26.65% to 2.45% when SAF was connected to the grid at time t=0.4sec. It also showed that the major current harmonic components were considerably reduced e.g. I^{5th}, I^{7th}, I^{11th} and I^{13th} were reduced from 25.99%, 8.64%, 5.67% and 5.40% to 0.46%, 0.51%, 0.16% and 0.03% respectively. Graphical representation for FFT analysis is given in the **Appendix [D.2].**

5.2. Case 2: one converter under unbalanced & distorted voltages with balanced load

Simulations were performed for the rated grid voltage at 398 [$V_{L\text{-}L,rms}$]. The unbalanced and distortion has been introduced in the supply voltage as described in the section 4.2. Three phase balanced load is connected as distributed load which includes bridge rectifier load and passive load. Sum of loads is 17 [kW]. Simulation results are shown in the Figure 5.4, simulation time is 1.0 second and the converter is connected at time t=0.5 sec.

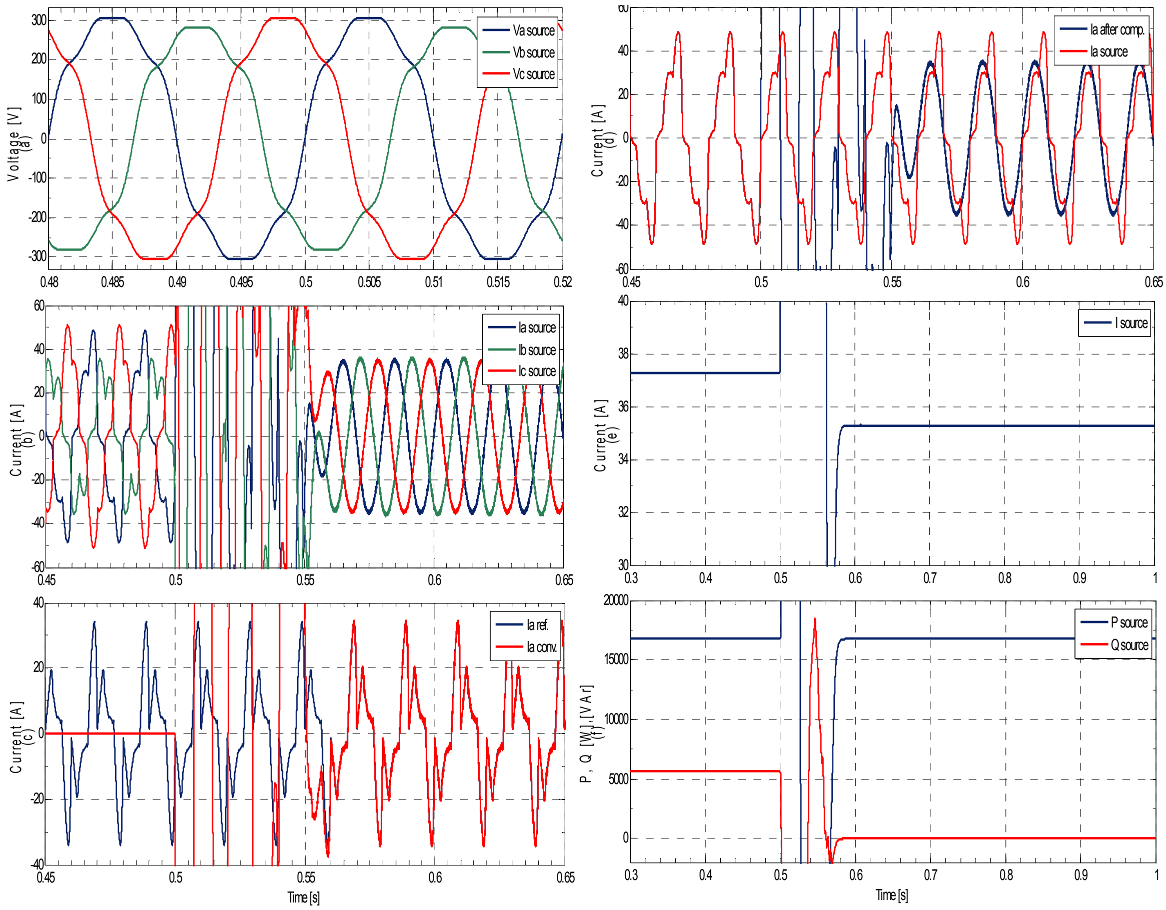

Figure 5. 4: Grid supply parameters and converter performance: (**a**), Three phase voltage supply voltage. (**b**), Three phase load current. (**c**), Converter performance for phase ‘a’. (**d**), Source and load current for phase ‘a’. (**e**), Magnitude of source/load current, (**f**), Active and reactive powers drawn by the distributed load.

Three phase representation of the voltage is given in the Figure 5.4(**a**). It is shown that the voltage remains the same before and after the converter is connected to the network. Figure

5.4(**b**) shows the three phase grid supply current. It is clear from the Figure that before the connection of SAF, the supply current is highly distorted but when converter starts working, current becomes pure sinusoidal. This shows that the control of converter is working properly when it is connected at time t=0.5 sec. Figure 5.4(**c**) represents the phase 'a' of current supplied by the converter. It is clear that converter current is strictly following the reference current.

Phase 'a' representation of load/source current is given in the Figure 5.4(**d**). Figure shows that load is drawing highly distorted current but it becomes pure sinusoidal when VSC is connected at PCC. When VSC starts supplying reactive and oscillating current components, the magnitude of supply current is decreased by 2 [A] as shown in the Figure 5.4(**d**). the converter control is working according to our requirements, the reactive power drawn by the distributed load becomes zero when it is connected at PCC. Figure 5.4(e) is the representation of source active and reactive power. It is clear from the Figure that active power drawn by the connected load remains the same both before and after the connection of VSC while the reactive power has reduced to zero from 5.67 [kVAr].

FFT Analysis

FFT analysis was performed for the harmonic contents in the source current. Simulations were performed for the supply voltage 398 [$V_{L\text{-}L,rms}$]. Table 5.2 shows the percentage of different harmonic components before and after the VSC is connected to the grid supply.

Parameter	**Harmonic contents before VSC is connected**	**Harmonic contents after VSC is connected**
Fund.	100%, 39.5 [A_{peak}]	100%, 35.41 [A_{peak}]
I_{3rd} [% of I_1]	20.80%	1.93%
I_{5th} [% of I_1]	20.91%	0.19%
I_{7th} [% of I_1]	6.77%	0.23%
I_{9th} [% of I_1]	4.18%	0.05%
I_{11th} [% of I_1]	3.97%	0.12%
I_{13th} [% of I_1]	5.84%	0.06%
I_{15th} [% of I_1]	5.40%	0.02%
I_{17th} [% of I_1]	1.12%	0.04%
T.H.D	31.14%	2.27%

Table 5. 2: FFT Analysis for the source current

Table 5.2 shows the harmonic contents in the source current before and after the converter is connected to the distribution network. It is shown that the Total Harmonics Distortion (THD) has been considerably reduced from 31.14% to 2.27%. The major harmonic components are 3^{rd}, 5^{th}, 7^{th}, 9^{th}, 11^{th} and 13^{th} and they are reduced from 20.80%, 20.91%, 6.77%, 4.18%, 3.97% and 5.84% to 1.93%, 0.19%, 0.23%, 0.05%, 0.12% and 0.06% respectively. It is seen that 3^{rd} harmonic has major contribution due to artificial injection.

5.3. Case 3: one converter under unbalanced & distorted voltages with unbalanced load

In the previous section, simulations were performed under unbalanced and distorted voltage conditions with balanced three phase load. Here an unbalanced additional single phase diode bridge is connected between the phase ‘a’ and phase ‘b’. Simulation results for the given load conditions are given as:

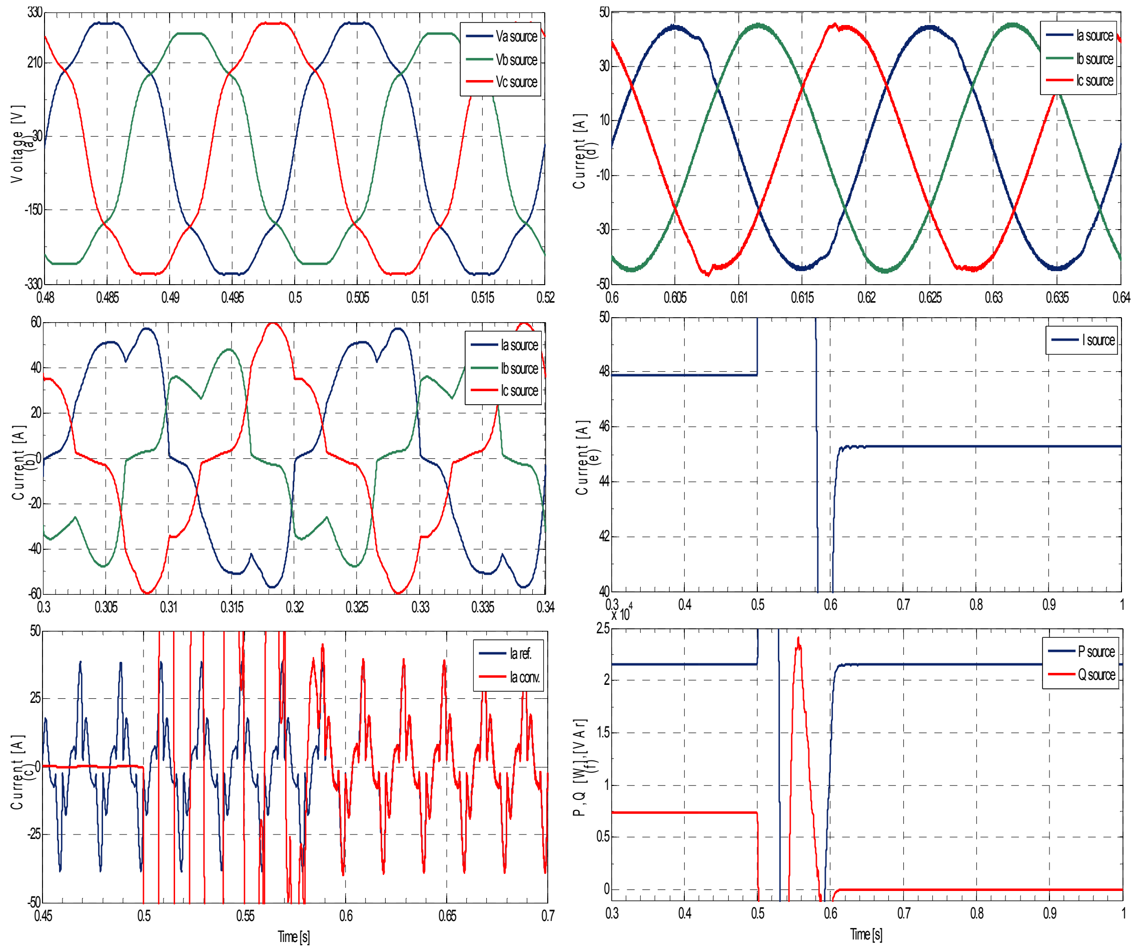

Figure 5. 5: Distribution network and VSC parameters: (**a**), Three phase supply voltage. (**b**), Three phase source current. (**c**), Converter performance. (**d**), source current for phase after compensation. (**e**), Magnitude of supply current. (**f**), Magnitudes of source active and reactive powers.

Fundamental of the source voltage is separated with positive sequence detector and the the distortion in the source voltage is removed with the help of Low Pass Filter (LPF). Simulation time is 1.0 second and converter is connected at time t=0.5 sec.

With unbalanced and distorted voltage condition, source is supplying current to the balanced load and unbalanced load. 5.5 (**b**) shows that the three phases of source current are not sinusoidal, but when converter starts operation at time t=0.5 sec. it becomes pure sinusoidal as shown in the 5.5 (**d**). VSC is working according to the requirements and is following its reference signals strictly. 5.5 (**c**) is representation of the converter performance for phase ‘a’, which shows that converter currents are same in magnitude and direction as required by the control parameters. Since there is an extra unbalanced load of 5 [kW]. So it is drawing a total current of 47.9 [A] before the converter starts working but when SAF is connected at PCC, the magnitude of supply current is decreased by 2.7 [A]. This is less than before because now the oscillating and reactive current is supplied by the shunt connected converter.

Source current magnitude is shown in the 5.5 (**e**). One of our requirements for controlling the converter is that the reactive power should become zero. 5.5 (**f**) shows that it has become zero when VSC starts its operation and there is no effect on active power supplied by the distribution grid.

Circuit diagram for the additional load is mentioned as:

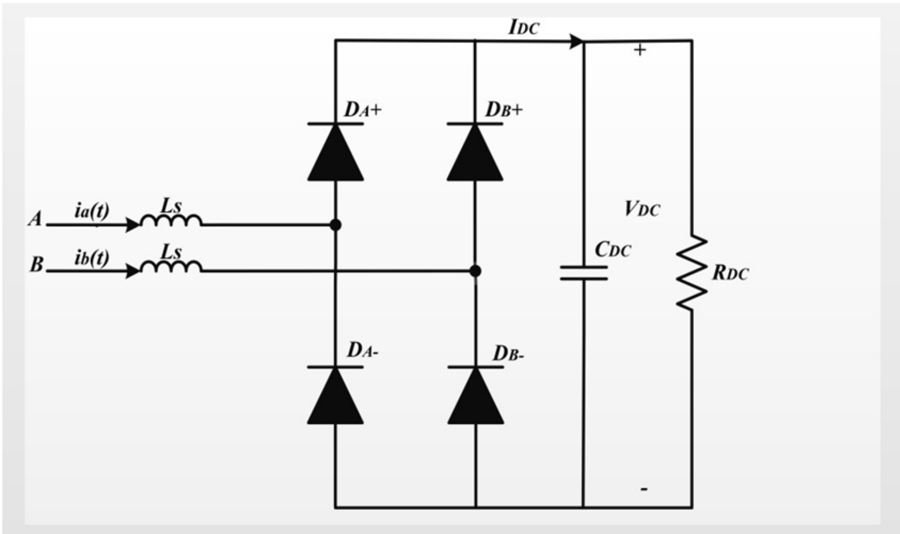

Figure 5. 6: single phase Diode Bridge

FFT Analysis

FFT Analysis was performed to see the contents of different harmonics in the source current when the source is not only distorted and unbalanced but the load as well. Figure 5.7 shows the graphical representation of FFT Analysis for both before and after the connection of SAF.

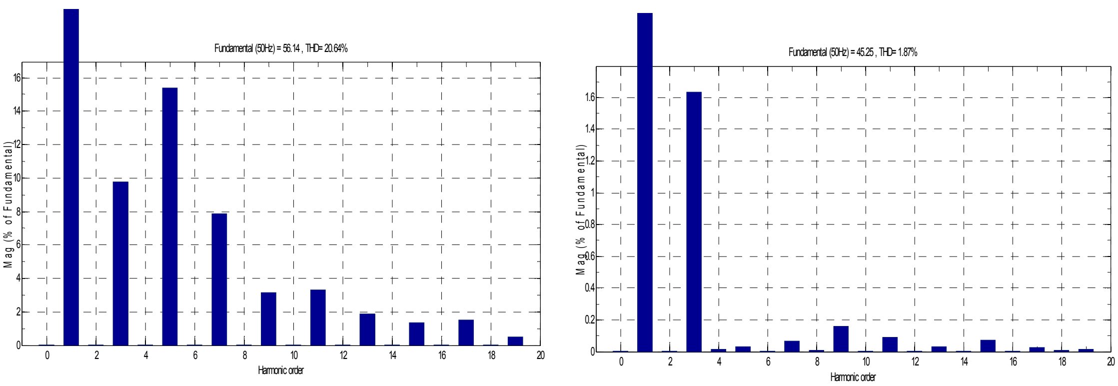

Figure 5. 7: THD for before and after the VSC started compensation

Figure 5.7 shows that the THD was reduced to 1.91% from 20.64% when VSC started working. Some major harmonic components e.g. 3^{rd}, 5^{th}, 7^{th} and 9^{th} order harmonics were reduced from 9.77%, 15.41%, 7.84% and 3.16% to 1.64%, 0.03%, 0.07% and 0.16% respectively.

5.4. Case 4: Two Telecom sites under balanced load and balanced source Conditions

Telecom sites are located close to each other. In this model two telecom sites are connected to the LV distribution lines and supposed to be located 100m apart, inductance and resistance between these sites are considered to be 0.1 [mH] and 0.01 [mΩ] respectively. An additional load is connected as a distributed load with network supply. Block diagram for this network is given below.

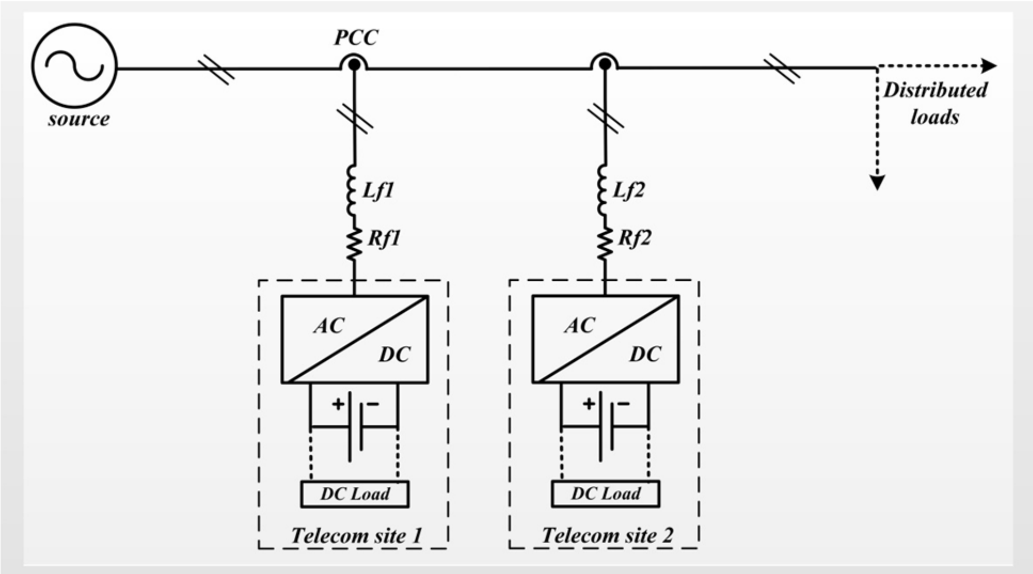

Figure 5. 8: Two Telecom sites connected to the LV AC distribution network

5.4.1. Harmonics and reactive power compensation

Control structure of two Telecom sites have been explained in the chapter 4 and simulation model is given in the **Appendix [D.3].** PI regulators were tuned manually and they give optimal results on these values for both the telecom sites.

Kp=13

Ki=600

Simulations were performed for the rated Grid voltage and frequency of 50 [Hz]. Simulation time is 1.0 second and the converters are connected at PCC at time t=0.4 sec. results are shown for both before and after the converters start working.

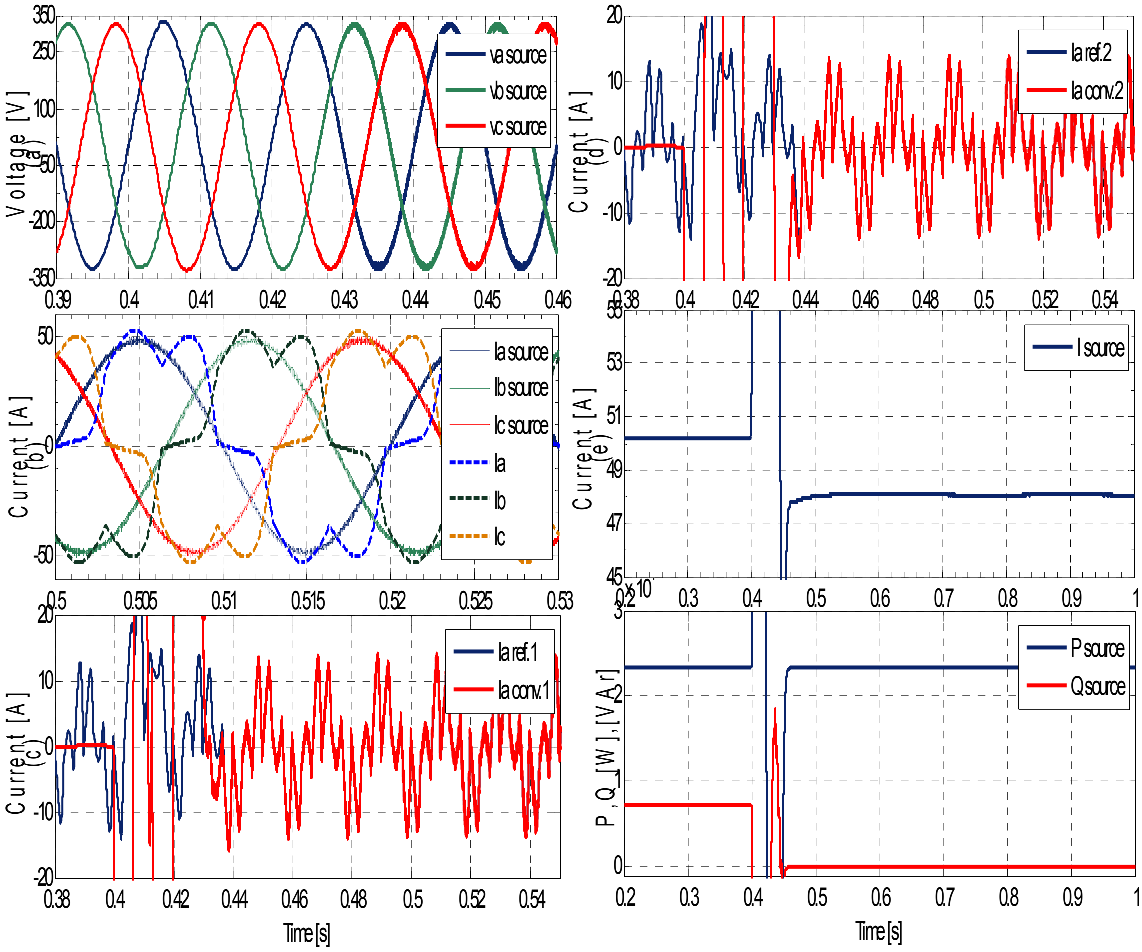

Figure 5. 9: Network and Converter Parameters: (**a**), Three phase supply voltage. (**b**), Three phase source/load current. (**c**), Performance of converter 1. (**d**), Performance of converter 2. (**e**), Magnitude of supply current. (**f**), Magnitudes of source active and reactive powers.

For the balanced three phase grid supply, voltage of distribution network remains the same before and after the converters start working. Figure 5.9 (**a**) shows the grid voltages. It is clear from the Figure that the voltages are pure sinusoidal before and after the time t=0.4 sec. Figure 5.9 (**b**) demonstrates the source/load current before and after compensation. Solid lines present three phases of source current after the compensation while three phases of current drawn by connected loads are explained by the dotted lines. It is well defined from the Figure that supply current has become pure sinusoidal at the point of connection of VSCs at time t=0.4 sec. In our network, the objective of two SAFs is to share the reactive and oscillating current components equally. From Figures 5.9 (**c**) and 5.9 (**d**), it is clear that the phase 'a' reference current is provided by the two equal sources e.g. the peak of reference current is 26 [A] and the peak current provided by each converter is 13 [A]. These currents are injected when the PE interfaces start their operation at point 0.4 sec.

The magnitude of grid current is reduced by 5.1 [A] when the converters are coupled at PCC at time t=0.4 sec. source current magnitude is given in the Figure 5.9 (**e**). It is evident from the Figures 5.9 (**c**) and 5.9 (**d**) that converters are working perfectly, so the reactive power drawn from the source becomes zero when they are connected with the grid supply.

Figure 5.9 (**f**) shows that the active power remains the same before and after the connectivity of converters while the reactive power drops down to zero which indicates the perfect performance of the SAFs.

FFT Analysis

In this section, two VSCs or telecom sites are coupled with the distribution network and mitigation of current harmonics depends upon the proper working of these VSCs. FFT Analysis was performed in order to observe the harmonic contents in the source current. Table 5.3 summarizes the results for harmonic contents in the source current for both before and after the operation of converters.

Parameter	**Harmonic contents before VSC is connected**	**Harmonic contents after VSC is connected**
Fund.	100%, 50.2 [A_{peak}]	100%, 48.0 [A_{peak}]
I_{5th} [% of I_1]	21.11%	0.15%
I_{7th} [% of I_1]	6.52%	0.19%
I_{11th} [% of I_1]	3.65%	0.05%
I_{13th} [% of I_1]	5.63%	0.12%
I_{17th} [% of I_1]	1.23%	0.07%
I_{19th} [% of I_1]	0.99%	0.04%
T.H.D	25.64%	2.31%

Table 5. 3: FFT Analysis for the supply current

It is shown that THD has been considerably reduced from 25.64% to 2.31% when VSCs start supplying the opposite harmonics at PCC. Table also shows that the major harmonic current components are 5^{th}, 7^{th}, 11^{th} and 13^{th} order harmonics and they are reduced from 21.11%, 6.52%, 3.65% and 5.63% to 0.15%, 0.19%, 0.05% and 0.12% respectively.

5.5. Case 5: Two converters under balanced load and unbalanced source Conditions

In this case, source conditions are the same while one converter is replaced by two with the same capacities, compensation of reactive and oscillating current components will be achieved by sharing required amount of current between these two active filters equally.

Simulations were performed for the grid voltage 398 [$V_{L-L,rms}$]. Simulation time is 1.5 seconds and the converters are connected at the time t=0.5 sec. Results are shown for the compensation of reactive power and harmonics in the source current.

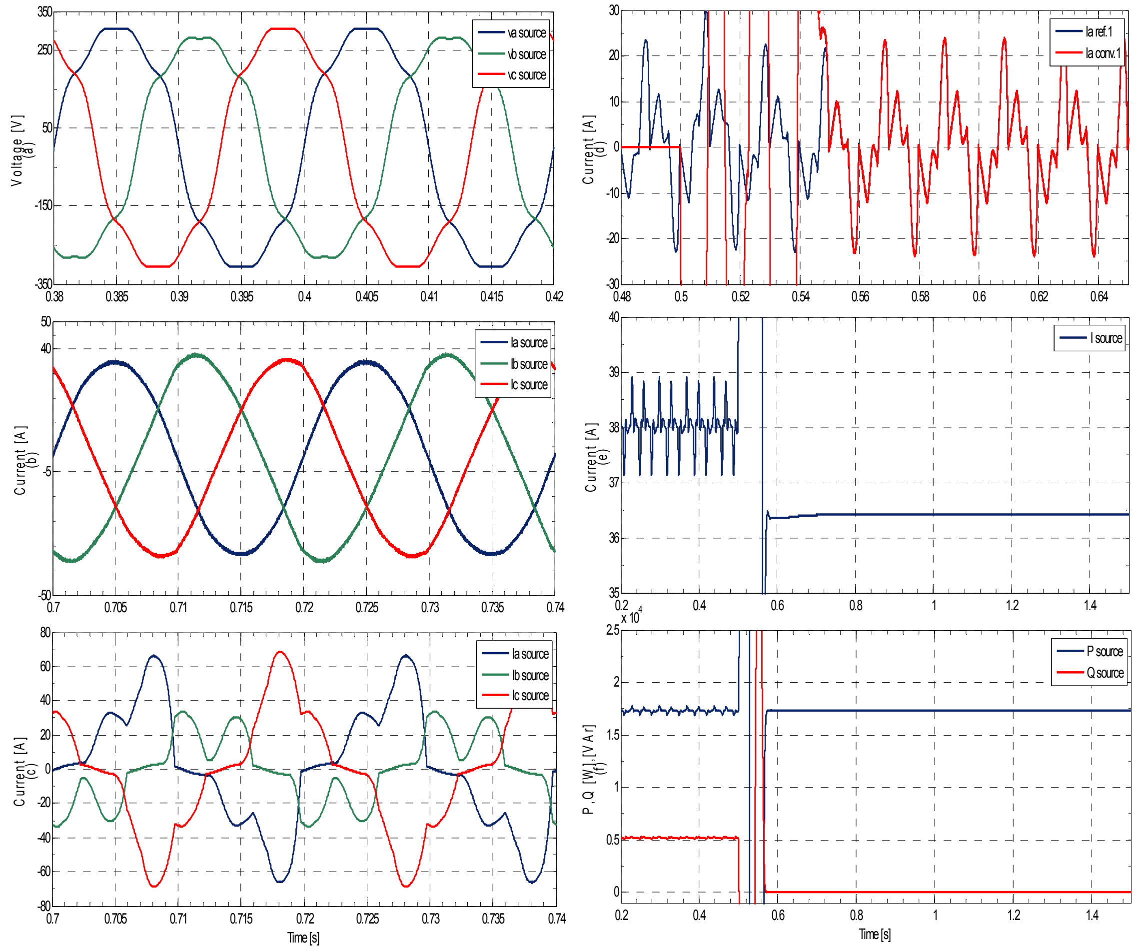

Figure 5. 10: Distribution Network and Converter Parameters: (**a**), Three phase supply voltage. (**b**), Three phase source/load currents after compensation. (**c**), Three phase source/load currents before compensation. (**d**), Performance of converter 1. (**e**), Magnitude of source current. (**f**), Magnitudes of active and reactive powers consumed by the load.

Unbalance and distortion in the supply network by reducing the phase ‘b’ voltage and by adding 3^{rd}, 5^{th} and 7^{th} harmonics artificially in the source. Figure 5.10 (**a**) illustrates three phase voltages of the distribution network. It shows that the phase voltages are distorted in nature and they are not making pure sinusoidal waveforms.

Non-linear loads connected with distribution network are the major source of current harmonics but this is a severe case in which loads as well as source causes the distortion which makes the supply current even more distorted as shown in the Figure 5.10 (**c**). It shows the three phases of source/load current before they were compensated. After the telecom sites start feeding the grid with harmonics and reactive current, three phases of the load current become sinusoidal, displaced by 120^0 from each other as shown in the Figure 5.10 (**b**).

In this case both of telecom sites are sharing the required current equally. Each converter is supplying half of the reference current. Figure 5.10 (**d**) demonstrates the phase ‘a’ of the reference current and the phase ‘a’ of the supplied current.

It is clear from the Figure that converter is supplying half of the reference current and is in phase with the reference signal. Due to distortion and disturbance in the source of the supply network, current becomes severely distorted and the magnitude was oscillating between 37 [A] and 39 [A]. These kinds of oscillations cause troubles for the other loads connected in the network. But after the converters start working, source current waveforms become sinusoidal and the magnitude flattens at 36.4 [A] as shown in the Figure 5.10 (**e**). Figure 5.10 (**f**) shows active and reactive powers of the supply network both before and after the converters are connected at time t=0.5 sec. It is evident from the Figure that active power remains constant at 17.5 [kW] while reactive power goes down to zero when VSCs are connected at PCC.

FFT Analysis

FFT analysis of source current was performed for two telecom sites connected with grid under unbalanced and distorted conditions with balanced load. Simulation war performed with rated grid voltage and frequency. Table in **Appendix [D.4]** summarizes the result from FFT analysis.

Table shows that THD was reduced significantly from 43.01% to 3.42% which is well within the allowable power quality limits It also shows that the major harmonic components e.g. 3^{rd}, 5^{th}, 7^{th}, 9^{th}, 11^{th} and 13^{th} order harmonies were reduced from 30.13%, 28.91%, 4.35%, 6.05%, 3.97% and 4.69% to 3.28%, 0.20%, 0.47%, 0.23%, 0.14% and 0.04% respectively.

5.6. Case 6: Two converters under unbalanced load and unbalanced source Conditions

The grid supply is unbalanced and distorted as discussed for the Case 5 but there is an additional bridge rectifier load shown in the Figure 5.5 is added as a distributed load between the phase 'a' and phase 'b'. Besides this, a passive load described in the section 4.3.1 is replaced by a passive *'RL'* load with Delta connection as shown in the Figure 5.11.

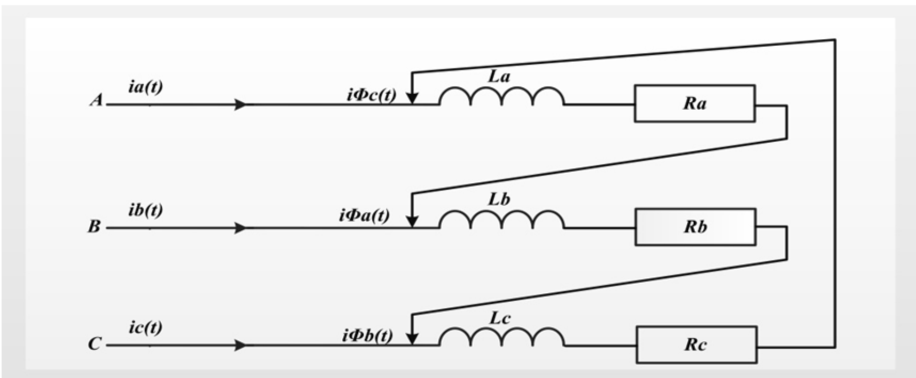

Figure 5. 11: Delta connected Passive Load

Control of telecom sites was achieved by Clark and Park transformation methods with the same PCC. Simulations were performed for the mitigation of harmonics and reactive power with the help of these converters. Simulation time is 1.0 second and the converters start feeding the network at time 0.5 sec. Figure below summarizes the simulation results as:

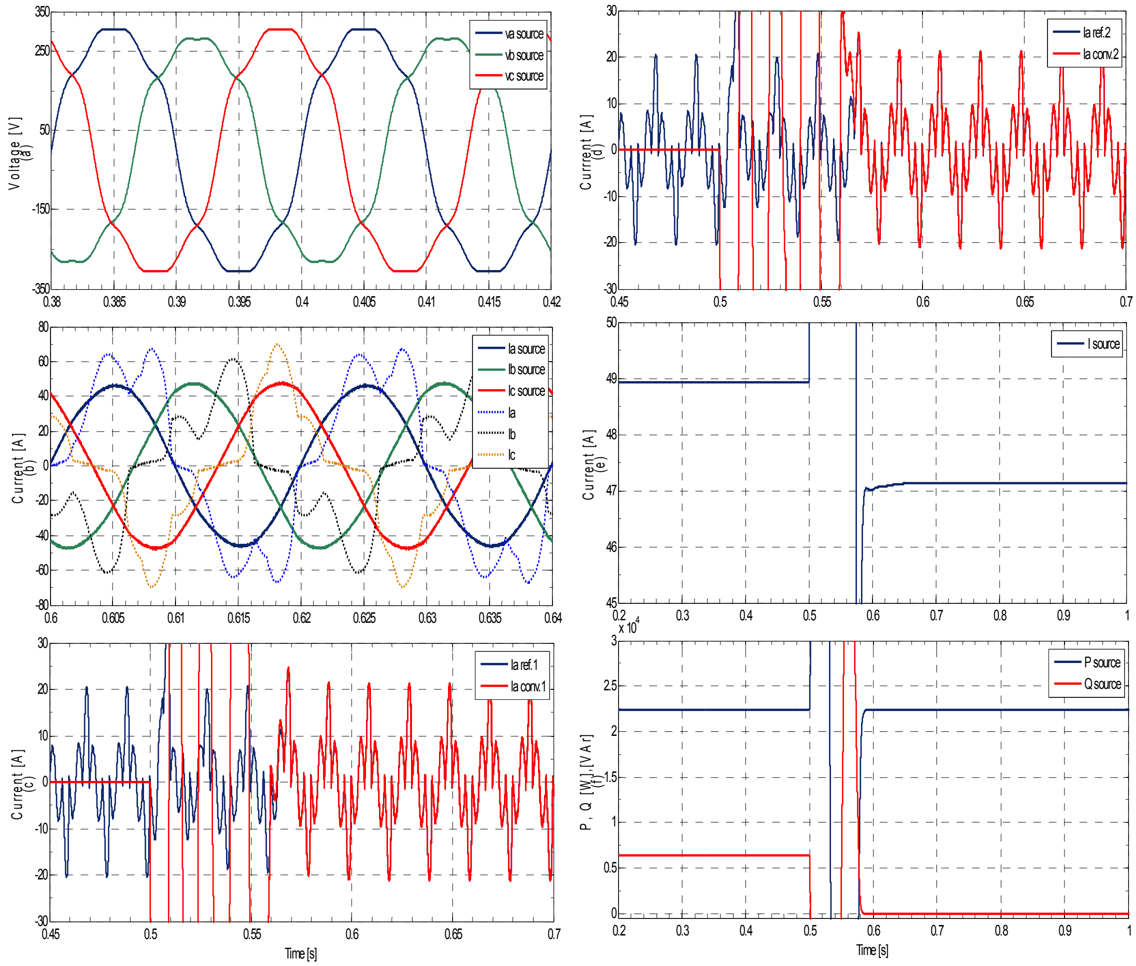

Figure 5. 12: Supply and converters parameters: (**a**) Three phase supply voltage. (**b**), Three phase source/load currents. (**c**), Performance of converter 1. (**d**), Performance of converter 2. (**e**), Magnitude of source current. (**f**), Magnitudes of active and reactive powers.

Due to introduction of harmonic components and phase unbalance in the supply, three phase voltages doesn't remain pure sinusoidal in nature as shown in the Figure 5.12 (**a**). Supply current before and after the compensation at PCC, are shown in the Figure 5.12 (**b**). Solid lines show the source current after compensation and dotted lines show the currents before the mitigation of harmonics and reactive power. It is clear from the Figure that after Telecom sites were connected at time t=0.5 sec, three phases of source current become sinusoidal without any distortion. It is also shown that when the reactive power was supplied by the active filters, Power Factor PF becomes unity. Since two telecom sites are connected with the grid, they share the required amount of current equally. Converters performances are shown in the Figures 5.12 (**c**) and Figure 5.12 (**d**). Figures show that the phase 'a' of the reference signal and phase 'a' of the current provided by the converter are in phase. In addition to it, each converter is supplying half of the total amount of required current. Magnitude of source current is decreased by 2 [A] when converters start working as shown in the Figure 5.12 (**e**).Figure 5.12 (**f**) represents the active and reactive powers drawn by the distributed loads. It is evident from the Figure that reactive power drops down to zero from 6.0 [kVAr] when VSCs start their operation while active power remains the same before and after the connection of converters i.e. 22.5 [kW] which validates the accurate functioning of converter control parameters.

Source Current Harmonics

Harmonic components in the source current are analysed by performing FFT analysis of the current. Simulations were performed for time t=1.0 second and telecom sites are connected with the supply network at instant t=0.5 sec. Results for this analysis is given in the **Appendix [D.5].**

Results show that THD was reduced substantially from 24.19% to major 2.77%. It is also evident that the major current harmonic components are 3rd, 5th, 7th, 9th, 11th and 13th order harmonics. These components were reduced from 6.63%, 21.34%, 7.02%, 3.16%, 3.46% and 1.63% to 1.64%, 0.36%, 0.06%, 0.35%, 0.15% and 0.13% respectively.

5.7. Case 7: Three converters under balanced load and balanced source Conditions

In this case, number of VSCs is increased to three which proves to be very beneficial for the whole system e.g. the current rating of each converter is decreased, the reliability will be increased accordingly. Control of these converters is achieved by Clark and Park transformations with the same PCC, neglecting any load connected to the lines of distribution network, in between these converters. Figure 5.13 explains the block diagram of given network model.

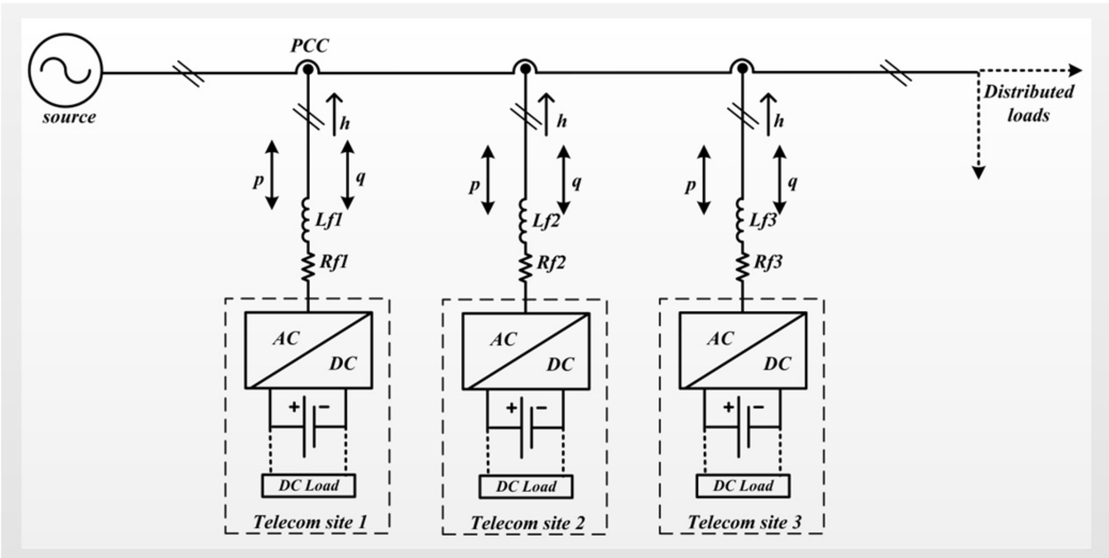

Figure 5. 13: Three Telecom sites connected to the LV AC distribution network

Tuning of PI regulators connected within the control part of converters is done manually. Values Kp and Ki, giving the optimal results are given in Table 5.4.

	Kp	Ki
VSC 1	37	1950
VSC 2	42	1950
VSC 3	37	1950

Table 5. 4: Optimal values of Kp and Ki

An additional 5.5 [kW], Thyrsitor bridge load is connected with the distribution network. Different simulations were performed to analyse the performance of active filters and the effects of their connection to the grid network. Simulation time is 1.0 second and the converters are connected at time t=0.5 sec. Detailed control structural representation is given in the **Appendix [D.6]** and simulation results are given in the Figure 5.14.

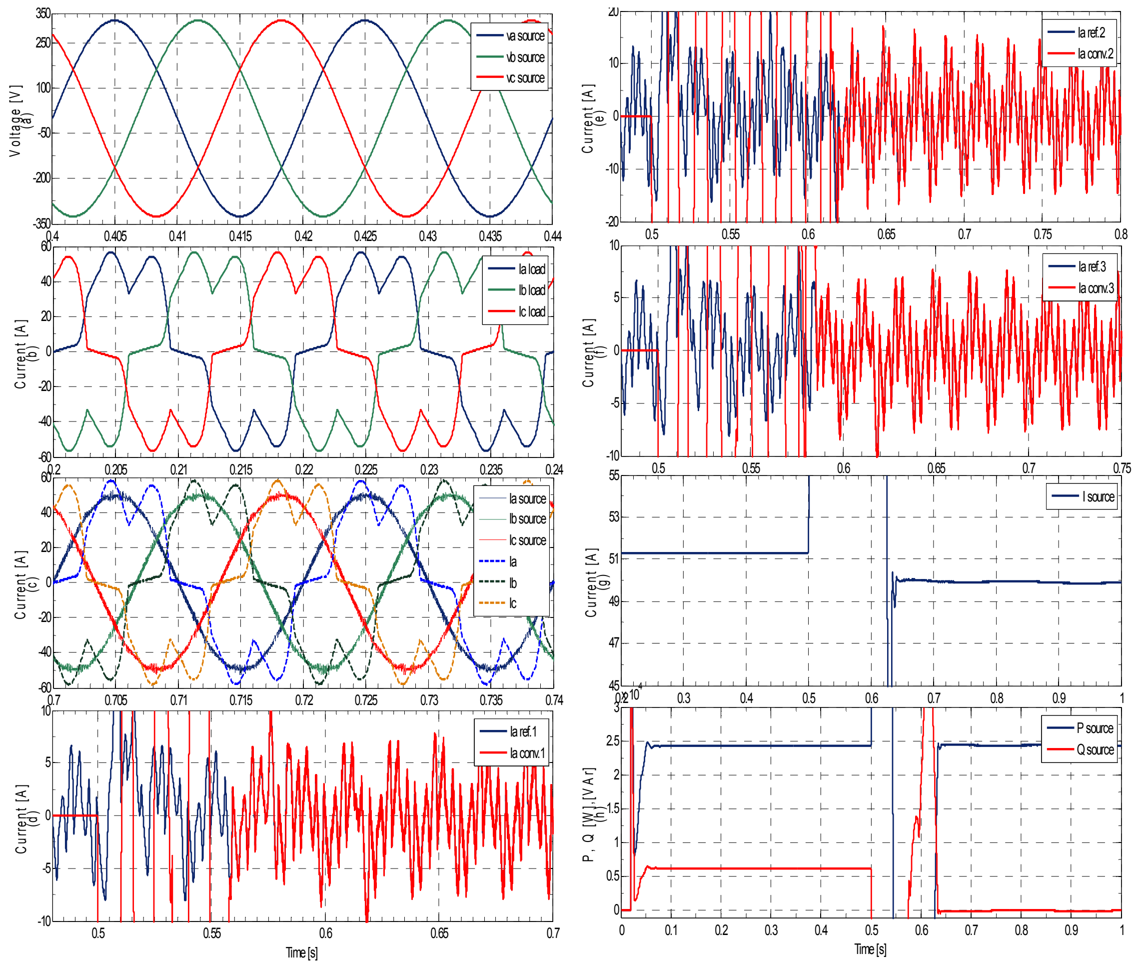

Figure 5. 14: Grid source and converters parameters: (**a**), Three phase supply voltage. (**b**), Three phase load currents. (**c**), Three phase source/load currents. (**d**), Performance of converter 1. (**e**), Performance of converter 2. (**f**), Performance of converter 3. (**g**), Magnitude of source current. (**h**), Magnitudes of active and reactive powers.

In this case, the distribution load is connected with the voltage source which is neither unbalanced nor distorted. Each phase is displaced 120^0 from each other. Three phase representation of source voltage is given in the Figure 5.14 (a). Figure 5.14 (b) shows the current drawn by the load coupled with the distribution grid.

It is clear from the Figures that three phases of source current are not in phase with the supply voltage and connected load is drawing harmonics from the source. Currents drawn by the connected load and compensated source current at PCC are shown in the Figure 5.14 (**c**). Figure shows that after the connection of active filters, source current becomes sinusoidal and in phase with the phase voltage while the load current remains same before and after the working of VSCs. Solid lines represent the compensated current waveforms while dotted lines show the load currents. In our converter control mechanism, it is defined that the converter 2 is responsible for compensating half of the required amount of currents while both converters 1 & 3 share the remaining half equally with each other. Figures 5.14 (**d**), (**e**), and (**f**) show the performance of three converters for the phase ‘a’ only. It is shown in these Figures that the supplied current are in phase and exactly same as that required by the reference signals.

The total current required for the connected load is decreased by 1.2 [A] when converters start supplying the required the currents as shown in the Figure 5.14 (**g**). This is because oscillating and reactive current components are supplied by the active filters when they start working. Active and reactive powers both before and after the operation of VSCs are shown in the Figure 5.14 (**h**), The active power remains same before and after the time t=0.5 sec. while reactive power reduces to zero.

Harmonics Analysis

Harmonic contents in the source current are analysed with the FFT analysis. Table 5.5 summarizes the results from Fourier analysis.

Parameter	**Harmonic contents before VSC is connected**	**Harmonic contents after VSC is connected**
Fund.	100%, 51.3[A_{peak}]	100%, 49.91 [A_{peak}]
I_{5th} [% of I_1]	24.99%	0.73%
I_{7th} [% of I_1]	7.87%	0.08%
I_{11th} [% of I_1]	5.3%	0.05%
I_{13th} [% of I_1]	5.76%	0.26%
I_{17th} [% of I_1]	1.99%	0.43%
I_{19th} [% of I_1]	1.76%	0.22%
T.H.D	27.02%	3.28%

Table 5. 5: FFT Analysis for the source current

Table shows that THD was considerably reduced from 27.02% to 3.28% and the other major harmonic components e.g. 5^{th}, 7^{th}, 9^{th}, 11^{th} and 13^{th} order harmonics were also significantly reduced..

5.8. Case 8: Three converters under balanced load and unbalanced source Conditions

The presences of power electronic devices in the distribution system cause distortion in the supply voltage. In this case, distortion is created by the introduction of 3rd, 5th and 7th order harmonics in the source and unbalance is created by reducing the phase 'b' voltage by 30 [$V_{L\text{-}L,rms}$] and keeping the other phases remains unchanged.

Tuning of PI regulators was done manually and the distributed load same as that of case 7. Simulations were performed for the compensation of harmonics and reactive power. Simulation time is 1.5 seconds and the converter are connected at time t=0.5 sec. The results are given as:

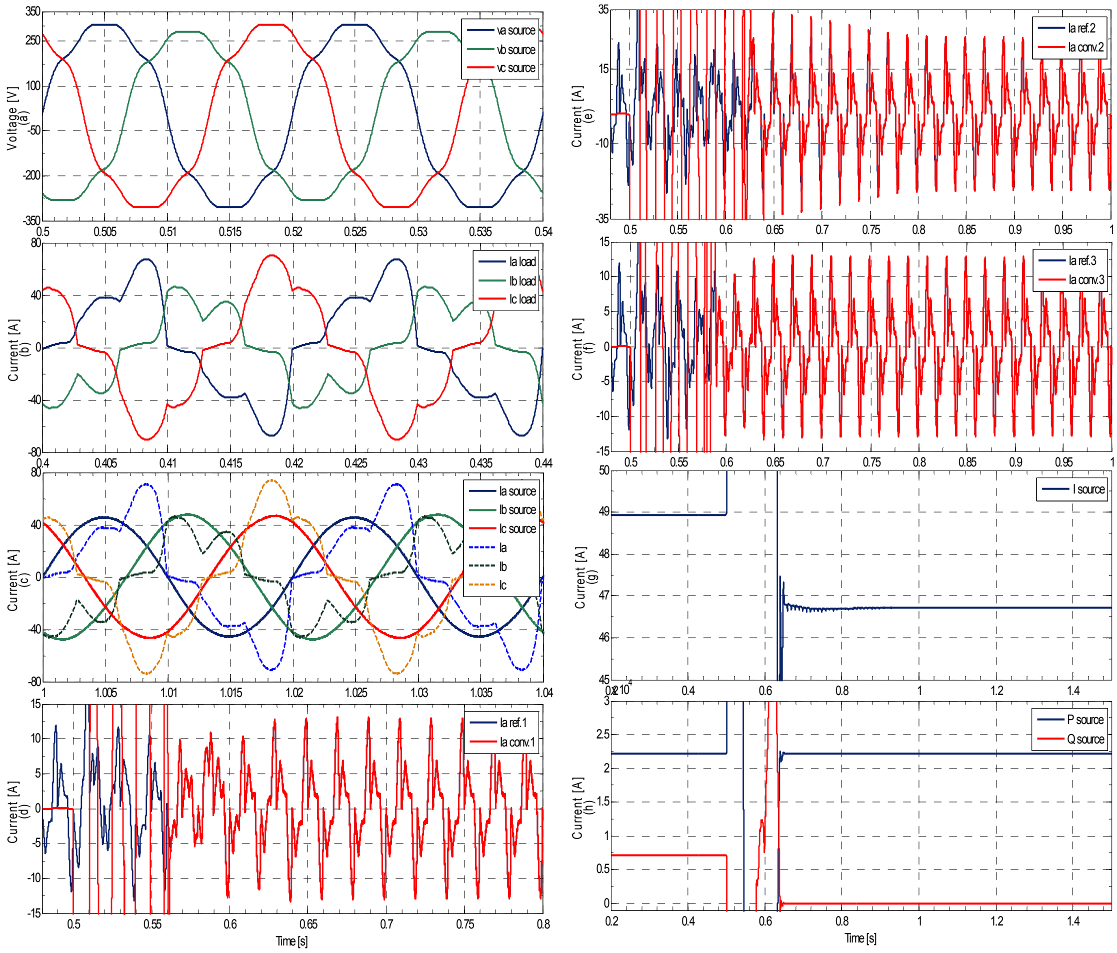

Figure 5. 15: Source and converters parameters: (**a**), Three phase supply voltage. (**b**), Three phase load currents. (**c**), Three phase source/load currents. (**d**), Performance of converter 1. (**e**), Performance of converter 2. (**f**), Performance of converter 3. (**g**), Magnitude of source current. (**h**), Magnitudes of active and reactive powers.

Figure shows the different parameters related to network and the converters. Figure 5.15 (**a**) shows three phase voltage supply. It shows that the voltage is distorted and unbalanced as we have introduced these constraints in our network model. Figure 5.15 (**b**) and 5.15 (**c**) represent three phase source or load currents supplied to the distributed loads. Solid and dotted lines show the source current waveforms before and after the compensation respectively.

It is clear from the Figures that there was distortion in the source current and waveforms were not in phase with the supply voltage but when converters started their operation current became pure sinusoidal with minimum distortion, in addition to becoming in phase with the applied voltage.

Figures 5.15 (**d**), 5.15 (**e**) and 5.15 (**f**) show the performance of connected converters for phase 'a'. It is evident from the figures that converter currents are following the reference signal strictly. Also, converter 2 is supplying the current twice than converter 1 and 3. The magnitude of applied current is shown in the Figure 5.15 (**g**), it is clear from the Figure that current magnitude before compensation started, was 48.9 [A] and after VSCs were connected at time t=0.5 sec. it decreases to 46.6 [A]. This is because oscillating and reactive currents are now being supplied by the converters.

One of basic requirements of our converter control is to compensate the reactive power as well. Figure 5.15 (**h**) shows the active and reactive powers drawn by the connected loads. Figure shows that active power remains the same before and after the time t=0.5 sec. but reactive power falls down to zero which validates our converter control methods.

Harmonics in the source current

Network source has been polluted when different harmonics were introduced. 3rd, 5th and 7th harmonics were introduced in the supply. Fourier Transform Analysis was performed to investigate the level of different harmonics in the source current. Results were obtained and are summarized as follows:

Parameter	**Harmonic contents before VSC is connected**	**Harmonic contents after VSC is connected**
Fund.	100%, 55.5 [A_{peak}]	100%, 46.21 [A_{peak}]
I_{3rd} [% of I_1]	23.72%	1.89%
I_{5th} [% of I_1]	25.55%	0.11%
I_{7th} [% of I_1]	6.70%	0.27%
I_{9th} [% of I_1]	4.69%	0.05%
I_{11th} [% of I_1]	4.09%	0.12%
I_{13th} [% of I_1]	3.14%	0.10%
I_{15th} [% of I_1]	5.59%	0.05%
I_{17th} [% of I_1]	1.17%	0.03%
T.H.D	34.34%	2.91%

Table 5. 6: FFT Analysis for the source current

FFT analysis for the source current shows that THD was reduced from 34.34% to 2.91% which is quite well within the allowable limits. Data also shows that the major harmonic current components are 3rd, 5th, 7th, 9th, 11th and 13th order harmonics and they are reduced from 23.72%, 25.55%, 6.70%, 4.69%, 4.09% and 3.14% to 1.89%, 0.11%, 0.27%, 0.05%, 0.12% and 0.1% respectively.

5.11. Import & Export of Active Power

Simulations were performed for 1, 2 and 3 telecom sites connected to the network to observe the effects of charging and discharging the battery banks by importing and exporting the active power respectively. For simplicity, here results are shown for two telecom sites. Simulation time is 35 sec., converters are connected to the network from the beginning but start their operation at time t=5 sec. Simulation results are given as:

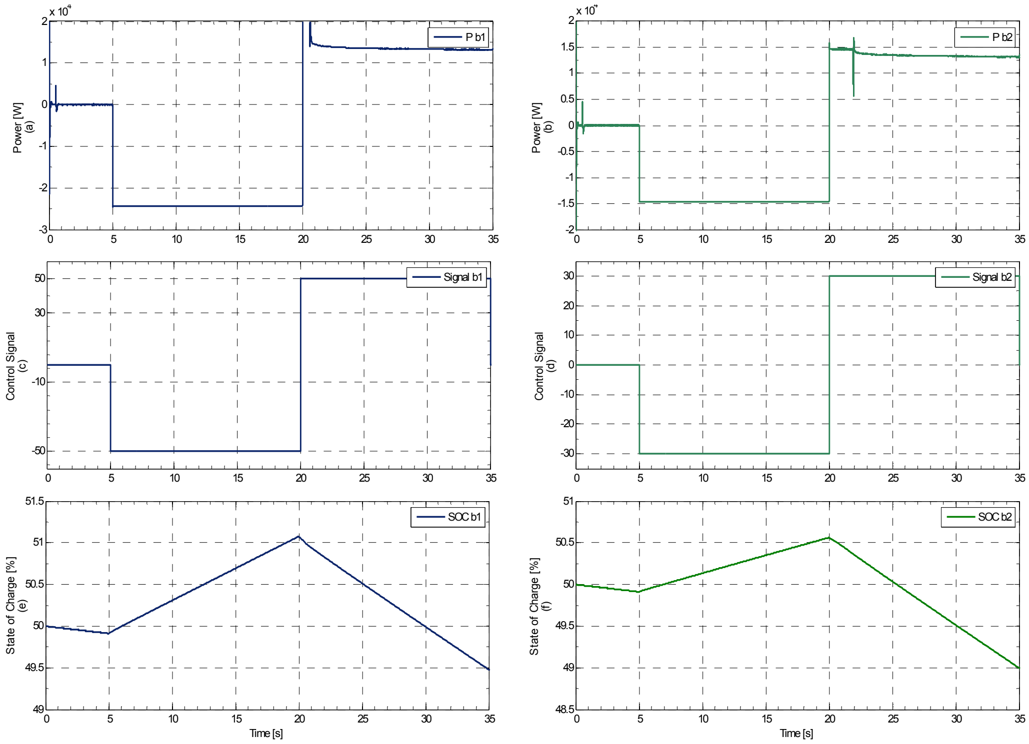

Figure 5. 16: Import and export of active power: (**a**), Import and export for storage unite at site 1. (**b**), control signal provided to the converter of site 1. (**c**), State of Charge for battery bank at site 2. (**d**), Import and export for storage unite at site 2. (**e**), control signal provided to the converter of site 1. (**f**), State of Charge for battery bank at site 2.

Figure 5.16 verifies the performance of Voltage Source Converters for the import and export of active power to recharge and discharge the available surplus active power.

It is shown in the Figures 5.16(**a**) and Figure 5.16 (**b**) that battery banks start absorbing the power at time t=5 sec and it continuous till time instant t=20 sec. During this time batteries 'b1' and 'b2' takes power at the rate of 2.5 [kW] and 1.5 [kW] per time interval respectively. But after time instant t=20 sec, battery banks start exporting power to the grid. The ability of battery bank to consume or inject the active power depends upon the control signal given to these storage units. Figures 5.16(**c**) and Figure 5.16 (**d**) show the control signals provided to the battery bank 1 and battery bank 2.

When active power is given or taken, to or from the grid, State of Charge (SOC), for each battery bank is changed as shown in the Figures 5.16(**e**) and Figure 5.16 (**f**). It is seen that for site 1 that battery bank was charged from 50% to 51.2% during import of active power while battery at site 2 was charged to 50.7%. Similarly, during discharging, states of charge dropped down to 49.5% and 49% respectively for each unit. Charging and discharging depends upon the control signals provided to the Telecom converters. These abilities of bi-directional converters can be used for peak shaving. For example, battery banks can be allowed to recharge during off-peak hours and discharge during peak-hours load demand.

Telecom Load

The battery banks are supplying power for harmonics and reactive power compensation. In addition to this, they can also import or export active power to or from the grid. But during these operations, it is observed that they have always been supplying power to the telecom loads without any interruption.

Summary

In this chapter, various cases have been developed according to number of different loads, types of loads, configuration of loads and number of telecom sites connected to the network. Simulation results were analysed and discussed with the ideal voltage source and non-ideal voltage source. In non-ideal voltage source distortion and phase displacement were created in the network model to introduce distortion and un-balance in the system voltage.

Performance of converters was verified for different loads and grid parameters such as harmonics current and reactive power drawn by the distributed loads; harmonics and reactive power supplied by the telecom batteries, FFT analysis for harmonic distortion in the source current, active and reactive power supplied or absorbed by the battery banks, etc. Results show that harmonics and reactive power were compensated and THD level in the source current was reduced considerably to the levels specified by IEEE, IEC and EN

Telecom sites with provided control strategies also allow to import and export the active power from or to the grid respectively. Import of active power is useful in charging the battery banks during off-peak hours. It was also shown that by increasing the connection of number of telecom sites to the network, services provided by the PE interface get stable, reliable and efficient.

Chapter 6: Grid Voltage Support

Distributed Energy Sources consist of Combined Heat and Power (CHP), energy storage units and loads under active demand side management; special attention is given to the wind and solar power among DG due to the environmental concerns [62]. From the past few years, particularly Europe has experienced a significant increased in wind power generation; only in Germany installed wind power turbines have been increased to 30GW in 2011 compared to 5GW in 2000 [63]. In this chapter, Induction Generator based wind turbine is connected to the MV grid via a transformer. Available small energy storage units in the form of telecom sites are connected to LV side of the grid. These telecom sites help in the improvement of voltage sag; number of telecom sites is three and the simulation results are discussed accordingly.

6.1. AC Distribution System

Electricity distribution is final stage in the delivery to the consumer. AC distribution consists of Medium and low voltage systems with some distributed generations. Distributed power generation should also be as close to the consumers as possible because long distance power delivery causes several kinds of losses e.g. about 8-10% of electrical energy appearing at generator terminal is lost in transmission and distribution [64]. AC distribution system is generally connected in radial structure but large customers may be directly fed with two radial feeders with automatic switching in case of power cut [37]. Low Voltage AC distribution system is composed of different loads connected to it and also distributed generation on some points. Figure 6.1 below shows modern LV AC Distribution System.

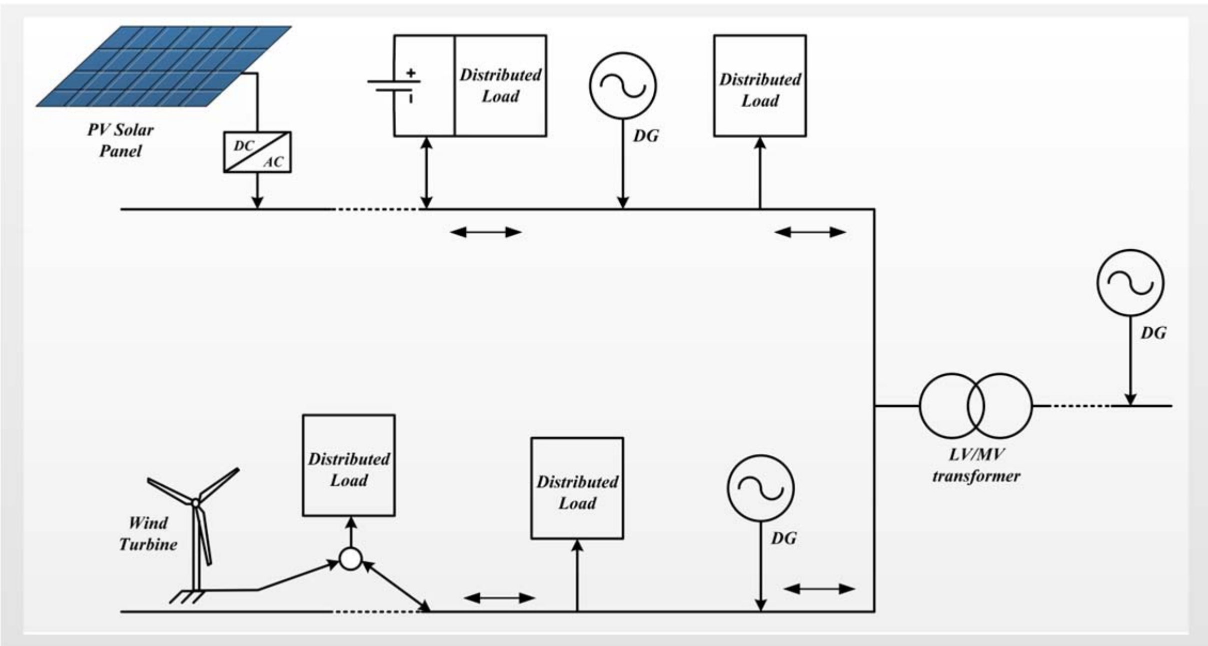

Figure 6. 1: Modern LV/MV AC Distribution System

Various Environmental factors and fast depleting fossil fuels are forcing the world to embrace renewable energy sources with conventional grid supply. Electricity from wind power parks and PV panels are perhaps the most common of all these sources [65]. That is why power flow from the distribution grid may not be unidirectional all the time anymore, because it also depends upon the generation from these renewable energy sources which enable customers to sell surplus supply to the grid.

6.2. Proposed Network Model

Numerous Telecom sites/stations are located on different locations of the cities. Each site is composed of PE interface, battery bank and telecom load. Battery banks on these sites act as DERs, these DERs will not only be used to supply power for the telecommunication services but also to improve the voltage sag whenever a fault occurs either on grid side or LV side of the network [66]. Figure below shows the block diagram of the system under investigation, when three telecom sites are used for grid voltage support during faults.

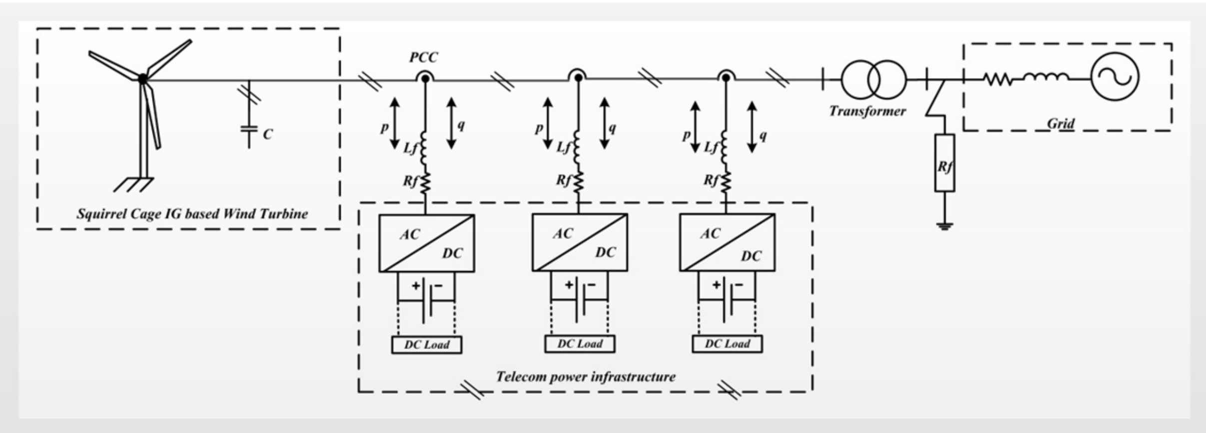

Figure 6. 2: Proposed network model for grid voltage support

It consist of a fixed speed 38kW wind turbine with a squirrel cage IG connected directly to the grid through a transformer of 50 kVA and battery banks connected with PE interface at the terminals. DC load is a 3kW telecom load being supplied by the battery bank and is connected to the low voltage side of the grid. The inductance '*L'* of distribution line is taken as 1*mH* per kilometre. The transformer is rated for turbine power and DC load. Here are the parameters for Grid, transformer, IG and telecom load.

6.3. Working Principle of Telecom sites

Vector control principle has been used to supply reactive current component. Structural operation of PE interfaces has been explained in the section 3.3.4 in detail. Here, only the difference is to supply reactive power required by the IG to support the voltage, i.e. 'i_{d_ref}' in this case would be zero for all three telecom sites and they will not be providing any active power to the grid. Figure below shows the schematics of three telecom sites control principles to achieve the desire results.

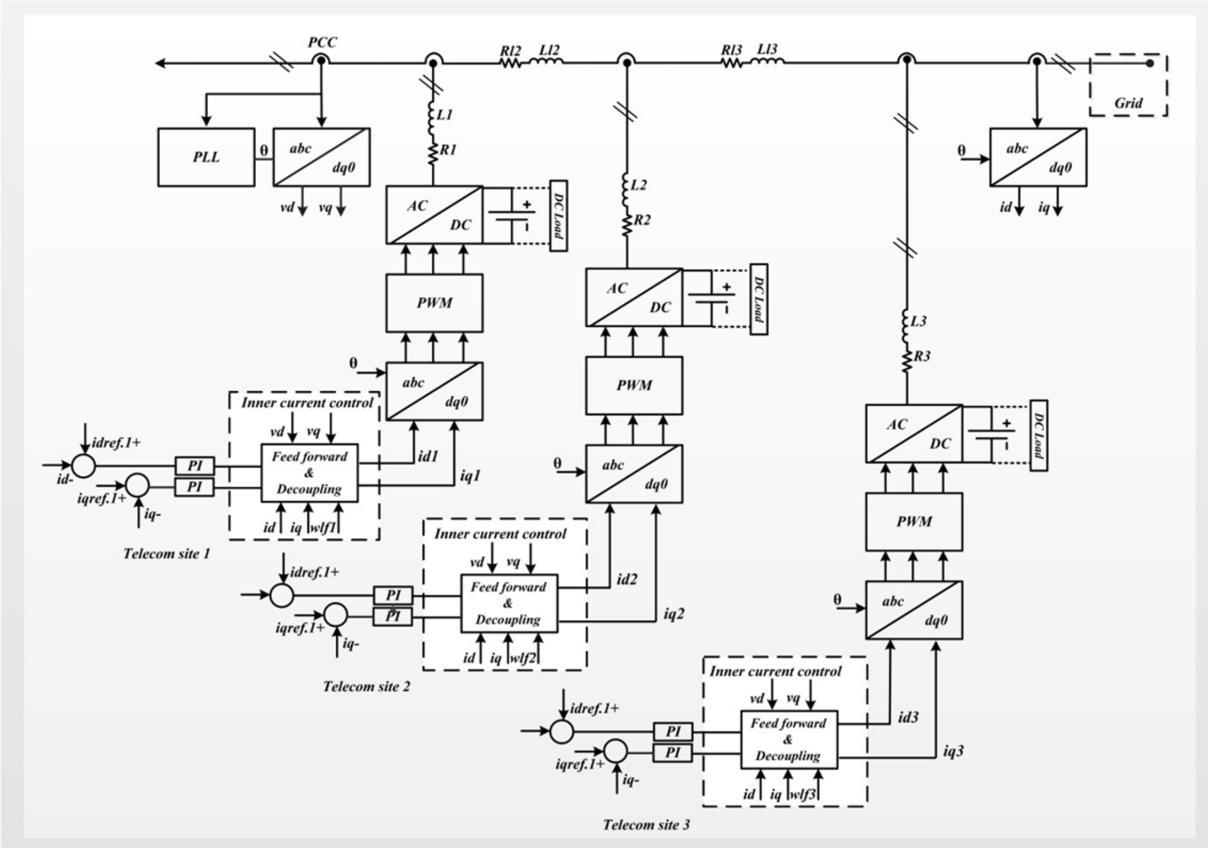

Figure 6. 3: Control Principle of power electronic interfaces for three Telecom sites

In the Figure shown here, the reactive power is translated by the reactive component of the reference current. It means that the battery banks will only provide the reactive power to the grid.

Complete Control Algorithm of these telecom PE interfaces together with wind power generation and are given in the **Appendix [E.1].**

6.4. Network parameters

Below, different network components are explained along with their operation parameters.

6.4.1. Telecom sites

Telecom sites along with the PE interface are connected to the LV grid side. Each telecom site consists of PE interface to the utility, apparatus for providing communication services and battery banks which provide power to this apparatus. Total load is taken as approximately 3 [kW] DC loads.

Telecom site 2 is 100m apart from site 1 and site 3 is located 200m away from site 2. Inductance between each telecom site is taken as 1 *‘mH’* per *‘km’* while the resistance is neglected due to very small distance between them.

6.4.2. MV Distribution Grid

The main grid is three phase AC source with internal impedance. Different grid parameters are summarized in the Table 6.1.

Voltage, v_s	11 [$kV_{L\text{-}L,rms}$]
Frequency, f	50 [Hz]
'*X/R*' ratio	7
Short Circuit Capacity	100 [MVA]

Table 6. 1: Parameters of MV Distribution Grid

The impedance between LV grid and MV grid is taken as '$1.0+j1.0m\Omega$'.

6.4.3. Transformer

Power generation from wind turbine is delivered to MV grid with the help of Star/Delta, LV/MV windings connected transformer. Transformer is rated for telecom load and wind power. Parameters related to step-up transformer, are given below.

Nominal Power, P	50 [kVA]
Nominal Frequency, f	50 [Hz]
Magnetizing Resistance, Rm	1.48 [kΩ]
Magnetizing inductance, Lm	Inf.
Winding 1 Voltage, $V1$	381 [$V_{L\text{-}L,rms}$]
Winding 1 Resistance, $R1$	2.48 [mΩ]
Winding 1 Inductance, $L1$	1.97 [mH]
Winding 2 Voltage, $V2$	11 [$kV_{L\text{-}L,rms}$]
Winding 2 Resistance, $R2$	3.93 [mΩ]
Winding 2 Inductance, $L2$	3.13 [μH]

Table 6. 2: Parameters for the Transformer

6.4.4. Induction Generator IG

Wind turbine with squirrel cage induction generator has been connected with the Grid via a transformer. Defining parameters of IG can be summarized in the Table 6.3.

Nominal Voltage, v_g	381 [$V_{L\text{-}L,rms}$]
Frequency, f	50 [Hz]
Nominal Power, p	3.75 [kW]
No. of Pole Pairs	2
Torque, T	-0.65 [pu]
Inertia Constant, $H_{(s)}$	0.19050 [pu]
Stator Resistance, R_s	0.01756 [pu]
Stator Inductance, L_{ls}	0.05762 [pu]
Rotor Resistance, $R_{r'}$	0.01029 [pu]
Stator Inductance, $L_{lr'}$	0.05762 [pu]
Friction Factor, F	0.02084 [pu]

Table 6. 3: Parameters for the Induction Generator

Y-connected capacitor bank connected with induction generator is rated as rated as 20.25 [kVAr].

6.5. Simulation Results and Discussion

In this section, a comprehensive simulation investigation has been carried out to explore the possibilities of Grid voltage support with the help of telecom sites. Simulations were performed for three telecom sites connected to LV side of the distribution network. Rated voltage is 381 [$V_{L\text{-}L,rms}$], simulation time is 10.0 seconds and converter are connected to the grid at time t=2.0 seconds. Simulation results for different scenarios are given below.

6.5.1. Three phase Generator Terminal Voltage and Current

Fault occurs on distribution lines with the fault resistance *'Rf=2.63Ω'* at time t=3.0 sec. and the fault clearing time is 4.5 seconds. Simulation results for generator terminal voltage and generator terminal currents before and after the fault are given as:

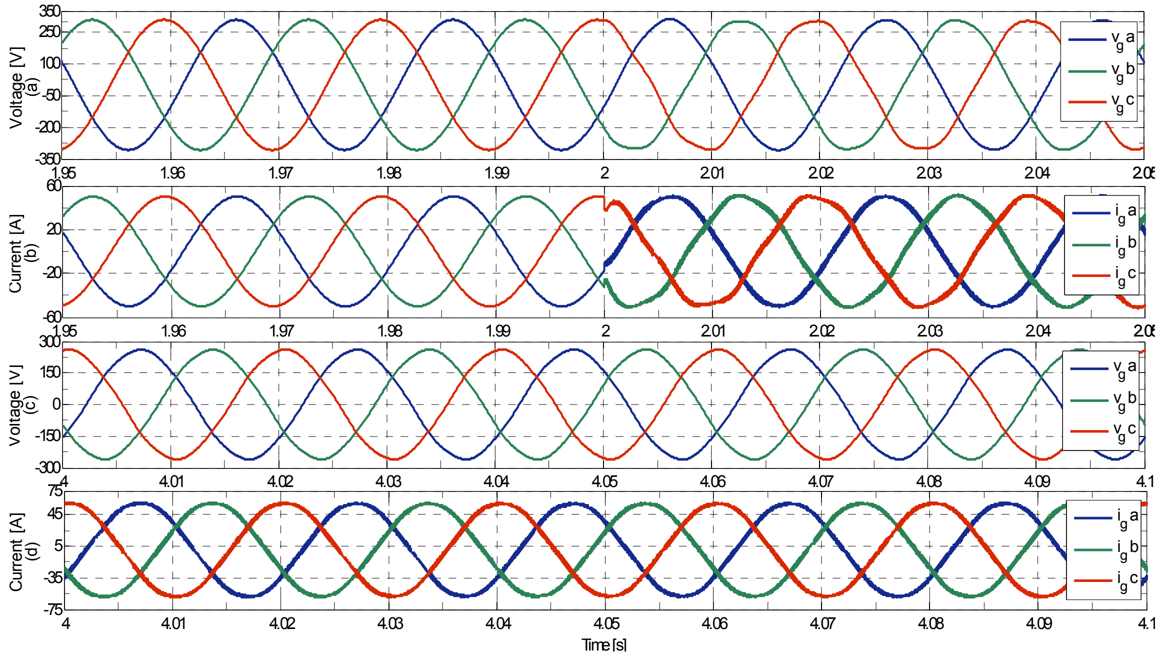

Figure 6. 4: Simulation results for three phase generator terminal voltage and current: (**a**), Pre-fault generator terminal voltage. (**b**), Pre-fault generator current. (**c**), Post-fault terminal voltage. (**d**), Post-fault terminal current.

Generator terminal voltage and currents get affected when a fault occurs on in the line. In this master thesis, we are concentrating only on the three phase faults in the distribution system and asymmetric faults are not considered in this research dissertation. Figure 6.4, shows the IG terminal voltage and current. It is shown in the Figure 6.4(**a**) that before and after the connection of telecom sites at time t=2.0 sec. voltage is symmetric three phase, each phase displaced by 120 Degrees and peak to peak voltage is 381 [$V_{L\text{-}L,rms}$]. Terminal currents also remain sinusoidal without any prominent disturbance and their peak to peak magnitude is 50 [A] as shown in the Figure 6.4(**b**).

Three phases to ground fault occurs in the distribution lines with the fault resistance *'2.3Ω'* at time t=3.0 sec. voltage at generator terminal falls down to about 315[$V_{L\text{-}L,rms}$], however, the voltage remains sinusoidal due to the balanced nature of the grid fault as shown in the Figure 6.4(**c**). Waveforms showing the post-fault currents in the Figure 6.4(**d**) explain the behaviour of current appearing at generator terminals. It is clear from the Figure that current waveforms remain sinusoidal even after the fault occurs but the peak to peak current magnitude has been increased to 60 [A_{peak}] to maintain the magnitude of power produced.

6.5.2. Operation of telecom converters for voltage support

Telecom sites were connected with the distribution lines at time t=2.0 sec. and fault occurs at time t=3.0 sec. Telecom sites 1,2 and 3 are connected at the time instants 4.5 sec, 6.5 sec and 6.5 sec. respectively. Simulation results for converters operations are given as:

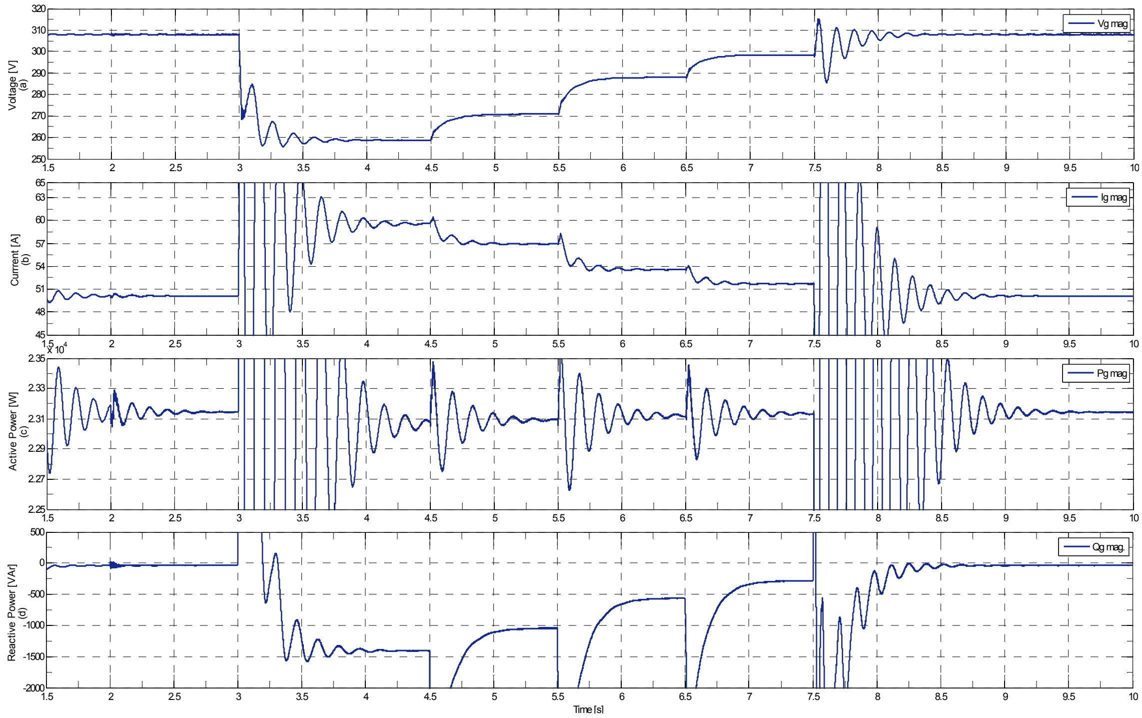

Figure 6. 5: Simulation results for converters operation and their effects on grid parameters: (**a**), Generator terminal voltage magnitude. (**b**), Generator terminal current magnitude. (**c**), Active power supplied by the IG. (**d**), Reactive power absorbed by the IG.

Figure 6.5 investigates the effects of fault on generator voltage, current, active power and on reactive power. Generator terminal voltage magnitude is reduced from 308 [V] to 258 [V] when the fault occur in the lines at time t=3.0 sec. About 16.5% reduction in the terminal voltage is due to a three phase to ground fault and it is cleared at time t=7.5 sec. But until it is cleared with protection devices, voltage level is improved stepwise with the help of VSCs connected on LV side of the grid. Figure 6.5(**a**), shows the magnitude of voltage before and after the fault appearance. It is evident from the Figure that when conv.1, conv.2 and conv.3 started working, the voltage magnitude was improved to 270 [V], 288 [V] and 298 [V] respectively. With combination of three converters voltage rose to 298 [V] which is quite significant improvement and within the allowable limits of power quality standards of $\pm$5%.

As explained in the previuse section, generator terminal current rises due to the occurrence of the fault. Figure 6.5(**b**), confirms its rising trend but it also shows that with the operation of converters rising trend recovers. Figure shows that with the occurrence of fault, current magnitude is increased to 71.5[A] from the pre-fault condition i.e. 66[A]. With the operation of *'conv.1'*, *'conv.2'* and *'conv.3'*, the fault current falls down to 69.8[A], 67.8 [A] and 66.8[A] respectively.

Before the fault occurs, connection of telecom sites has no significant impact on the normal operation of IG except on active power supplied by the generator as shown in the Figure 6.5(**c**). It also predicts that the active power is improved when VSCs started supporting grid with reactive power. Figure shows that there is a substantial amount of oscillations in the active power when telecom sites are connected, when fault occurs, when telecom sites start supporting the grid and even after the clearance of the fault. These oscillations are due to the inductive nature of the generation system and the lower value of the inertial constant [ref.]

The most important purpose of connecting the telecom sites is to provide reactive power to the grid because in case of fault, IG absorbs much more reactive power from the grid which causes instability and leads to disconnection of the turbine. Figure 6.5(**d**) investigates the reactive power support from by the telecom sites. It explains that before the fault appear on the lines, IG was absorbing only 40 [VAr] from the grid but when fault occurred at time t=3.0 sec., it went up-to 1400[VAr]. However, with the proper control strategies of back-up power available at telecom sites, the absorption dropped down to 300 [VAr]. It is clear from the Figure that when conv.1, conv.2 and conv.3 started supporting the grid, reactive power rose to 1050[VAr], 650[VAr] and 300 [VAr] respectively.

6.5.3. Grid Parameters

When fault occurred on distribution lines on MV side of the grid, there was a considerable drop of voltage on LV side of the grid as shown in the Figure 6.6. Voltage, current, etc. on MV grid side also face the consequences of the fault. Effects on MV grid side are described in Figure given below:

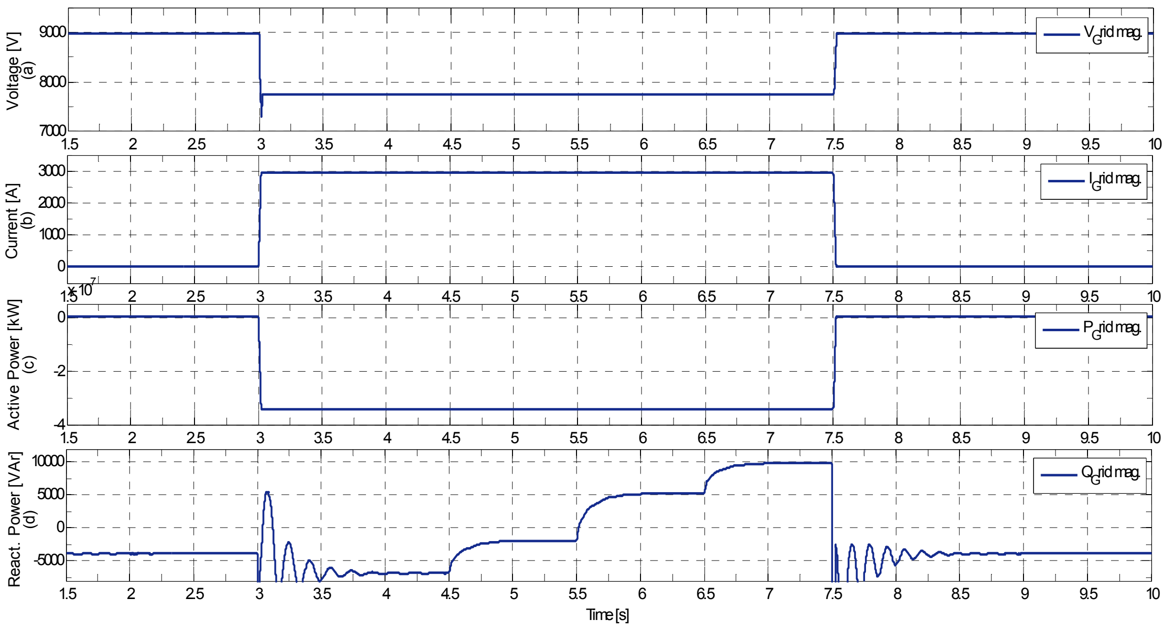

Figure 6. 6: Simulation results for MV grid parameters: (**a**), Magnitude of grid voltage. (**b**) Magnitude of current supplied by the grid. (**c**), Magnitude of active power from the grid. (**d**), Reactive power supplied by the grid.

Figure 6.6 explains the different parameters related to MV grid of the network. It shows that connection of telecom sites with LV grid has no effect on MV grid parameters, not even on the active power.

Due to fault appearance, magnitude of the voltage drops down to 7.7 [kV] from Pre-fault voltage of 8.9[kV] as shown in the Figure 6.6 (**a**). Telecom sites connected at LV side for voltage support causes very nominal improvement on MV side; close inspection showed that with the connection of each converter, voltage rises approximately 1 [V] which has very small impact on 1.2 [kV] fall. The same is the situation with the grid current magnitude and the active power provided from the grid. It is clear from the Figure 6.6 (**b**), that it goes from nearly zero to 2.9 [kA] and doesn't come down with the available or provided reactive power support on the LV side. Moreover, rise of grid active power is not so significant and can be neglected. Figure 6.6 (**c**), shows the magnitude of active power provided from the grid. It shows that with the occurrence of the fault it drops from 23 [kW] to -3.15x10E7 [W] and remains almost constant until and unless the fault is cleared at time t=75 sec.

As we discussed earlier that when fault occurs, IG starts absorbing reactive power from the grid and continues until it is disconnected from the main grid as apparent in the Figure 6.6 (**d**). Figure describes the effect of fault on grid reactive power. It demonstrates that when fault occurred at time t=3.0 sec., grid reactive power deteriorates from initial -4.0 [kVAr] to -7.0 [kVAr] up-to time instant t=4.5 sec. When supporting devices started working, they not only supply rated reactive power but also supply surplus to grid. Figure describes that with start of operation of conv.1, conv.2 and conv.3, reactive power supplied from grid was raised to 2.0 [kVAr], 6.0 [kVAr] and 9.9 [kVAr] respectively.

6.5.4. Telecom Sites/Converters Operation

Telecom sites with bidirectional PE interface are used in this research work to improve the stability of system by providing reactive power support to the grid. Telecom sites are connected to the grid at different time intervals and supply the reactive power to the grid as shown in the Figure below:

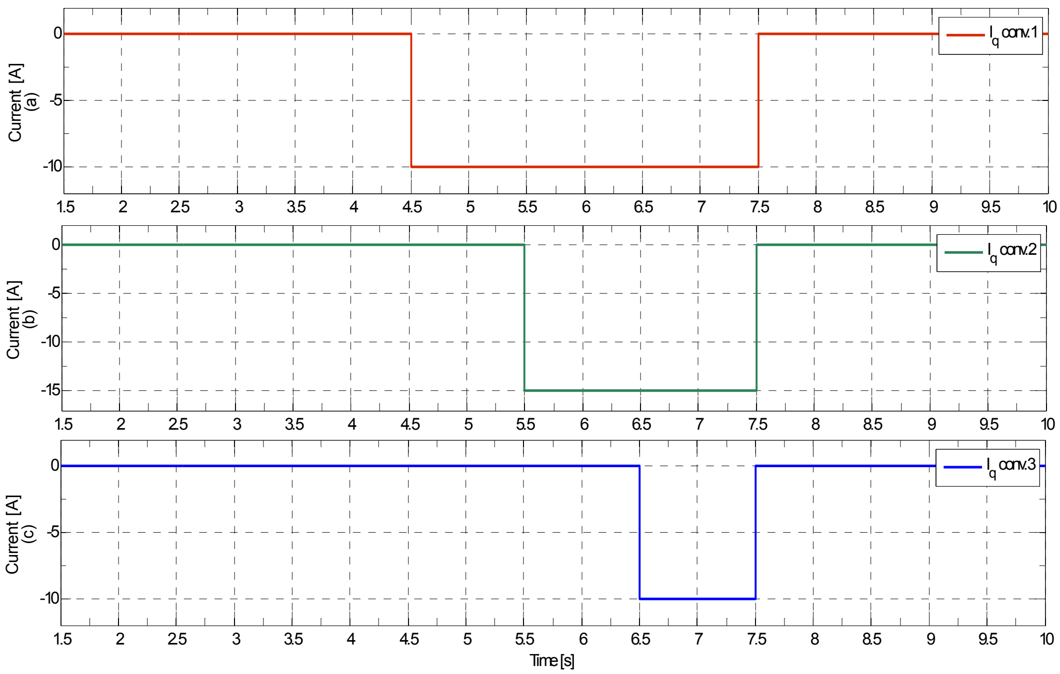

Figure 6. 7: Simulation results for converters operation: (**a**), Performance of the Telecom site. (**b**), Performance of the Telecom site 2. (**c**), Performance of the Telecom site 3.

Figure 6.7 demonstrates the supplied amount of reactive current by each telecom site together with the time of its connection with grid.

Telecom sites are connected to the grid at time t=2.0 sec. and fault occurs at time instant t=3.0 sec. Site 1 is starts supporting the grid at time t=4.5sec with reactive current 10 [A] and supply remains continues till time t=7.5 sec, when fault is cleared with protective devices as shown in the Figure 6.7 (**a**). Telecom Sites 2 and 3 supply reactive current of 15 [A] and 10 [A] respectively, Figure 6.7 (**b**) and Figure 6.7 (**c**) show the current waveforms supplied by these sites. It is shown in the Figure that site 2 and 3 start supporting the grid at time instants t=6.5 sec and t=6.5 sec until time t=7.5 sec respectively. Figure 6.7 depicts that the reactive currents supplied by the telecom sites stay constant during their operation.

6.6. Telecom Load

Telecom load is on average 3 [kW] DC load fed from the battery banks at telecom sites. Through simulation studies, it was observed that battery banks were continuously supplying power to DC load for telecom services. Battery banks are used for grid voltage support when they have Surplus amount of power.

Summary

Most of the grid instability is due to the faults in the distribution system. In this chapter, structure of modern AC distribution network is shown and the importance of integration of renewable energy generation e.g. winds power and solar power, has been explained. It is also described that how Telecom sites, interfaced through bi-directional converters can be used to improve the stability of Induction Generator based wind turbines under symmetrical voltage dips by providing the reactive power.

A network model is developed in the software MATLAB/SIMULINK® and control schemes of telecom PE interfaces developed in Chapter 4 have been used with some modifications for grid voltage support. Simulations were carried out to examine the different parameters of LV/MV grid and telecom converters.

It was seen that the connection of telecom sites with the grid has no impact on its specification except active power which oscillates. With the appearance of a fault on grid side, voltage on both sides of the transformer falls down and IG starts consuming significant amount of reactive power from the grid. But, when each converter started supplying reactive power at different intervals, according to the set points, considerable amount of voltage was improved. In addition to this, telecom load during this activity remained operational.

Chapter 7: Conclusion and Future Work

This chapter summarizes the results and achievements of the presented work with a brief conclusion. In addition to this, possibilities and recommendations for the future work are also given at the end.

7.1. Conclusion

Literature studies and measurements analysis show that the voltage dips, current harmonics and reactive power consumption are the most frequent and severe power quality issues in the AC distribution network supply. It is also realized that the cost of improving net efficiency of the whole power system is less than the investments in the new power plants and the Grid and the cost of the reduction of greenhouse gas emissions.

Whenever a grid, connected with distributed IG based wind turbine experiences a fault, a voltage dip appears on the lines and IG starts absorbing much reactive power from the grid. Moreover, the extensive use of static switching devices in the power system causes power factor variation and distortion in the source current. Voltage dips, harmonics pollution and reactive power loss give rise to the voltage variations and hence grid instability.

Advancements in communication technologies and available energy storage units at Telecom sites and electric vehicles provide the opportunity to realize the benefits of Smart Grid. Although differences in the energy policies of different grid operators, uncertainty in the market and reluctance of customers to accept new changes are key obstacles in the deployment of Smart Grid. However, several environmental and economic indicators are driving utilities to embrace Smart Grid as an emerging Grid. Smart Grid is a new concept of future grid which ensures the environment friendly, reliable, efficient, secure and better quality of supply by using different technologies and distributed energy resources.

A basic distribution network model was developed in MATLAB/SIMULINK® with network supply, various distributed loads and Telecom sites. Conventional power electronic interfaces of these Telecom sites were replaced by bi-directional AC/DC converters. Measurements were taken for ideal/non-ideal voltage source and by varying the number of Telecom sites up-to three. Artificial waveform distortion and un-balance was created by introducing number of harmonics and phase imbalance in the supply.

A vector control technique was used to achieve the co-ordinated control of utility interfaces as it offers dynamic response and flexibility to control active and reactive powers independently. It was observed that the injection of measured amount of currents at PCC minimizes the reactive power loss, improves source current waveforms and provides the possibility of voltage support during the grid fault. Simulation results verify the performance of converters and show that the absorption of reactive power dropped down to zero, system voltage increased to 97.5% of the magnitude and ‘THD’ declined to 3.4%; when three Telecom converters started supporting the grid. These measurements are within the permissible power quality standards defined by IEEE, IEC and EN. Moreover, results also show that utility interfaces allow the charging of battery banks by importing the active power from the grid. Charging of battery banks during off-peak hours and discharging during peak hours will help the utilities for peak shaving.

It is projected; globally there will be 1.03million electric vehicles comprising of Vehicle-to-Grid (V2G) technology in 2020 with maximum per capita share of Norway. Integration of increasing EVs and Telecom sites with proper Energy Management System (EMS) will ensure the reliability, efficiency, security and better quality of electricity supply.

Integration of energy storage units would only be possible if present PE utility interfaces will have the capabilities of bi-directional power flow. Bi-directional converters presented in this master thesis meet these requirements and provides a step towards the implementation of Smart Grid.

7.2. Future Work

Work presented in this maser thesis, gives an overview of Smart and establishes a relationship between benefits that can be achieved by implementing Smart Grid together with available Telecom power infrastructure and other energy storage units. However, still there is a lot of work required to understand the broad spectrum of Smart Grid and its utility applications. Some of the possibilities to improve the presented work are as follows:

- A brief analysis was done to understand the Smart Grid; however, there is a need to look at different technologies, driving factors and barriers for its implementation; in more details to achieve maximum benefits.
- Vector control technique has been used to achieve the desired results for three sites; number of telecom sites can be extended by using droop control method.
- Telecom batteries are only fed by AC distribution network; other renewable energy sources like solar and wind power can also be implemented to enhance the reliability.
- To develop an integrated control of other renewable energy sources with the bi-directional converters, can be a challenging task.
- Tuning of PI regulators was done by hit and trial method; however, more systematic approaches can be adopted for tuning the PI regulators.
- Oscillations in the active power and current at the IG terminals cause further instability; further work is required to understand and minimize the oscillations.
- Charging and discharging cycles of battery banks have very crucial role in the deployment of Smart Grid. A detailed analysis is necessary to analyse the charging and discharging characteristics of energy storage units.
- The work presented in this master thesis, can be implemented and verified by experimental results.

References

[1] Z. Liping, G. Ying and L. Ning, "The Greenhouse Gas Emission Factors Study in Construction Industry," in *Water Resource and Environmental Protection (ISWREP), Int. Symp.*, Xi'an, 20-22 May 2011.

[2] G.-J. v. d. Zanden, "The Smart Grid in Europe: The Impact of Consumer Engagement on the Value of the European Smart Grid," M. S. Thesis, The international Institute for Industrial Enviornmental Economics (IIIEE), Lund, Sweden, 2011.

[3] R. Belmans, "Smart Grid; Strategic Deployment Document for Europe's Electricity Networks of the Future," SmartGrids ETP Forum, April 2010.

[4] F. Rotaru , G. Chicco , G. Grigoras and G. Cartina, "Two-stage distributed generation optimal sizing with clustering-based node selection," *Int. Journal of Electrical Power & Energy Systems,* vol. 40, no. 1, p. 120–129, Sep. 2012.

[5] Y. Song and B. Wang, "Survey on Reliability of Power Electronic Systems," *IEEE Transaction on Power Electronics,* vol. 28, no. 1, pp. 591-604, Jan. 2013.

[6] E. Styvaktakis, "Automating Power Quality Analysis," P.hD. Dissertation, Department of Electric Power Engineering and department of signals and systems, Chalmers University of Technology, Gåteborg, Sweden, 2002.

[7] E. K. Hart, E. D. Stout and M. Z. Jacobson, "The Potential of Intermittent Renewables to Meet Electric Power Demand: Current Methods and Emerging Analytical Techniques," *Proceedings of the IEEE ,* vol. 100, no. 2, pp. 322 - 334, Feb. 2012 .

[8] S. M. Amin and B. F. Wollenberg, "Towards a smart grid: power delivery for the 21st century," *IEEE Power and Energy Magazine,* vol. 3, no. 5, pp. 31-41, Sept.-Oct. 2005.

[9] J. Ekanayake, K. Liyanage and J. Wu, Smart Grid: Technology and Applications, West Sussex, United Kingdom: John Villey & Sons, Ltd, April 24, 2012.

[10] L. F. Ochoa, C. J. Dent, Member and G. P. Harrison, "Distribution Network Capacity Assessment: Variable DG and Active Networks," *IEEE Transaction on Power Systems,* vol. 25, no. 1, pp. 87-95, Feb. 2010.

[11] Q. Sun, J. Wu, W. Zhang, N. Jenkins and J. Ekanayak, "Comparison of the Development of Smart Grids in China and the United Kingdom," in *IEEE PES Conf. on Innovative Smart Grid Technologies Europe*, Gothenburg, Sweden, 11-13 Oct. 2010.

[12] U.S Department of Energy (DoE), "IEEE Smart Grid," [Online]. Available: http://smartgrid.ieee.org/resources/public-policy/united-states. [Accessed 28 Aug. 2013].

[13] Encyclopedia of the nations, “Norway - Energy and power,” 16 Jun 2010. [Online]. Available: http://www.nationsencyclopedia.com/Europe/Norway-ENERGY-AND-POWER.html. [Accessed 28 Aug. 2013].

[14] K. Sand, “Smartgrids.no; National Smart Grid Strategy Report,” 03 March 2012. [Online]. Available: http://smartgrids.no/. [Accessed 03 September 2013].

[15] NIST, National Institute of Technology, “Smart Grid: A Beginner's Guide,” U.S. Department of Commerce, 2012.

[16] Chang Soon Ho, “Smart Grids for a Smart Future,” Korea Smart Grid Association, 17 July 2012. [Online]. Available: http://blog.investkorea.org. [Accessed 12 Sep. 2013].

[17] B. Kromhout, “Smart Grid Development,” M. Sc. Thesis, Faculty of Technology Policy and Managment (TPM), SEPAM, Uni. of Delft, Delft, Netherlands, 2010.

[18] Litos Strategic Communication, “The Smart Grid: An Introduction,” US Department of Energy (DoE), Jan. 2004.

[19] US Department of Energy: Office of Electricity Delievery and Energy, “Energy Storage: A key Enabler for Smart Grid,” National Energy Technology Department (NETL), 2009.

[20] Grønnbil, “Over 10,000 rechargable cars on Norwegian roads,” 01 Jan. 2013. [Online]. Available: http://www.gronnbil.no/. [Accessed 29 Aug. 2013].

[21] ZigBee, “Smart Grid Insights,” Zpryme Research & Consulting, LLC, July 2010.

[22] ABB: Power and Productivity for the better world, “Why smart grids?,” [Online]. Available: http://new.abb.com/smartgrids/why-smart-grids. [Accessed 2013 Aug. 24].

[23] McKensy Global Energy and Materials, “Unlocking Energy Efficency in the US Economy,” Mckensy&Company, July 2009.

[24] G. Rouse and J. Kelly, *Electricity Reliability: Problems, Pregress and Policy Solutions,* Galvin Eletricity Initiative, Feb. 2011.

[25] Vassa Energy Think Tank (ETT), European Residential Price Report 2011, Helsinki, Finland: VaasaETT Global Energy Think-Tank, March 2013.

[26] I. S. C. C. 2. o. P. Quality, “1159-1995 - IEEE Recommended Practice for Monitoring Electric Power Quality,” IEEE Standards Board, June 1995.

[27] D. T. Incorporated, The Dranets field hand book for Power Quality, New Jersey: Edison, 1991.

[28] S. Singh, K. Verma and D. Saxena, “Power quality event classification: an overview and key issues,” *Int. Journal of Engineering, Science and Technology,* vol. 2, no. 3, pp. 186-199, 2010.

[29] V. Azbe and R. Mihalic, “Computer-aided coordination of power system protection,” in *EUROCON 2003. Computer as a Tool. The IEEE Region 8*, Fac. of Electr. Eng., Ljubljana Univ.,

Slovenia, 22-24 Sept. 2003.

[30] M. McGranaghan and D. Sabin, "Monitoring morphs into customer service quid pro quo," *Electric Light & Power,* vol. 79, no. 6, pp. 15-16, 2001.

[31] A. Sumper and S. Galceran-Arellano, "Monitoring Power Quality," in *Handbook of power quality*, West Sussex, England, John Villey & Sons, 2008, pp. 445-462.

[32] F. Pilo, G. Pisano and G. G. Soma, "Considering Voltage Dips Mitigation in Distribution Network Planning," in *IEEE Power Tech Conf.*, Laussane, 1-5 July 2007.

[33] Z. Hanzelka, "Voltage Dips and Short Supply Interruptions," in *Handbook of power quality*, West Sussex, England, John Villey & Sons, 2010, pp. 79-131.

[34] R. C. Leborgne, D. Karlsson and G. Olguin, "Analysis of Voltage Sag Phasor Dynamic," in *IEEE Power Tech*, St. Petersburg, Russia, 27-30 June, 2005.

[35] C. Radhakarishna, M. Eshwardas and G. Chebiyam, "Impact of voltage sags on practical power system networks," in *IEEE Transmission and Distribution Conference and Exposition*, Atlanta, GA , 28 Oct. 2001-02 Nov. 2001.

[36] J. P. Clerfeuille, P. Juston and M. Clement, "Extinguishing Faults Without Disturbances," in *Electricite de France*, Paris, Aug. 1997.

[37] J. Mackhowski, J. w. Bialek and J. R. Bumby, Power System Dynamics: Stability and Control, 2nd ed., West Sussex, United kingdom: John Villey & Sons, Ltd., 2008.

[38] N. Mohan, T. M. Undeland and W. P. Robbins, Power Electronics: Converters Applications and Design, Third ed., USA: John Villey & Sons, Inc., 2003.

[39] B. M. Saied and R. K. Antar, Harmonic mitigation technique for the power quality improvement of DC motor drives, Bodrum : IEEE International Aegean Conf. on Electrical Machines and Power Electronics ACEMP, 10-12 Sep. 2007.

[40] A. Baggini, Hand Book of Power Quality, West Sussex, United Kingdom: John Villey & Sons, Ltd., 2008.

[41] Suriadi, "Analysis of Harmonics Current Minimization on Power Distribution System using Voltage phase shifting Concept," M.Sc. Thesis, 2006.

[42] M. H. J. Bollen, S. Cundeva, S. K. Rönnberg, M. Wahlberg, K. Yang and L. Yao, "A wind park emitting characteristic and non-characteristic harmonics," in *IEEE 14th Int. Power Electronics and Motion Control Conf. (EPE/PEMC)*, Ohrid, 6-8 Sept. 2010.

[43] R. R. Verderber, O. C. Morse and W. R. Alling, "Harmonics from Compact Fluorescent Lamps," *IEEE transaction on Industry Applications,* vol. 29, no. 3, pp. 670 - 674, Aug. 2002.

[44] H. Akagi, E. H. Watanabe and M. Aredes, Instantaneous Power Theory and Applications to

Power Conditionaing, Hoboken, New jersey and Canada: John Villey & Sons, 2007.

[45] Elliot, Rod;, “Inrush Current Mitigation,” 25 August 2013. [Online]. [Accessed 15 September 15].

[46] C. Yuqing, J. Zhaojun, Z. Hongfeng, K. Feng and C. Lingzhi, “New Method to the Reactive Power Impact Caused by Harmonic,” in *IEEE Fourth Int. Conf. on Computer Sciences and Convergence Information Technology ICCIT*, Seoul , 24-26 Nov. 2009 .

[47] C. Lin, M. Tamayo and J. N. Jiang, “An Analysis of Transient Characteristics of Interconnected Wind Power Generation System with DFIG,” in *IEEE Int. Conf. on Sustainable Energy Technologies (ICSET)*, Kandy, 6-9 Dec. 2010.

[48] X. Dong, Y. Liu and J. Kappenman, “Comparative analysis of exciting current harmonics and reactive power consumption from GIC saturated transformers,” in *IEEE Power Engineering Society Winter Meeting*, Columbus, OH, 28 Jan-1 Feb 2001 .

[49] Y. Zou, M. Elbuluk and Y. Sozer, “Simulation Comparisons and Implementation of Induction Generator Wind Power Systems,” *IEEE Transactions on Industry Applications,* vol. 49, no. 3, pp. 1119 - 1128 , May-June 2013 .

[50] S. N. Patel, M. P. Rathod, K. C. Patel, P. H. Panchal and J. N. Prajapati, “Thyristorised Real Time Power Factor Correction (TRTPFC),” *Int. Journal of Engineering Research & Technology (IJERT),* vol. 2, no. 3, pp. 1-5, March - 2013.

[51] P. Sreejaya and D. S. R. Iyer, Reactive power control in AC systems, IEEE Int. Conf. on Future Electrical Power and Energy Systems, 2012.

[52] J. Dixon, L. Moran, J. Rodriguez and R. Domke, “Review, Reactive power compensation Technologies: State of the Art,” *Proceedings of the IEEE ,* vol. 93, no. 12, pp. 2144 - 2164 , Dec. 2005 .

[53] M. El-Habrouk, “A New Configuration for Shunt Active Power Filters,” Ph.D Dessertation, School of Engineering, Brunel University, UK, 1998.

[54] G. Galanos, C. Hatziadoniu, X. Cheng and D. Maratukularn, “Advanced static compensator for flexible AC transmission,” *IEEE Transactions on Power System,* vol. 8, no. 1, pp. 113 - 121 , Feb. 1993.

[55] R. Sedaghati, M. Ghasemi and M. Hayatdavudi, “Performance Study of Dynamic Voltage Restorer (DVR) in order to Power Quality Improvement,” in *IEEE 17th Conf. on Electrical Power Distribution Networks (EPDC)*, Tehran, 2-3 May 2012.

[56] M. Manyage and P. Pillay, *Definitions of Voltage Unbalance,* IEEE Power Engineering Review, May 2001.

[57] P. Channegowda and V. John, “Filter Optimization for Grid Interactive Voltage Source Inverters,” *IEEE Transactions on Industrial Electronics,* vol. 57, no. 12, pp. 4106 - 4114 , Dec.

2010 .

[58] H. Patel and V. Sood, “Comparison between Direct and Vector control Strategy for VSC-HVDC system in EMTP-RV,” in *Power Electronics, Drives and Energy Systems (PEDES) & 2010 Power India, 2010 Joint Int. Conf.*, Oshawa, Canada, 20-23 Dec. 2010.

[59] N. Mohan, Advanced Electric Drives: Analysis, Control and Modeling Using Simulink, Minnesota, USA: Minnesota Power Electronics Research & Education (MNPERE), 2001.

[60] J. Svennson, “Synchronisation methods for grid-connected voltage source converters,” *IEE Proceedings on Generation, Transmission and Distribution,* vol. 148, no. 3, pp. 229 - 235 , May 2001.

[61] K. Kim and C. R. Schaefer, “Tuning a PID controller for a digital excitation control system,” in *IEEE Pulp and Paper Industry Technical Conf.*, 27 June-1 July 2004 .

[62] A. M. Leite da Silva,, L. C. Nascimento, M. A. da Rosa, D. Issicaba and J. A. Peças Lopes,, “Distributed Energy Resources Impact on Distribution System Reliability Under Load Transfer Restrictions.,” *IEEE Transaction on Smart Grid,* vol. 3, no. 4, pp. 2048-2055, Dec. 2012.

[63] B. Udo, I. Erlich and W. Winter, “Advanced Grid Requirements for the Integration of Wind Turbines into the German Transmission System.,” in *IEEE Power Engineering Society General Meeting*, Montreal, Que., 2006.

[64] A. Stupar, T. Fried and J. W. Kollar, “Towards a 99% Efficient Three-Phase Buck-Type PFC Rectifier for 400-V DC Distribution Systems,” *IEEE transaction on Power Electronics,* vol. 27, no. 4, pp. 1732-1744, April, 2012.

[65] F. Dastgeer and A. Kalam, “Efficiency comparison of DC and AC distribution systems for distributed generation,” in *Power Engineering Conf., Australasian Universities*, Melbourn, Australia, 2009.

[66] G. Xu, L. Xu and M. D.J., “Wind turbines with energy storage for power smoothing and FRT enhancement,” IEEE Power and Energy Society General Meeting, San Diego, CA, 24-29 July 2011.

[67] J. A. Martinez-Vilasco, J. Martin-Arnedo and F. Castro-Aranda, “Modeling protective Devices for Distribution Systems with Distributed Generation using an EMTP-type tool,” *Ingeniare. Revista chilena de ingeniería,* vol. 18, no. 2, pp. 258-273, 2010.

[68] S. Khalid and B. Dwivedi, “Power Quality Issues, Problems, Standards and other effects in Industry with Corrective means,” *International Journal of Advances in Engineering & Technology, IJAET,* vol. 1, no. 2, pp. 1-11, May 2011.

Appendices

Appendix A: Energy Storage Devices

A.1: Distributed Energy Storage Units characteristics

Advanced Battery Type	**Capital Cost $kW-hr**	**Life cycle, no. of charge/discharged cycle to 80% DOD**	**% Round Trip Efficiency AC to AC**
Li-Ion	Very high 600-1200	Medium 2000-5000	Very high 85-95
VRB	Medium 350-500	High Up to 10,000	High 85-95
NaS	Medium 350-500	Medium 3000-5000	High 85-95
ZnBr	Low 150-250	High >10,000	Medium 70-75
Comments	-don't include cost of installation -which is 20-30%	For Storing wind or solar, cycle live of >10,000 needed	Efficiency is imp. For arbitrage but less for peak shaving, f regulation.

Advanced Battery Type	**Environmental Impact/Ease of permitting**	**Energy to size energy density Wh/L**	**Other issues or disadvantages**
Li-Ion	Low	Medium 80-200	-high self-discharge rate
VRB	High	Low 15-25	Environmental concern
NaS	Medium	High 145-150	Safety concerns, like packing etc.
ZnBr	Low	High 130-150	Energy density big issue
Comments		Energy density is not an issue unless land cost is high in Urban areas	

Table A. 1: Distribution Battery Technologies

Appendix B: Harmonics Limits

B.1: A measurement for multistage voltage dip

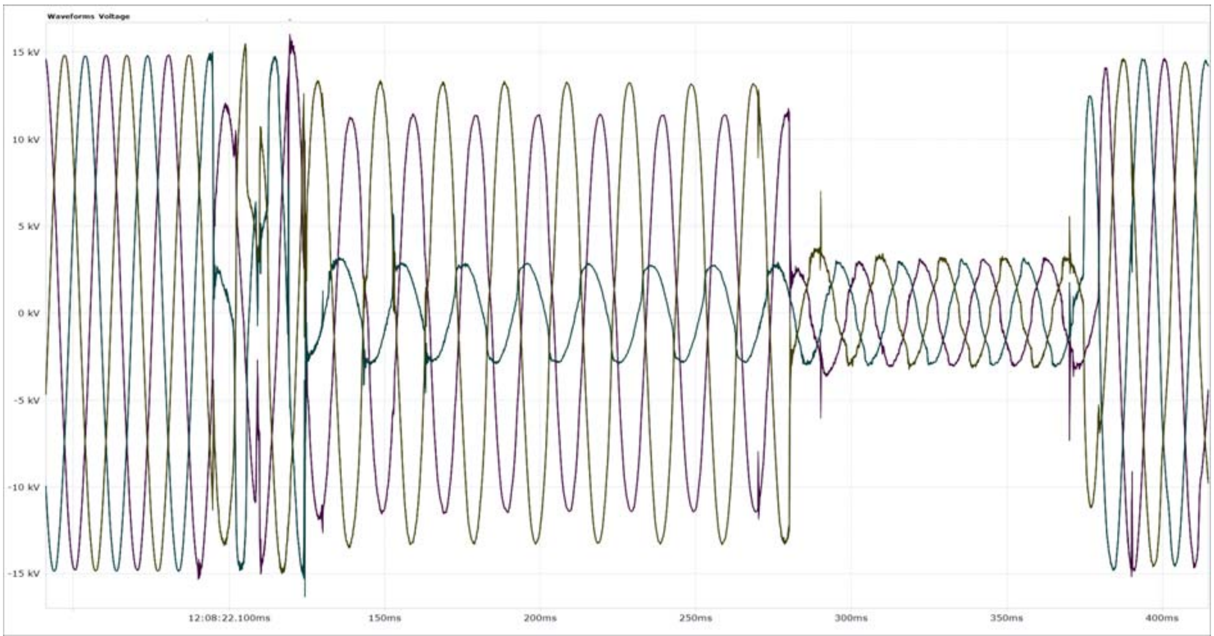

Figure B. 1: Measurement for a multistage voltage dip

B.2: Harmonics Distortion Limits for Voltage and Current

Bus Voltage at PCC (V_n)	Individual Harmonic	Total Voltage Distortion
$V_n \leq$ 69kV	3.0	5.0
69kV < $V_n \leq$ 161kV	1.5	2.5
V_n > 161kV	1.0	1.5

Table B. 1: Voltage Harmonics Distortion Limits

$V_n \leq 69kV$						
I_{sc}/I_L	**h<11**	**11≤h<17**	**17≤h<23**	**23≤h<35**	**35≤h**	**TDD**
<20	4.0	2.0	1.5	0.6	0.3	5.0
20-50	7.0	3.5	2.5	1.0	0.5	8.0
50-	10.	4.	4.	1.	0.	12.
69kV<Vn≤161kV						
<20	2.0	1.0	0.75	0.3	0.15	2.5
20-50	3.5	1.75	1.25	0.5	0.25	4.0
50-	5.	2.2	2.	0.7	0.3	6.
Vn>161kV						
<50	2.0	1.0	0.75	0.3	0.15	2.5

Table B. 2: Currents Harmonics Distortion Limits

Appendix C: Vector Control Principle

C.1: Mathematical representation of Clark and Park Transformation

Clark Transformation	**Park Transformation**
$\begin{bmatrix} v_\alpha \\ v_\beta \end{bmatrix} = \frac{2}{3}\begin{bmatrix} 1 & -\frac{1}{2} & -\frac{1}{2} \\ 0 & \frac{\sqrt{3}}{2} & -\frac{\sqrt{3}}{2} \end{bmatrix}\begin{bmatrix} v_a \\ v_b \\ v_c \end{bmatrix}$	$\begin{bmatrix} v_d \\ v_q \end{bmatrix} = \begin{bmatrix} \cos\theta & \sin\theta \\ -\sin\theta & \cos\theta \end{bmatrix}\begin{bmatrix} v_\alpha \\ v_\beta \end{bmatrix}$
$\begin{bmatrix} v_a \\ v_b \\ v_c \end{bmatrix} = \begin{bmatrix} 1 & 0 \\ -\frac{1}{2} & \frac{\sqrt{3}}{2} \\ -\frac{1}{2} & -\frac{\sqrt{3}}{2} \end{bmatrix}\begin{bmatrix} v_\alpha \\ v_\beta \end{bmatrix}$	$\begin{bmatrix} v_\alpha \\ v_\beta \end{bmatrix} = \begin{bmatrix} \cos\theta & -\sin\theta \\ \sin\theta & \cos\theta \end{bmatrix}\begin{bmatrix} v_d \\ v_q \end{bmatrix}$

Table C. 1: Clark and Park Transformation

Appendix D: Simulation models and results for power quality

D.1: Simulation circuit diagrams for one Telecom site

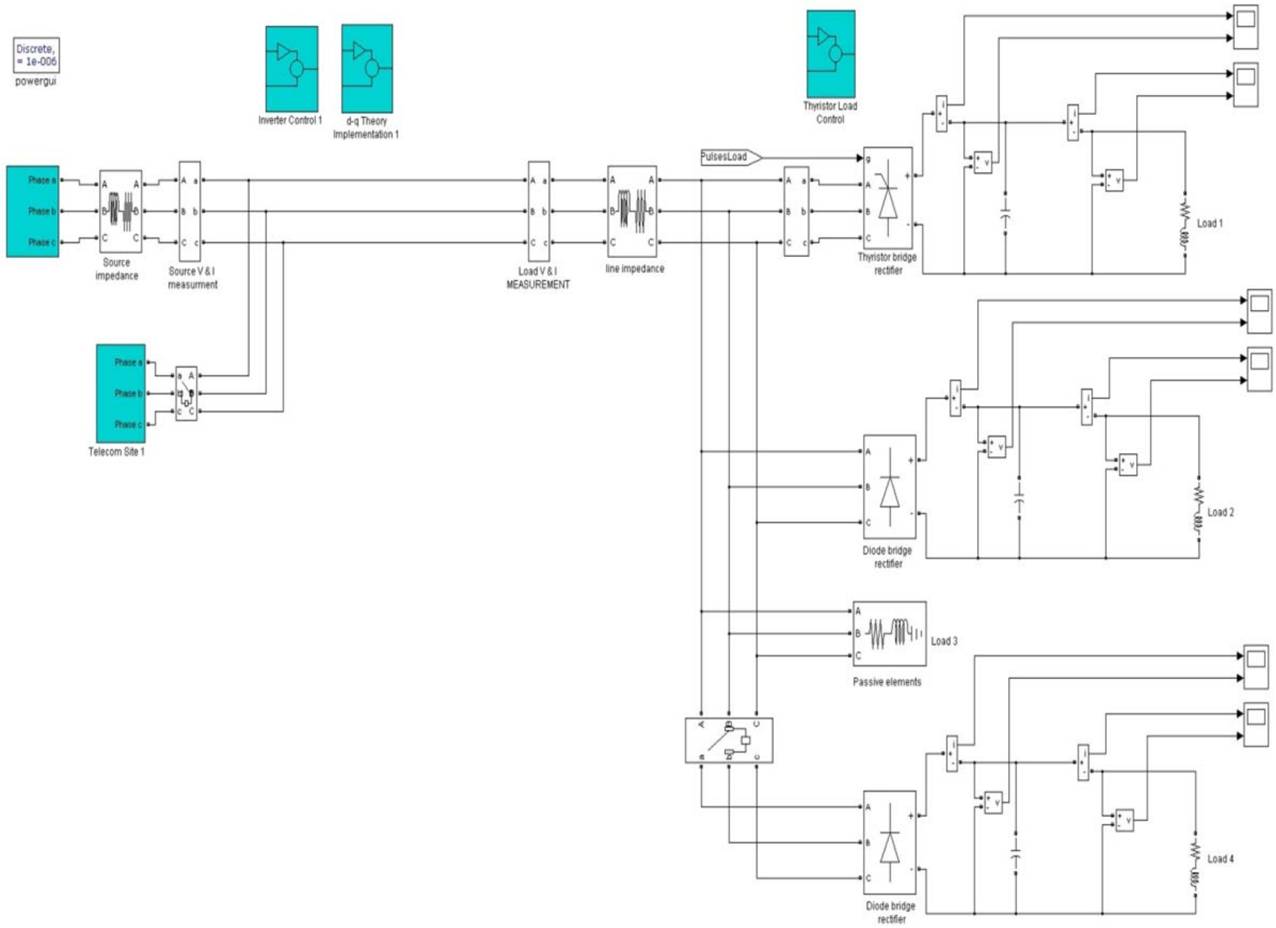

Figure D. 1: Simulation model for one telecom site connected to the network

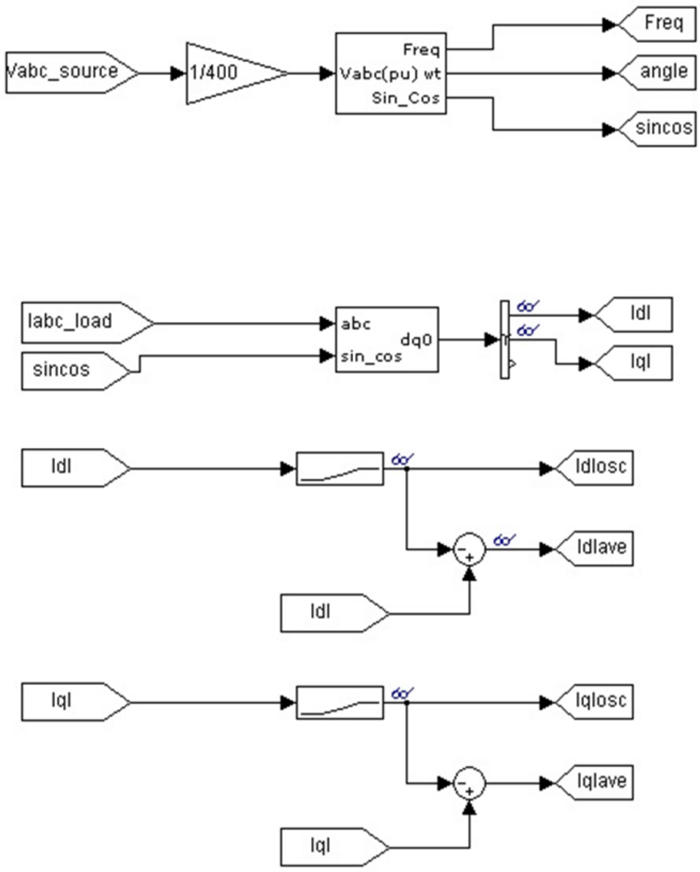

Figure D. 2: The Clark and Park transformation

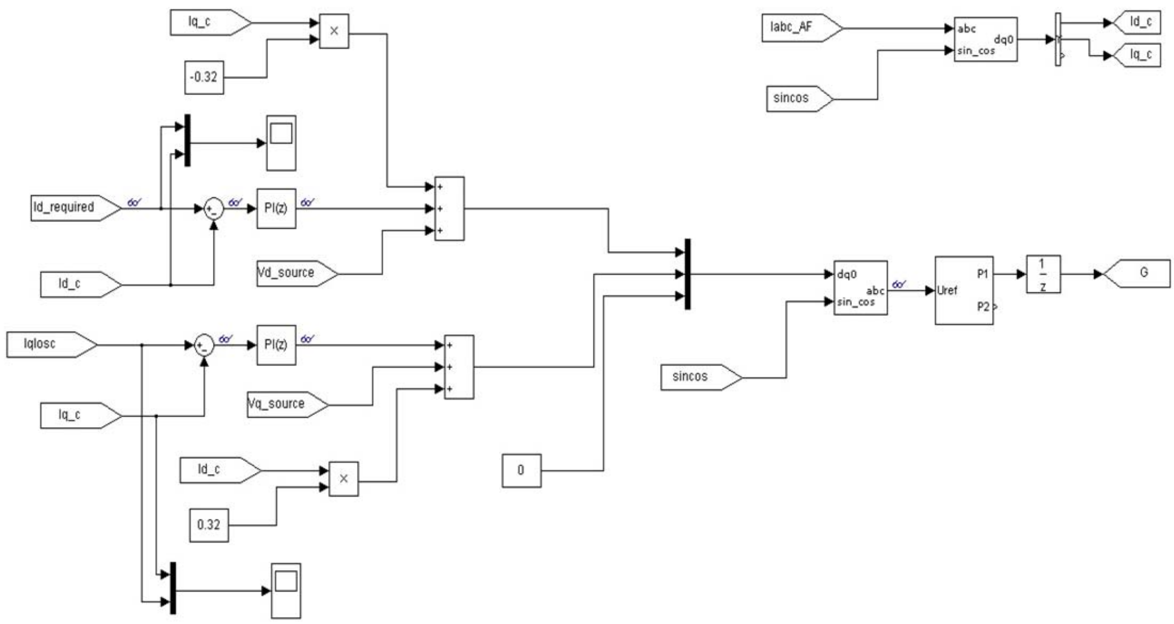

Figure D. 3: Inner current controller design for one converter

D.2: FFT Analysis

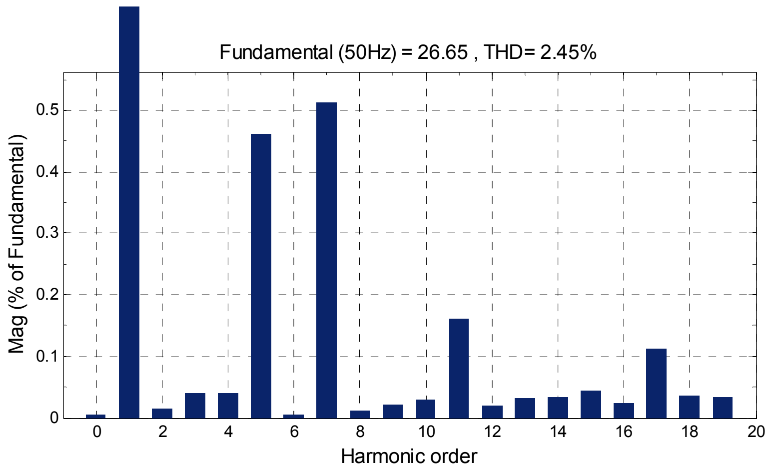

Figure D. 4: FFT Analysis for one converter

D.3: Simulation circuit diagrams for two Telecom sites

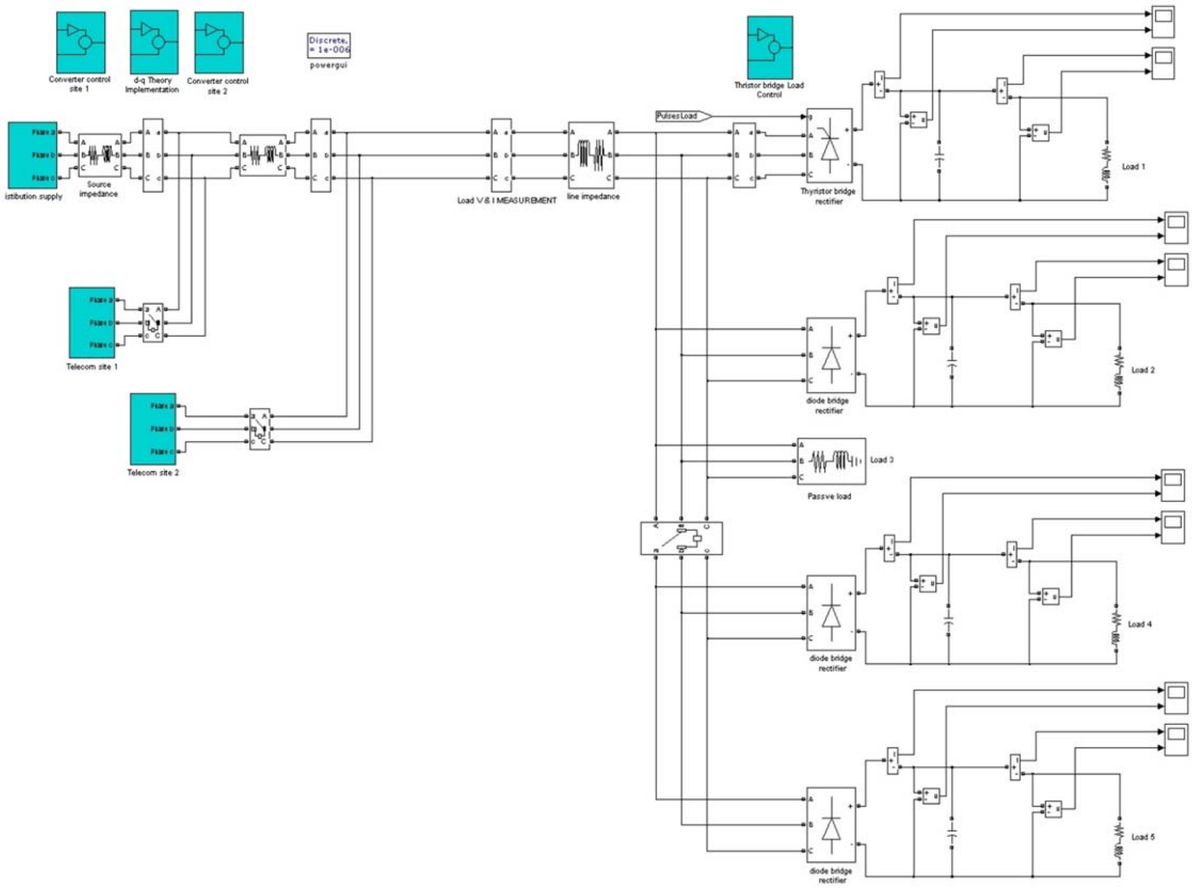

Figure D. 5: Simulation block diagram for two Telecom sites connected to the network

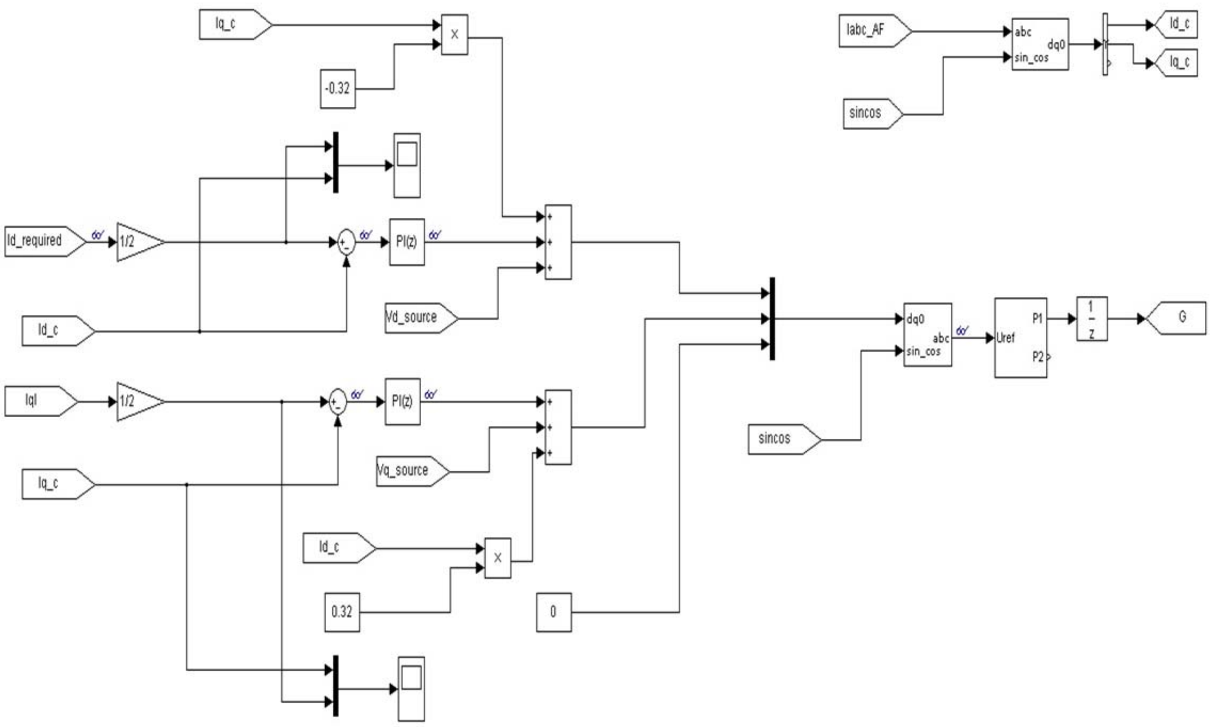

Figure D. 6: Inner current controller design for site 1

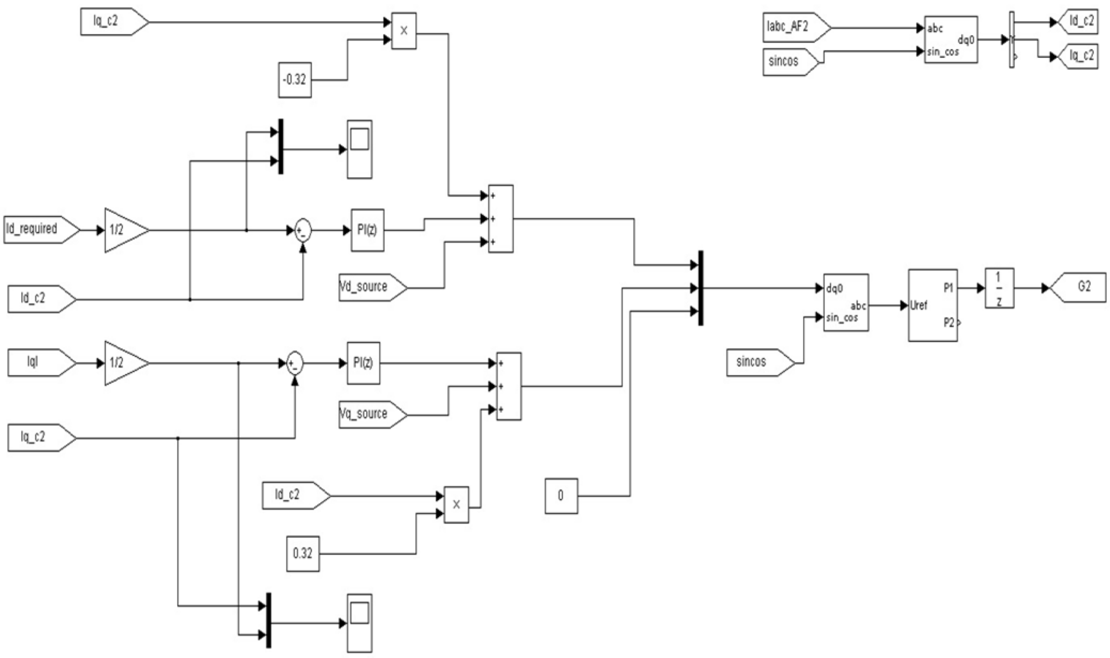

Figure D. 7: Inner current controller design for site 2

D.4: FFT Analysis for two converters under balanced load and unbalanced source conditions

Parameter	Harmonic contents before VSC is connected	Harmonic contents after VSC is connected
Fund.	100%, 44.5 [A_{peak}]	100%, 36.21 [A_{peak}]
I_{3rd} [% of I_1]	30.13%	3.28%
I_{5th} [% of I_1]	28.91%	0.20%
I_{7th} [% of I_1]	4.35%	0.47%
I_{9th} [% of I_1]	6.05%	0.23%
I_{11th} [% of I_1]	3.97%	0.14%
I_{13th} [% of I_1]	4.69%	0.04%
I_{15th} [% of I_1]	5.62%	0.12%
I_{17th} [% of I_1]	3.26%	0.02%
T.H.D	43.01%	3.42%

Table D. 1: FFT Analysis under balanced load and unbalanced source conditions

D.5: FFT Analysis for two converters under unbalanced load and unbalanced source Conditions

Parameter	Harmonic contents before VSC is connected	Harmonic contents after VSC is connected
Fund.	100%, 44.5 [A_{peak}]	100%, 36.21 [A_{peak}]
I_{3rd} [% of I_1]	6.63%	5.64%
I_{5th} [% of I_1]	21.34%	0.36%
I_{7th} [% of I_1]	7.02%	0.06%
I_{9th} [% of I_1]	3.16%	0.35%
I_{11th} [% of I_1]	3.97%	0.15%
I_{13th} [% of I_1]	3.46%	0.13%
I_{15th} [% of I_1]	1.63%	0.09%
I_{17th} [% of I_1]	1.28%	0.09%
T.H.D	24.19%	2.77%

Table D. 2: FFT Analysis under unbalanced load and unbalanced source conditions

D.6: Simulation circuit diagrams for three Telecom sites

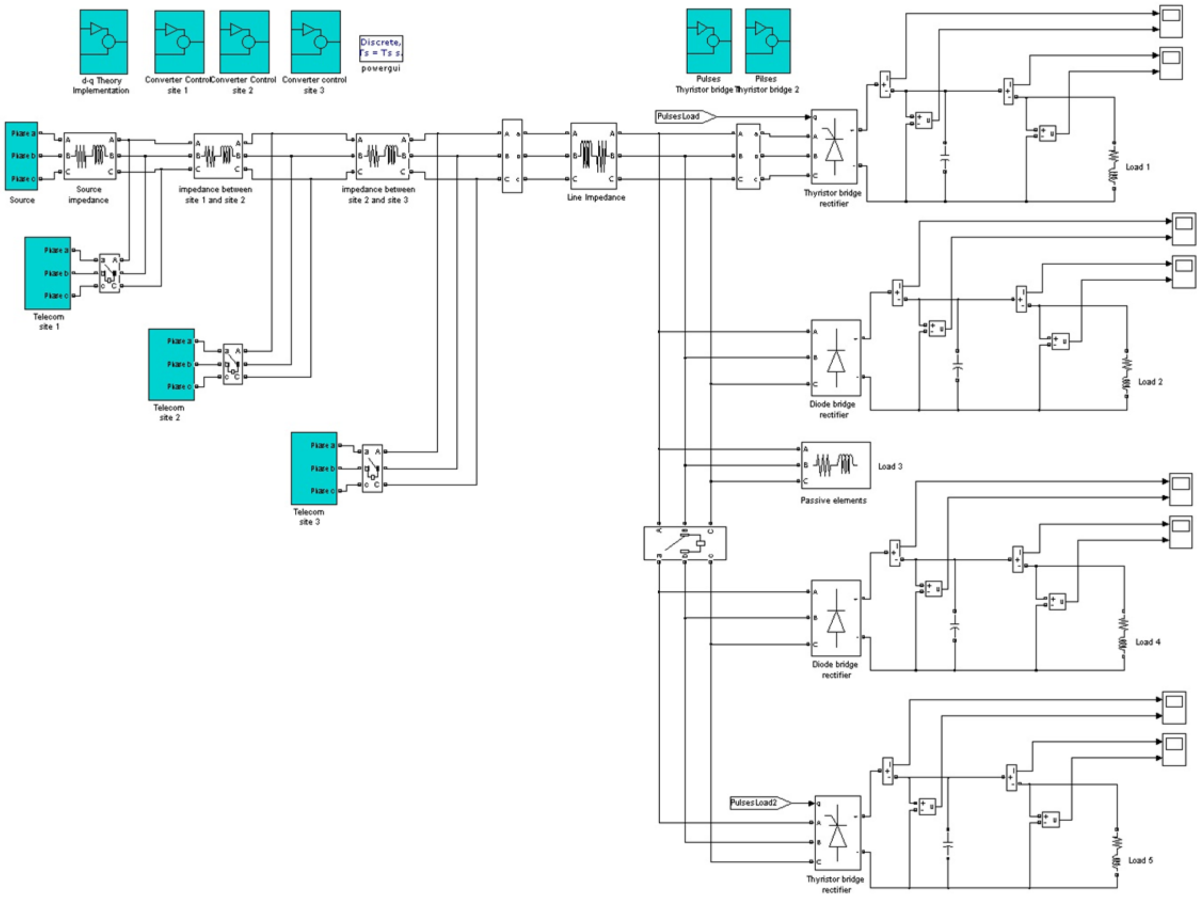

Figure D. 8: Simulation block diagram for three Telecom sites connected to the network

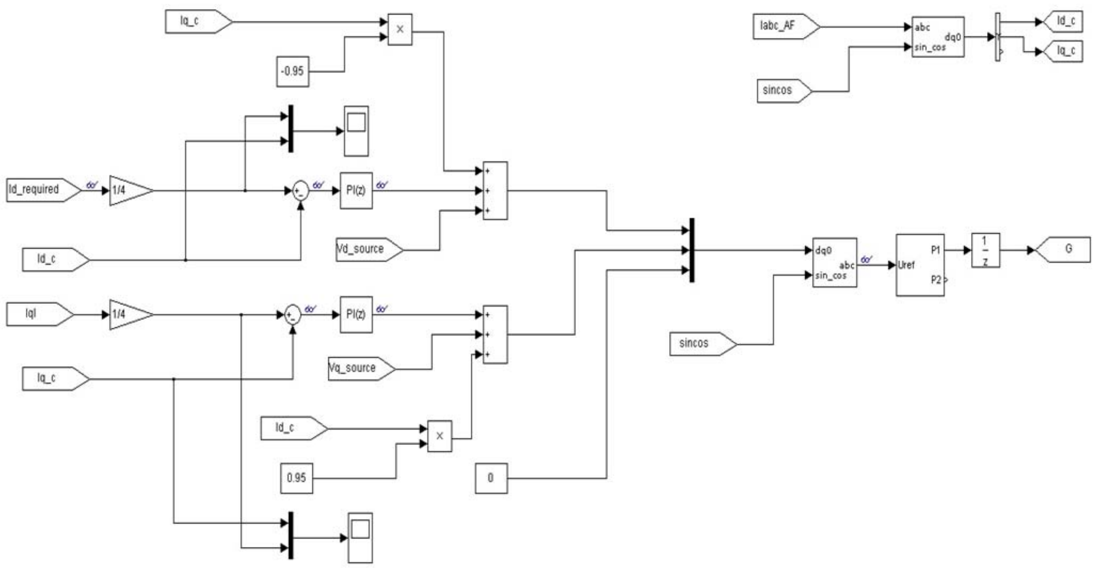

Figure D. 9: Inner current controller design for site 1

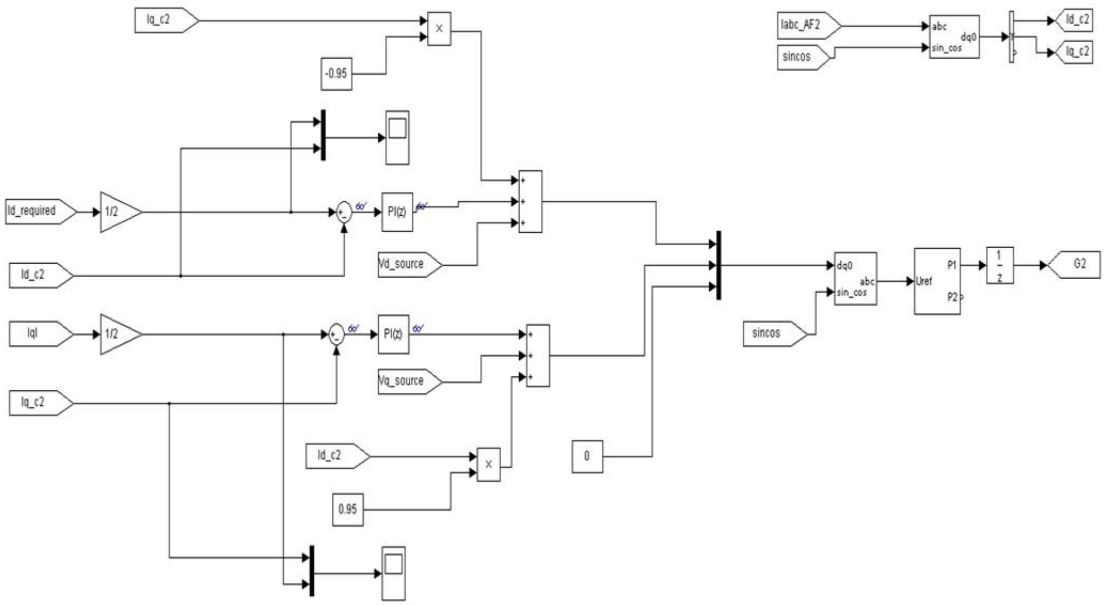

Figure D. 10: Inner current controller design for site 2

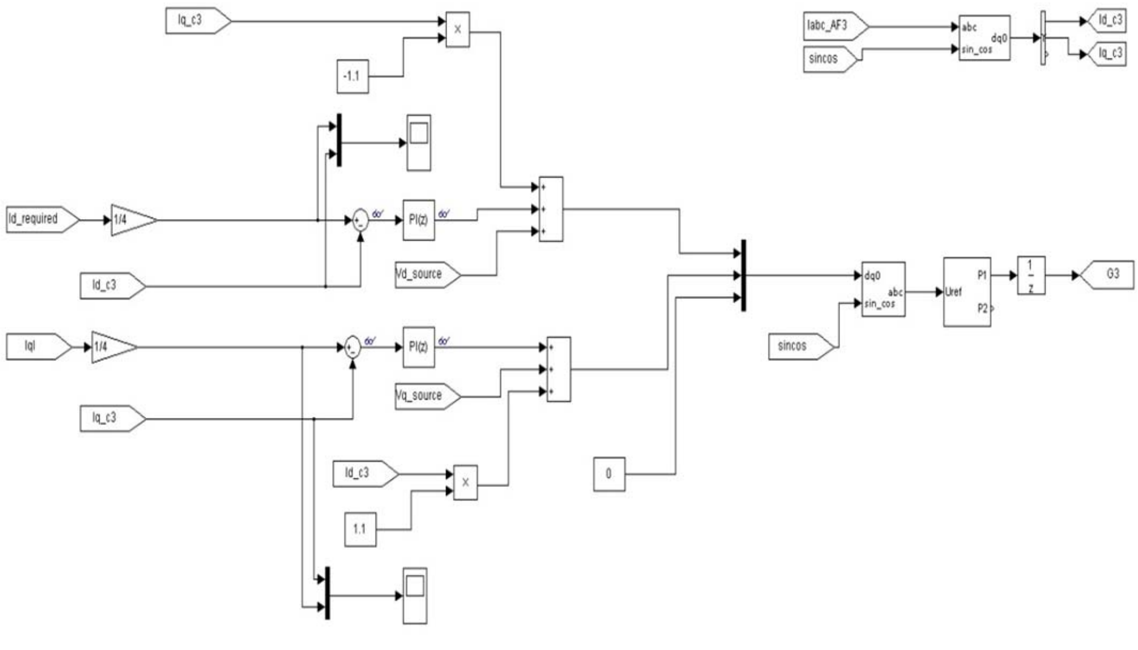

Figure D. 11: Inner current controller design for site 3

Appendix E: Simulation models for Grid Voltage Support

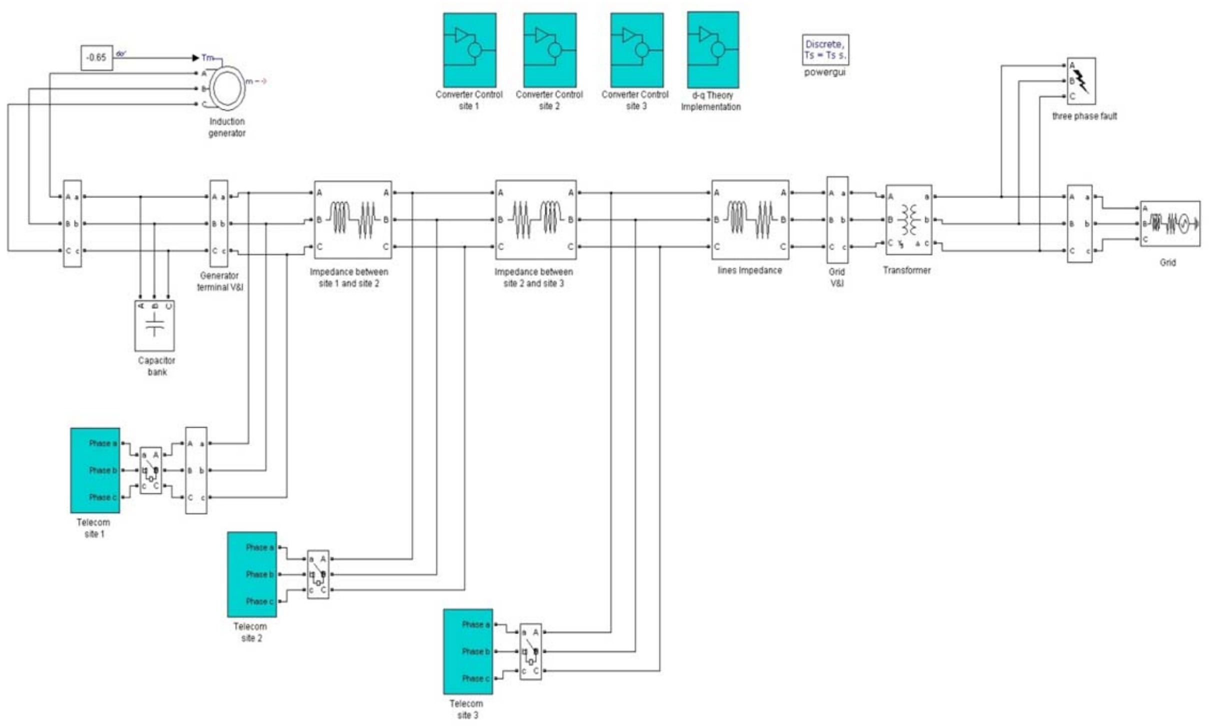

Figure E. 1: Three Telecom sites connected to IG based distribution grid

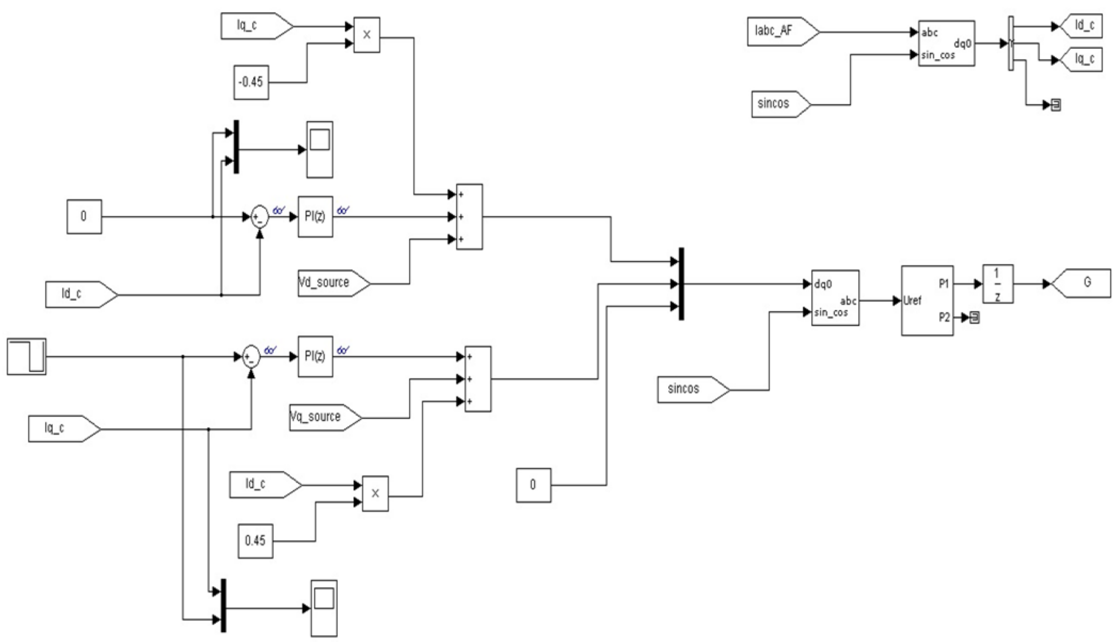

Figure E. 2: Inner Current Controller Design for Telecom site 1

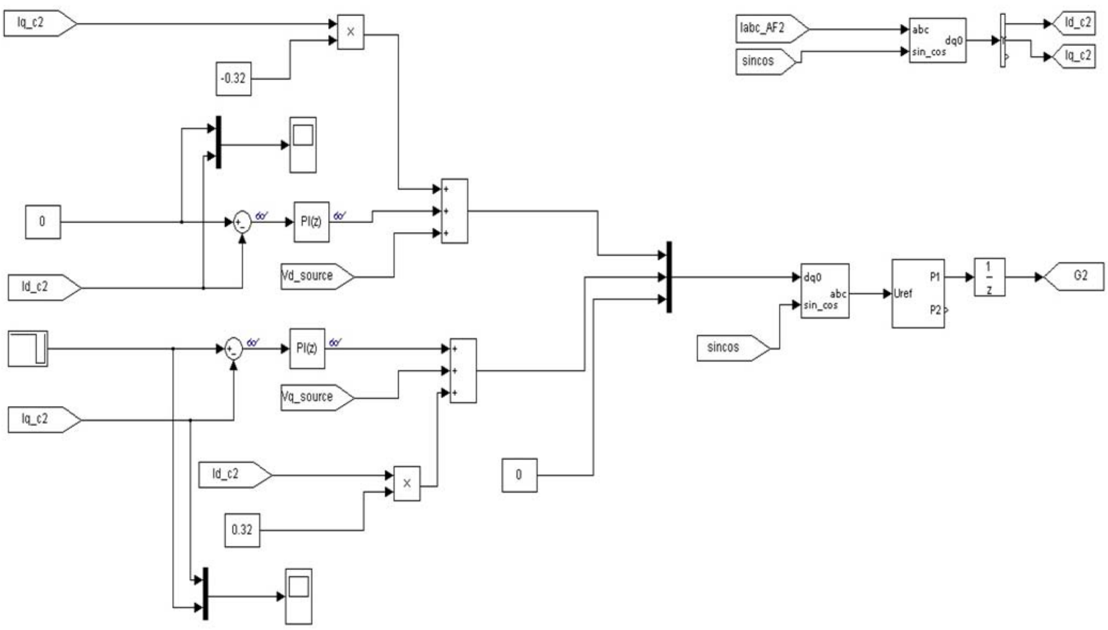

Figure E. 3: Inner Current Controller Design for Telecom site 2

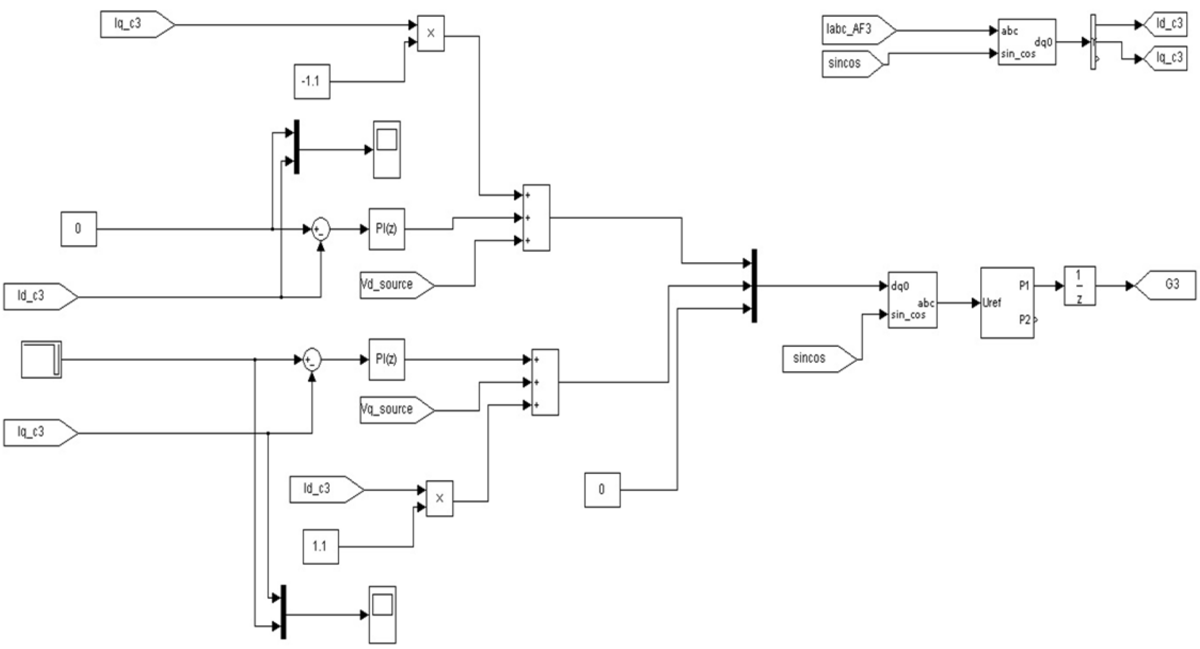

Figure E. 4: Inner Current Controller Design for Telecom site 3